Technical Report
ECOM-0274-F

1778-1-F = RL-2036

Reports Control Symbol
OSD-
May 1969

Investigation of the Rudimentary Horn

Final Report

26 April 1968 through 25 April 1969

Report No. 1

Contract DAAB07-68-C-0274
DA Project

Prepared by

Dipak L. Sengupta and Joseph E. Ferris

The University of Michigan Radiation Laboratory
Department of Electrical Engineering
Ann Arbor, Michigan

For

United States Army Electronics Command, Fort Monmouth, N J

ABSTRACT

The performance of a novel type of antenna named the Rudimentary Horn has been investigated both theoretically and experimentally. Detailed experimental investigation of the VSWR properties as well as the radiation characteristics of the antenna has been carried out over the frequency range 1 GHz to 10 GHz. Over this band of frequencies the antenna has been found to maintain its desirable impedance and radiation characteristics.

A first order theory has been developed for the radiation field produced by a symmetrical rudimentary horn having exponentially curved radiating elements . Fair agreement has been obtained between theory and experiment for the H-plane radiation patterns. Further improvement of the theory is desirable.

The rudimentary horn is found to be a broadband linearly polarized antenna. Its cross-polarization response in the direction of the main beam maximum is at least 30 dB down. The effects of the variation of the different physical parameters on the performance of the antenna are given. General design considerations are also given.

Possible applications of the rudimentary horn are also discussed. In particular, it has been found that in all aspects of electrical performance the rudimentary horn is competitive with commonly used antennas for HF long range communication.

FOREWORD

This report (1778-1-F) was prepared by The University of Michigan Radiation Laboratory, Department of Electrical Engineering under Contract No. DAAB07-68-C-0274, "Investigation of the Rudimentary Horn". This contract was initiated under United States Army Project No. PR and C-68-EL-7303. The work is administered under the direction of the Institute for Exploratory Research, Division C. Dr. Helmut L. Brueckmann is the Contract Monitor. This Final Report covers the period from 26 April 1968 through 25 April 1969.

The material reported herein represents the results of an investigation of the rudimentary horn.

TABLE OF CONTENTS

LIST OF ILLUSTRATIONS

I
INTRODUCTION

1.1 Preliminary Remarks

This is the Final Report on Contract DAAB07-68-C-0274, "Investigation of the Rudimentary Horn", and covers the period 26 April 1968 through 25 April 1969. The primary purpose of the Contract has been to investigate the properties of a new type of antenna called here the Rudimentary Horn with the specific goal of application in the HF range. In the following sections we discuss the origin of the antenna configuration and give a brief outline of the report.

1.2 Historical Background

The present antenna configuration was first proposed several years ago by J. Kerr of CS/TA Laboratory of the United States Army Electronics Command, Fort Monmouth. The antenna is an outgrowth of a broadband ridged horn and may be evolved from a ridged horn by removing the sides so that only the ridged back-cavity and the broadbanding ridges remain. A photograph of the original version of the complete antenna assembly is shown in Fig. 1-1. Initial unpublished work performed on this antenna was described to personnel of The University of Michigan Radiation Laboratory during the early part of 1966 (private communication with Mr. Charles Eason of USAECOM, Ft. Monmouth). At that time, typical experimental radiation pattern and VSWR data of the antenna obtained in 1964 were shown. Later at the Radiation Laboratory, we assembled a simplified model of the antenna and performed some limited experiments in order to obtain an understanding of its electrical characteristics.

To our knowledge, those who invented the antenna did not make any attempt to develop and pursue the concept further. In view of its excellent broadband characteristics both with respect to pattern and impedance and its simplicity of design and construction it was felt that it would be desirable to conduct a comprehensive investigation of this new antenna configuration.

1.3 Outline of the Report

As mentioned before, the rudimentary horn is a novel antenna. Hence, the major emphasis of our investigation has been devoted to the study of its radiation and impedance properties under various conditions. Besides understanding the performance of the antenna, the motivation of the entire investigation is also directed towards evaluating any possible application of the rudimentary horn to HF long range communication. The outline of the report is as follows.

Chapter II presents in detail the results of experimental investigations of the radiation and impedance properties of rudimentary horn antennas of different configurations. Whenever possible critical discussions of the results are given.

Theoretical analysis of the radiation field of a rudimentary horn is described in Chapter III.

In Chapter IV the properties of rudimentary horn antennas are compared with those of other commonly used HF antennas.

The general properties of the antenna and its possible applications are given in Chapter V.

Our conclusions and recommendations for further work are given in Chapter VI.

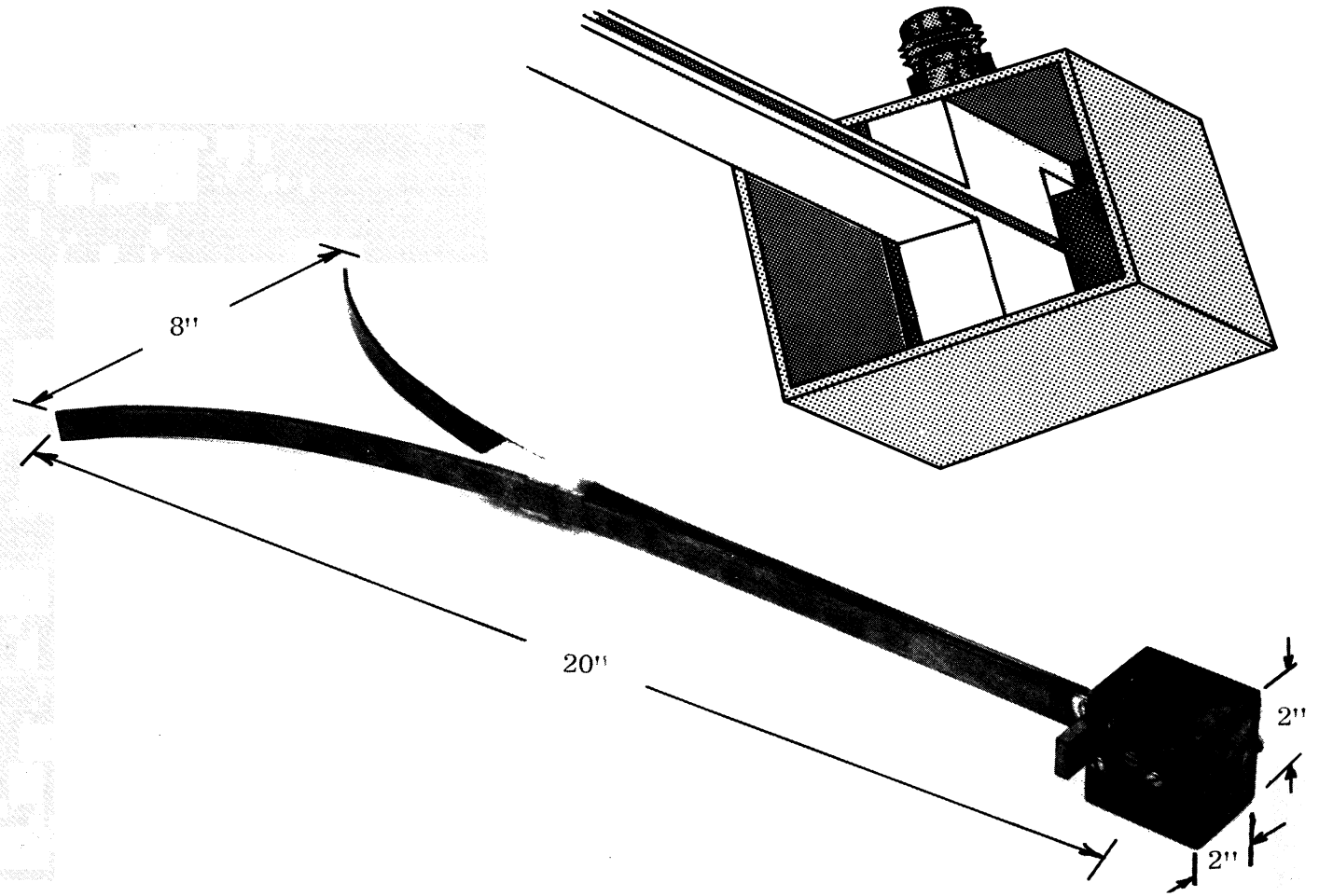

FIG. 1-1: PHOTOGRAPH OF THE RUDIMENTARY HORN ANTENNA. THE INSERT SHOWS THE STRUCTURE OF THE CAVITY.

II

EXPERIMENTAL STUDY OF THE RUDIMENTARY HORNS

2.1 Introduction

The results obtained from intensive experimental investigation of the various properties of rudimentary horn antennas are given in this chapter. Impedance and radiation pattern characteristics of different antenna configurations have been studied in detail and wherever possible, critical discussion of the results is given. Some information is also presented regarding the measured current distribution on the radiating elements of a few selected rudimentary horn antenna models.

2.2 A Discussion of the Measurement Techniques

As mentioned in the Chapter I, the primary purpose of the present investigation has been to determine any potential application of the rudimentary horn antenna to long range HF communication systems. From this point of view the frequencies of interest lie in the range 4.0 MHz to 24.0 MHz. However, at these frequencies the physical dimensions of the test antennas become too large to carry out any meaningful investigation of their radiation pattern characteristics. The results discussed in the following sections have been obtained by following the principle of model measurement in electromagnetic systems.

Detailed theory of models of electromagnetic system is discussed in the literature (Sinclair, 1948). Such model measurements ordinarily yield information of the radiation patterns of HF antennas under free space conditions and also when they are used in conjunction with perfectly conducting ground planes. Thus the information obtained in this manner will be found useful and meaningful only when the corresponding HF antennas are either used in free space or above a perfectly conducting ground. It is well known that in the HF range the ground has finite conductivity. Thus, in order to study the effects of the actual soil conditions on the radiation patterns of HF antennas, the appropriate ground constants are required to be scaled for proper model measurements. The dry ground constants in the HF range depend on the frequency of operation. For example (Ramsay, et al, 1967) the dry ground constants at two selected frequencies are:

permittivity $\epsilon = 15$
conductivity $\sigma = 15$ mʊ/meter — at 2 MHz,

and

permittivity $\epsilon = 5$
conductivity $\sigma = 1$ mʊ/meter — at 20 MHz .

It is known from the theory of model measurements (Sinclair, 1948; Ramsay et al, 1967) that if the relative dielectric constant of the model ground plane is kept constant at the value corresponding to the full scale frequency, the conductivity σ should be multiplied by the scale factor defined as the ratio of the model frequency to the full scale frequency. With this criterion it is found that the above ground when modelled will be required to have a large conductivity. Such a combination of electrical parameters in a material does not exist in nature. The model ground must therefore be made artificially. One of the difficulties in the technology of artificial ground fabrication is to produce a material with a relatively high conductivity while maintaining a preferred value of the dielectric constant. From this consideration it is preferable to choose the full scale frequency to be above 10 MHz (Ramsay et al, 1967). For example if the full scale frequency is 20 MHz and the scale factor is taken to be 100, then the model ground constants are required to be $\epsilon = 5$, $\sigma = 100$ m℧/meter and the loss tangent $\tan\delta = 0.018$ at the model frequency of 2 GHz. The characteristics of carbonated polyurethane elastometer developed by the Research Center of the Armstrong Cork Company, Lancaster, Pa., are $\epsilon = 4.75$ and $\tan\delta = 0.175$ at 2 GHz, which represents a close approximation to the required model dry ground. Limited amount of pattern studies for monopole antennas has been reported by Ramsay et al (1967) who used the above artificial ground to simulate the soil conditions in the HF range.

In view of the stated objective of the Contract it appears to be desirable to make radiation pattern measurements by modelling the actual soil conditions at HF in the above manner. However, we have not followed this procedure due to the excessive cost involved in the fabrication of such an artificial ground.

The results of our investigation which are reported in the following sections will thus pertain to the free space and perfectly conducting ground plane conditions only. The motivation behind writing this section has been that we are aware of this potentially important method of artificially simulating the necessary ground parameters during the model measurement of antenna radiation patterns. If necessary funds are available it would be preferable to follow this technique during the measurement.

The scale factor used during our experimental investigation was 333 so that the model frequency lies in the GHz range. The reason for choosing this particular scale factor has been the availability of the measuring equipment in the frequency range 1 - 10 GHz and also that the initial work done on the rudimentary horn was in this frequency range.

2.3 Description of the Test Antenna Models

In this section we describe the various rudimentary horn configurations that have been studied during the course of the investigation. For the purpose of identification, these test antenna models are numbered in the sequential order in which they were conceived. The rudimentary horns to be discussed in the following sections are given in Table II-1. The functional equations shown in the table describe the curvatures associated with the radiating elements. The geometrical arrangement and the relevant physical parameters of typical symmetrical and asymmetrical (with ground plane) rudimentary horn models are shown in Figs. 2-1 and 2-2 respectively. A photograph containing the three versions of an actual rudimentary horn model is shown in Fig. 2-3. Note that in Fig. 2-3 the antenna model 3 consists of radiating elements of conducting strips, the model 3W has the same configuration but its radiating elements are made of conducting round wires and model 3G is the ground plane version of the model 3.

The dimensions of the various design parameters of all the rudimentary horn models are given in Tables II-2 and II-3. All of the test models except the one numbered 3X are fabricated from 1/16"-thick brass strips. It is to be noted that the models 3, 3X and 3V are symmetrical and the remaining models numbered 4 through 10 are asymmetrical in nature, i.e. they employ ground plane.

It can be seen from Table II-1 that the models shown in the first row (i.e. 3, 3X, 6, 7, 8) employ exponential curvature of the radiating elements. The model 3V is a conventional V-antenna consisting of two linear elements of length L and inclined at an angle given by corresponding functional equation in Table II-1 . The models 4, 9C and 10C employ radiating elements having exponential curvature up to a length L_1 and then being continued linearly up to the rest of the length L_2 . The last model 5A shown in Table II-1 has been fabricated in a slightly different fashion. The functional equation shown here describes the variation of the characteristic impedance along the longitudinal direction when the antenna is viewed as a variable cross section strip transmission line. In Tables II-1 and II-3 the parameters Z_o and Z_{om} pertaining to the model 5A refer to the impedances of the input and the open ends of the antenna respectively. The first equation for model 5A in Table II-1 (Walton and Sundberg, 1964) determines the necessary length L of the antenna when the impedance variation in the longitudinal direction is specified. The second equation (Dukes, 1958) determines the height y of the radiating element above the ground plane so that the specified impedance Z_x may be achieved. It should be mentioned here that the necessary curvature of the radiating strip element to obtain the specified impedance variation given in Tables II-1 and II-3 has been found to be approximately exponential. Antenna models having the letter C associated with their identification numbers (e.g., 7C, 9C, etc) have been fabricated from conducting strips whose width (W) increase linearly from the corresponding values given in Table II-2 at the input ends to a value of 2" at the open ends. The reasons for following this procedure will be explained later.

TABLE II-1: RUDIMENTARY HORN CONFIGURATION

Configuration No.	Description
3, 3X, 6, 7, 8	$y = 10^{\left[\left(\frac{\log D - \log d}{L}\right)x + \log d\right]}$
3V	$y = \frac{D-d}{L}x + d$
4, 9C, 10C	$y = 10^{\left[\left(\frac{\log D_1 - \log d_1}{L_1}\right)x + \log d_1\right]}$ for $0 < x < L_1$ $y = \frac{D_2 - D_1}{L_2}x + D_1$ for $L_1 < x < L_2$
5A	$Z_x = Z_{om}\frac{Kx}{L}$ (Walton and Sundberg, 1964) also $Z_x = f\left(\frac{w}{y}\right)$ (Dukes, 1958)

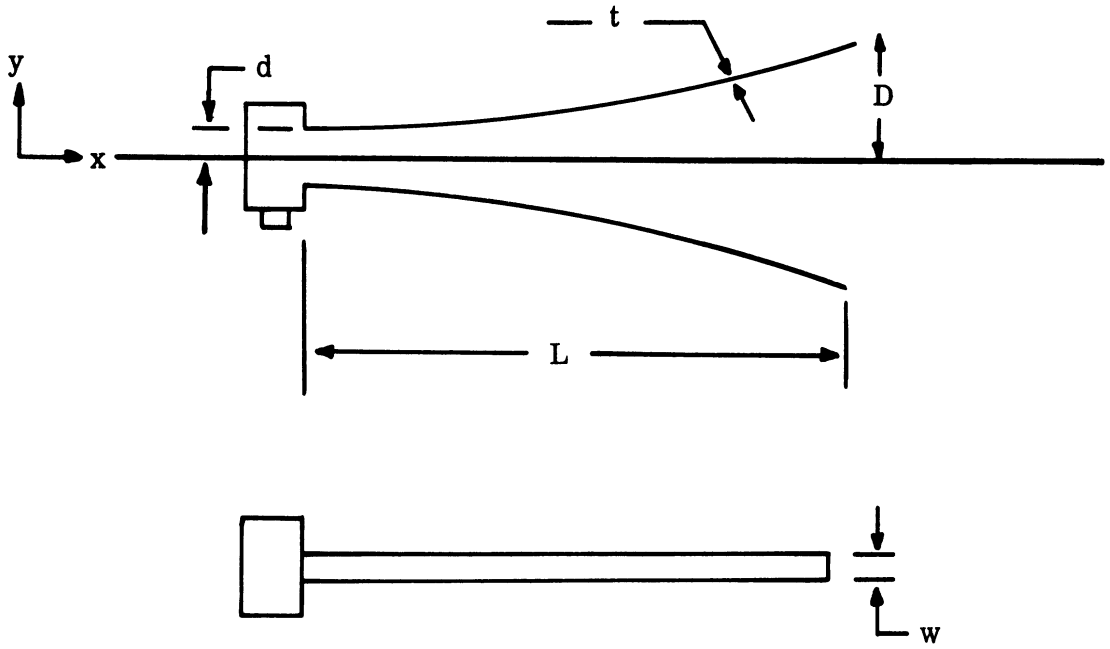

FIG. 2-1: GEOMETRICAL REPRESENTATION OF A SYMMETRICAL RUDIMENTARY HORN.

FIG. 2-2: GEOMETRICAL REPRESENTATION OF AN ASYMMETRICAL RUDIMENTARY HORN.

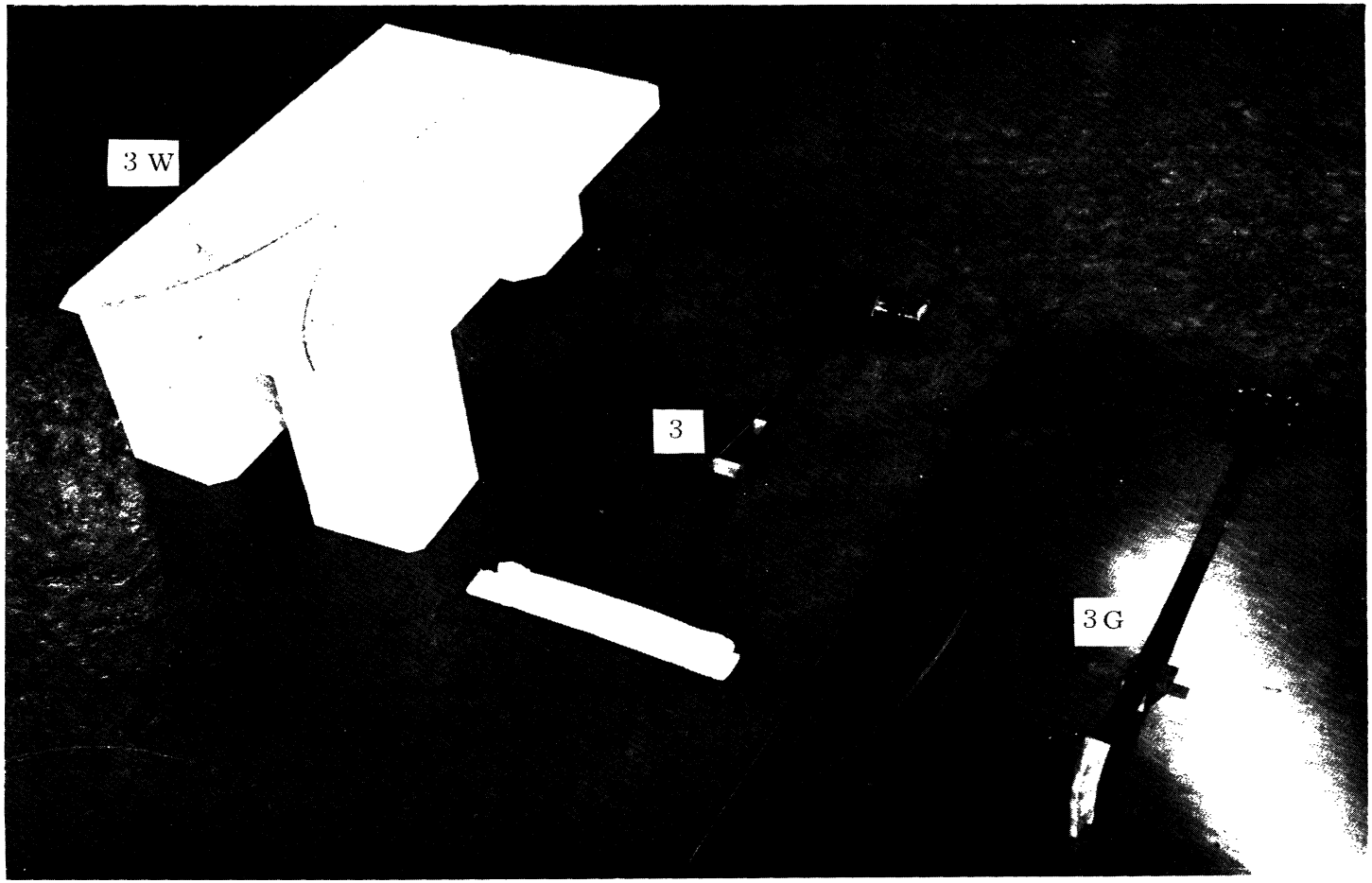

FIG. 2-3: PHOTOGRAPH OF THE THREE VERSIONS OF AN ACTUAL RUDIMENTARY HORN MODEL NO. 3.

TABLE II-2: DIMENSIONAL CHARACTERISTICS OF RUDIMENTARY HORN MODELS

Configuration No.	t (inches)	D (inches)	d (inches)	L (inches)	w (inches)
3	0.0625	6.00	0.025	18	0.0625
3X	0.625	6.00	0.025	18	0.625
3V	0.0625	6.00	0.025	18	0.625
6	0.0625	6.00	0.025	18	0.125
7	0.0625	6.00	0.050	18	0.250
8	0.0625	6.00	0.050	24	0.250

TABLE II-3: DIMENSIONAL CHARACTERISTICS OF RUDIMENTARY HORN CONFIGURATIONS 4, 5, 9C and 10C .

4 t=0.0625", D_1=0.075", D_2 = 3.00", d = 0.025", L_1= 10", L_2= 18", w = 0.625"

5 t=0.0625", w=0.250", L = 18", Z_o = 50 Ω, K = 2.92 Z_{om} = 215 Ω .

9C t=0.0625", D_1=1.260", D_2=6.00", d=0.025", L_1=10", L_2=24", w_1= 0.250", w_2=2.00" .

10C t=0.0625", D_1=0.676", D_2=3.00", d=0.025", L_1=10", L_2=24", w_1=0.250", w_2= 2.00" .

It is now appropriate to describe briefly the feeding system used for the antenna test models during the course of measurement. Each of the symmetrical models employed a double ridged waveguide concept at the input end for impedance matching purposes (Fig. 1-1). The original double ridged waveguide was designed to have a 50 Ω characteristic impedance over the frequency band of 1 - 10 GHz. The input back cavity in Fig. 1-1 forms an integral part of the feed for these models. The asymmetrical models employed a coaxial transition section in the feed similar to that used in standard stripline work. For the configuration 5A, an attempt was made to match gradually the stripline impedance to that of free space over the length of the antenna in a manner similar to that discussed by Walton and Sundberg (1964).

2.4 VSWR Characteristics

The VSWR characteristics of both symmetrical and asymmetrical configurations of rudimentary horns are discussed in the present section. Because of the interest of the sponsor, the asymmetrical antennas have been studied in more detail. The measurements reported here have been carried out over the frequency band of 1 - 10 GHz.

2.4.1 Symmetrical Configurations

The VSWR characteristics of the rudimentary horn models 3, 3X and 3W are shown in Figs. 2-4, 2-5 and 2-6 respectively. From Figs. 2-4 and 2-5 it is found that initially at the lower end of the frequency range the VSWR is in excess of 7 : 1 for antenna 3, and is in excess of 5 : 1 for antenna 3X ; however, over a major portion of the remainder of the frequency band it oscillates with a value of 3 : 1. The amplitude of these oscillations are found to be less for the model 3X which is made of thicker strips. It is thus observed that an antenna with wider radiating elements will have improved VSWR characteristics. Figure 2-6 shows the VSWR characteristics obtained from antenna 3W, made of round wires. Compared to the previous two antennas, it has poor VSWR characteristics over the entire band of frequencies.

Figure 2-7 shows the VSWR characteristics of a conventional V-antenna. This was investigated in order to obtain a comparison between a V-antenna and the rudimentary horn. It can be seen from Figs. 2-4, 2-5, 2-6 and 2-7 that compared to the rudimentary horns the V-antenna has considerably inferior VSWR characteristics.

2.4.2 Asymmetrical Configuration

Each of the configurations considered here consists essentially of a half rudimentary horn placed above a 36" x 14.5" conducting ground plane. The feeding system used during this part of the investigation consisted of a standard coaxial transition section commonly used in stripline work.

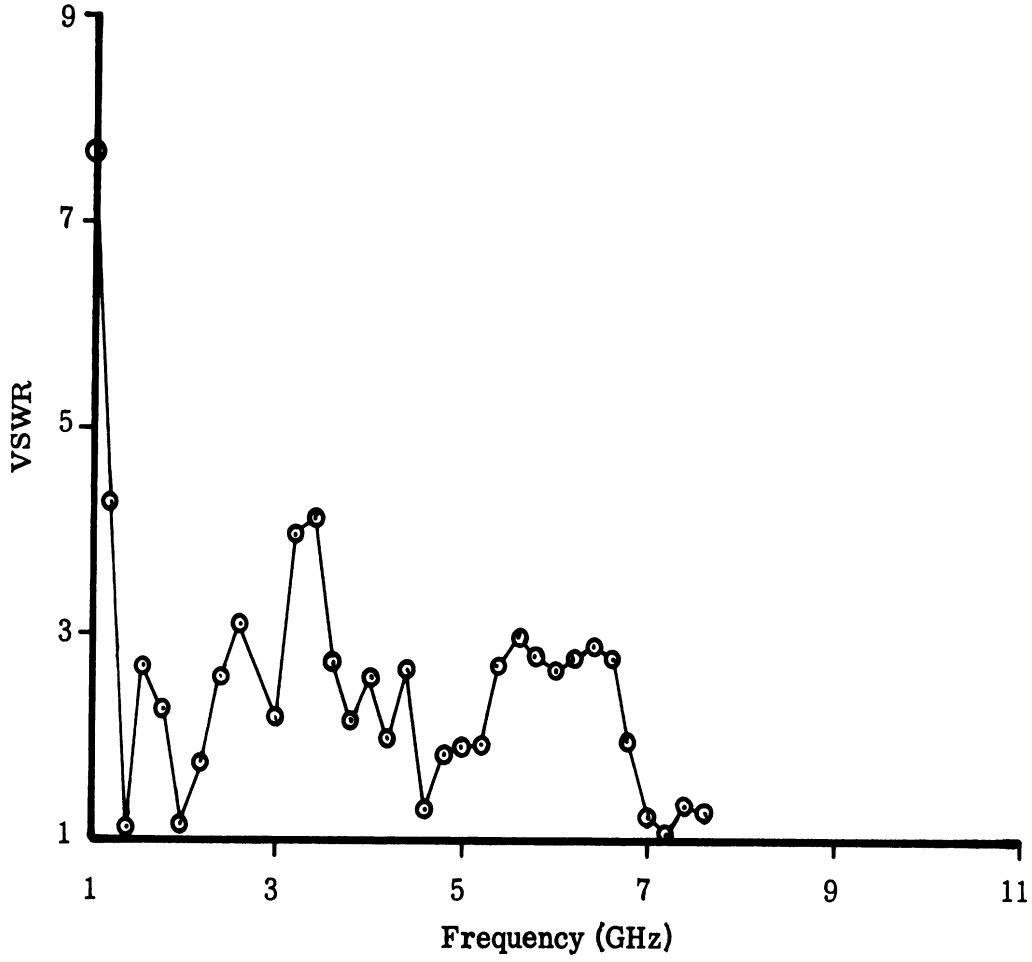

FIG. 2-4: VSWR CHARACTERISTICS OF RUDIMENTARY HORN NO. 3.

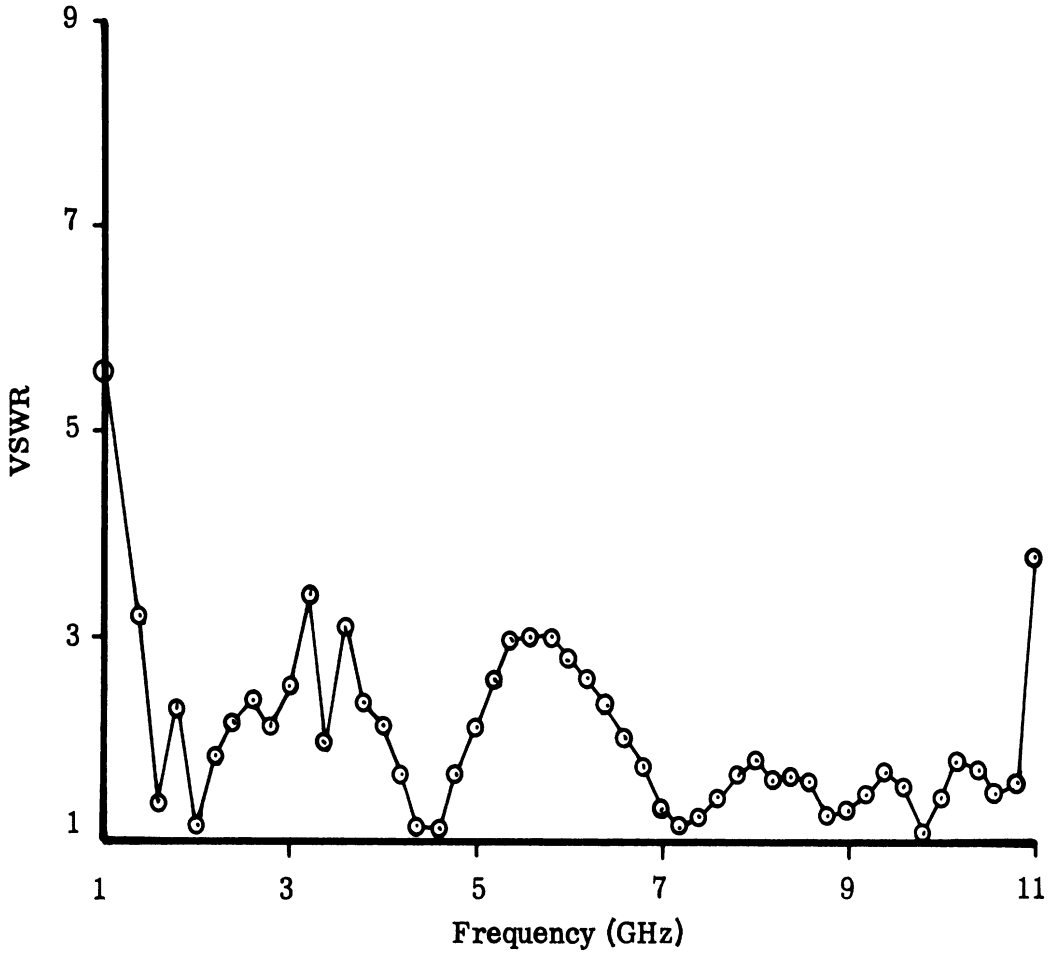

FIG. 2-5: VSWR CHARACTERISTICS OF RUDIMENTARY HORN NO. 3X.

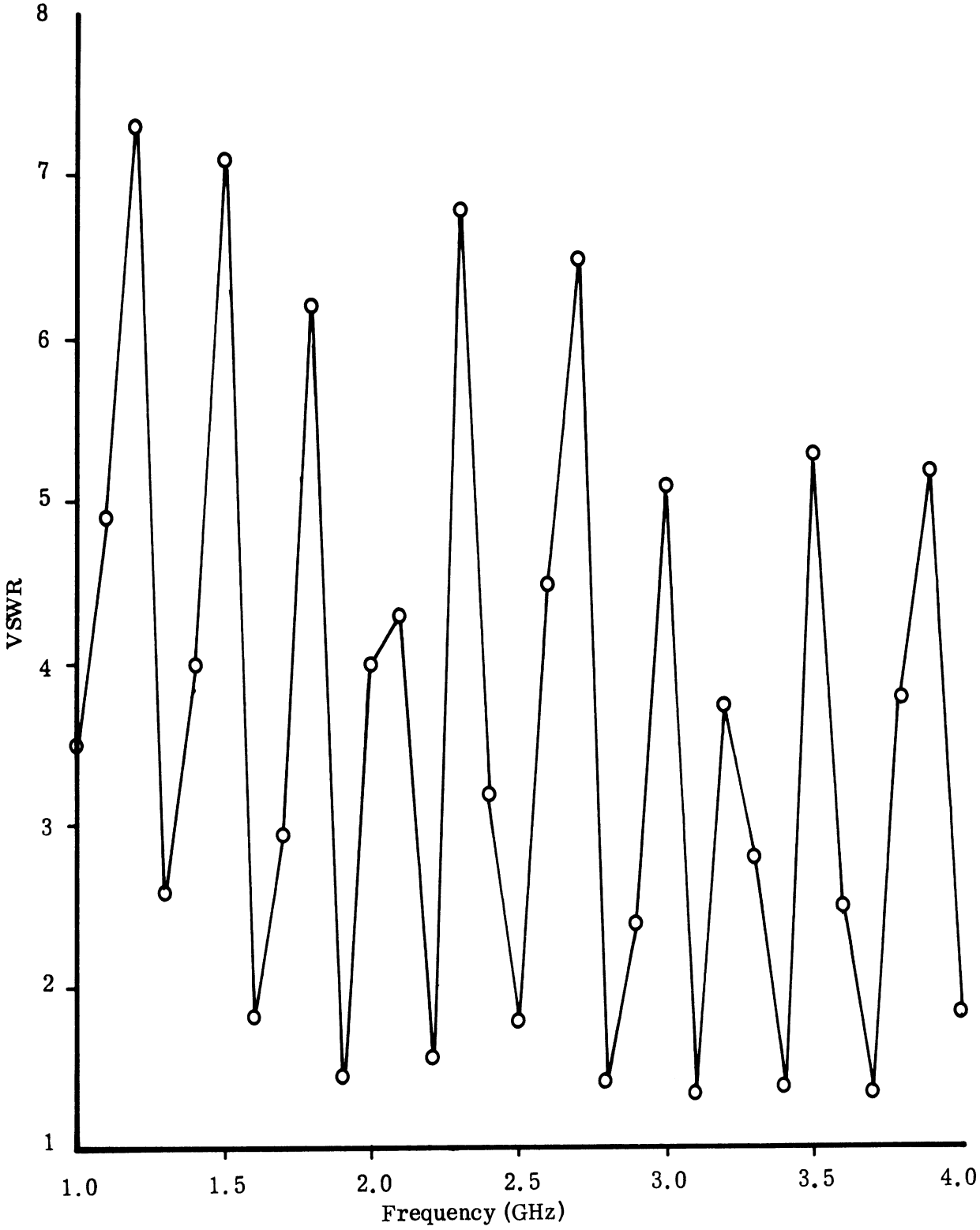

FIG. 2-6: VSWR CHARACTERISTICS OF RUDIMENTARY HORN NO. 3W.

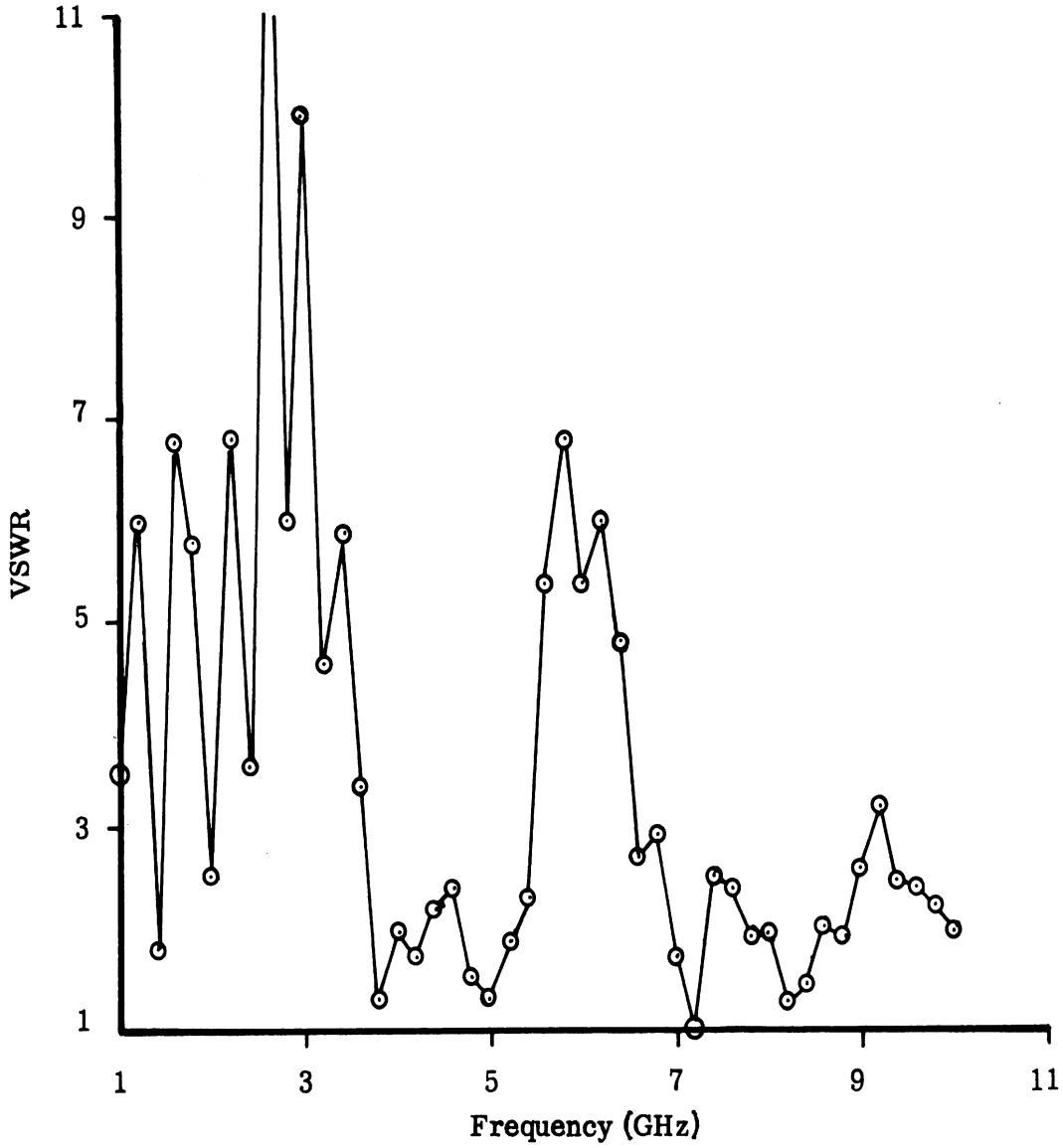

FIG. 2-7: VSWR CHARACTERISTICS OF RUDIMENTARY HORN NO. 3V.

In order to study the effects of the strip width w of the radiating element on the VSWR characteristics, models 6 and 7 were investigated. The width w = 0.125" for model 6 dictated that the parameter d = 0.025" so that an input impedance of 50Ω is obtained at the input end from uniform transmission line considerations (Dukes, 1958). Under the same criterion with w = 0.250" for model 7, the necessary d=0.05" . The observed VSWR characteristics for these two models are shown in Figs. 2-8 and 2-9. Figure 2-8 exhibits VSWR exceeding 3:1 at the lower frequencies and shows erratic variations of VSWR below the level 3:1 at the higher frequencies. Figure 2-9 clearly shows that the effect of using wider radiating strips produces well-behaved VSWR characteristics over the major portion of the frequency band; in this particular case the VSWR exceeds 3:1 at the lowest end of the frequency band but exponentially tapers off to less than 2:1 over the rest of the frequency band of interest.

Figure 2-10 shows the VSWR characteristics of model 8 which is similar to model 7 discussed above but with a longer effective length L. The general behavior of the VSWR in Fig. 2-10 is found to be similar to that in Fig. 2-9 but in the present case the performance may be considered to be slightly better. The better VSWR characteristics of model 8 may be attributed to its long length .

The set of VSWR characteristics shown in Figs. 2-11 to 2-13 have been obtained from rudimentary horn configurations which are similar to model 7 except that the widths of their radiating strips are linearly increased from the value w=0.25" at the input ends to larger values at the open ends. The models 7A, 7B, 7C and 7D considered here have strip widths at the open end 6", 4", 2" and 1" respectively. The motivation of this has been to ascertain how much the VSWR can be improved by increasing the strip without making the antenna mechanically heavy and unwieldy. After comparing Figs. 2-11 to 2-13 with Fig. 2-9 it is found that the VSWR characteristics can be considerably improved by following the above procedure. There appears to be an optimum strip width at the open end of the antenna which produced best VSWR. In the present case the test antenna model 7C with a radiating strip 2" wide at the open end has the best VSWR behavior.

Figure 2-14 shows the VSWR characteristics of model 4 which employs a radiating element having a combination of exponential and linear curvature. As can be seen from 2-14, this configuration has poor VSWR properties. Figure 2-15 shows the VSWR performance of rudimentary horn model 5A. Compared to the results shown in Fig. 2-14, the configuration 5A is found to have a VSWR variation which lies within 3:1 over most of the frequency band except near the lower end where the VSWR exceeds the value 3:1. It should be mentioned, however, that in the case of the model 5A the maintenance of the required curvature of the radiating element is quite difficult. This may be found to be a disadvantage in some practical situations.

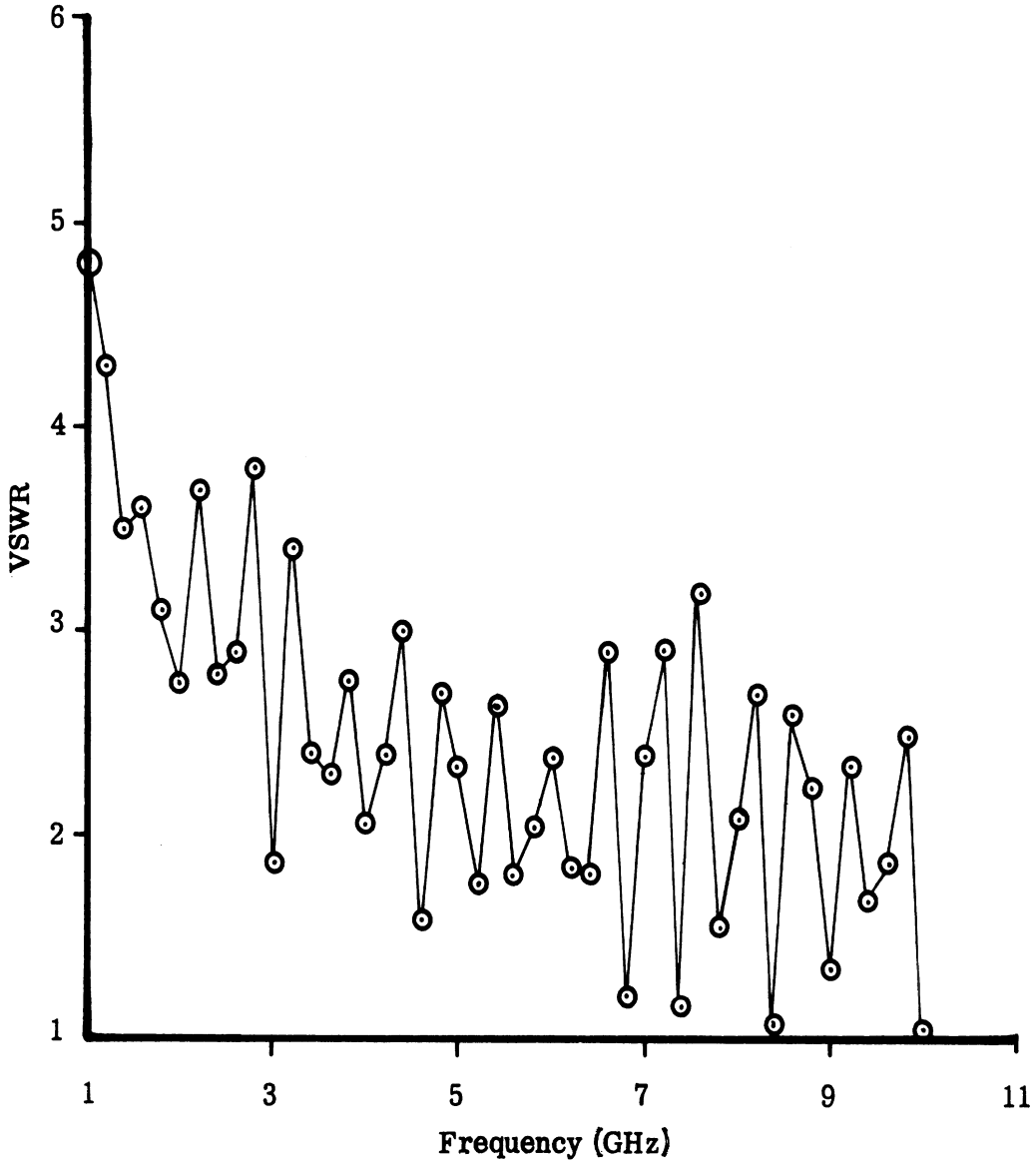

FIG. 2-8: VSWR CHARACTERISTICS OF RUDIMENTARY HORN NO. 6.

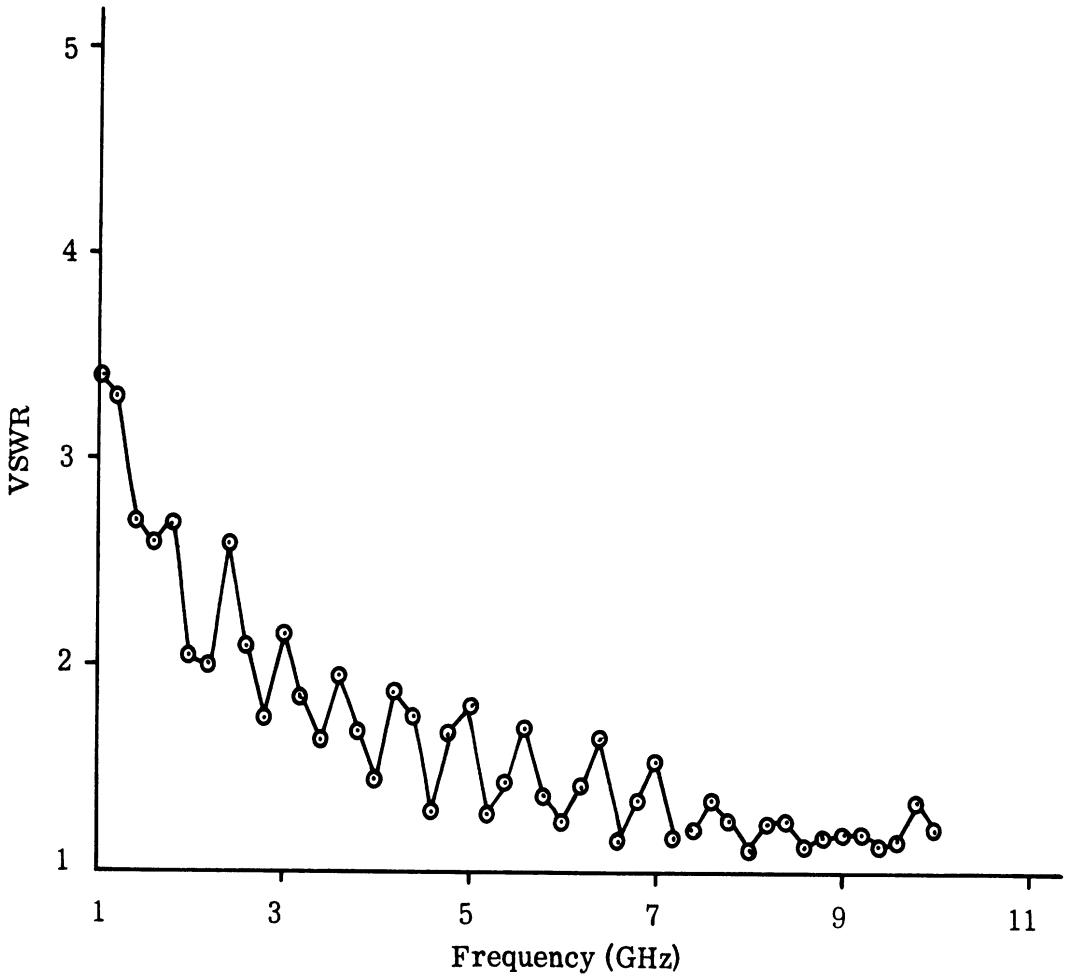

FIG. 2-9: VSWR CHARACTERISTICS OF RUDIMENTARY HORN NO. 7.

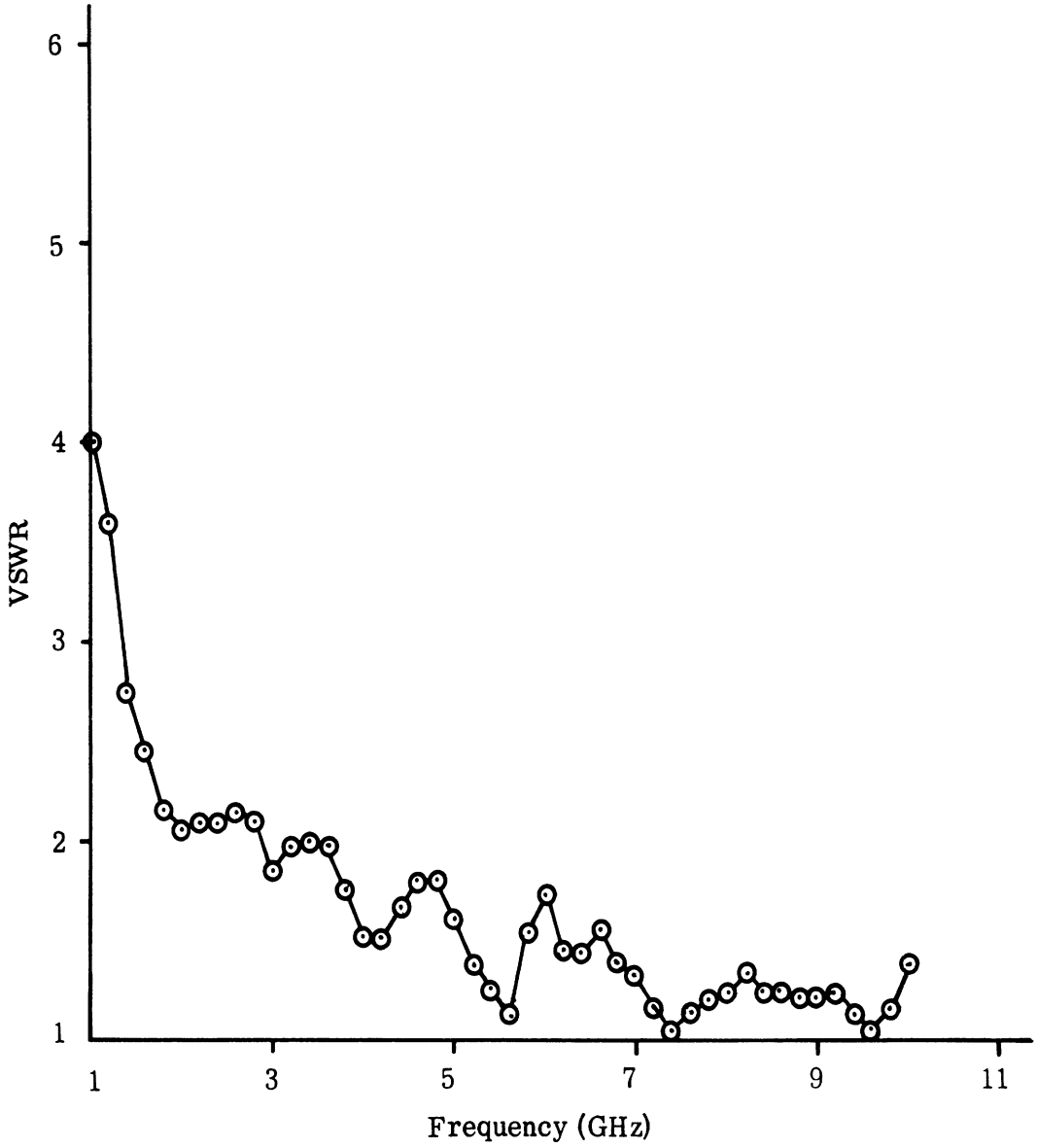

FIG. 2-10: VSWR CHARACTERISTICS OF RUDIMENTARY HORN NO. 8.

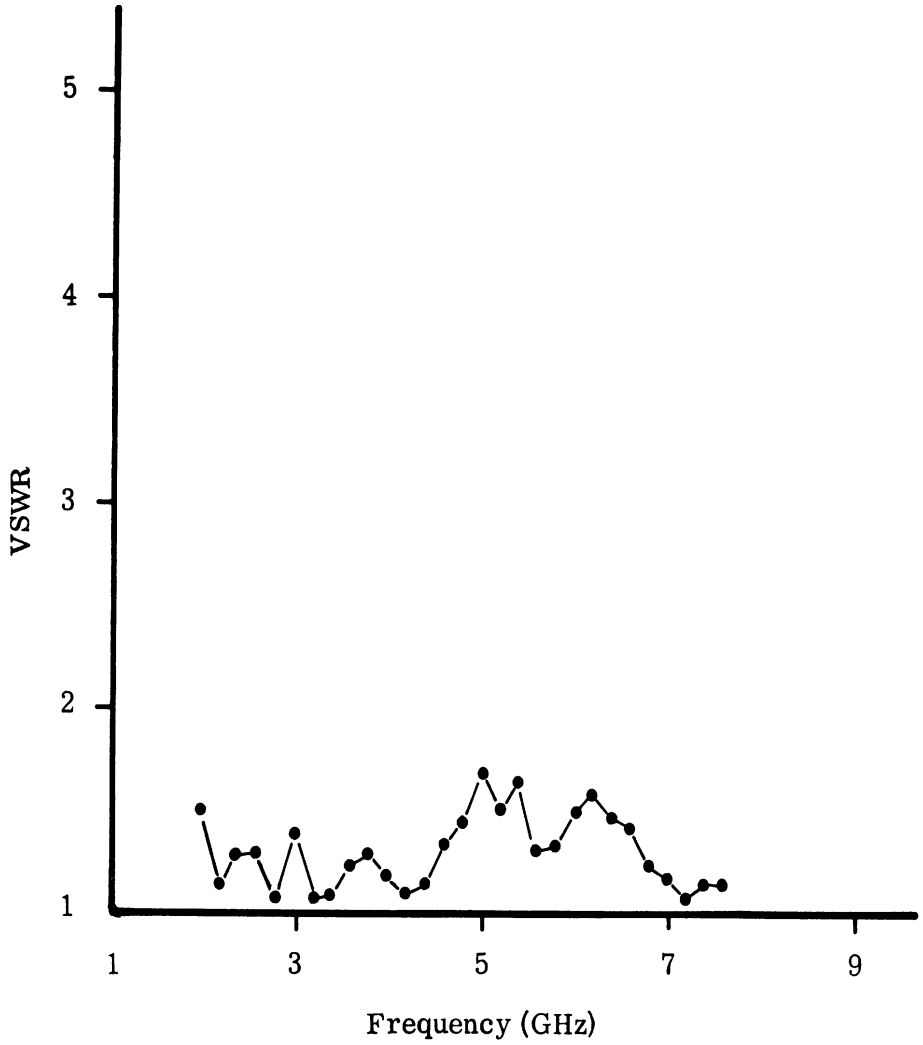

FIG. 2-11: VSWR CHARACTERISTICS OF RUDIMENTARY HORN NO. 7B.

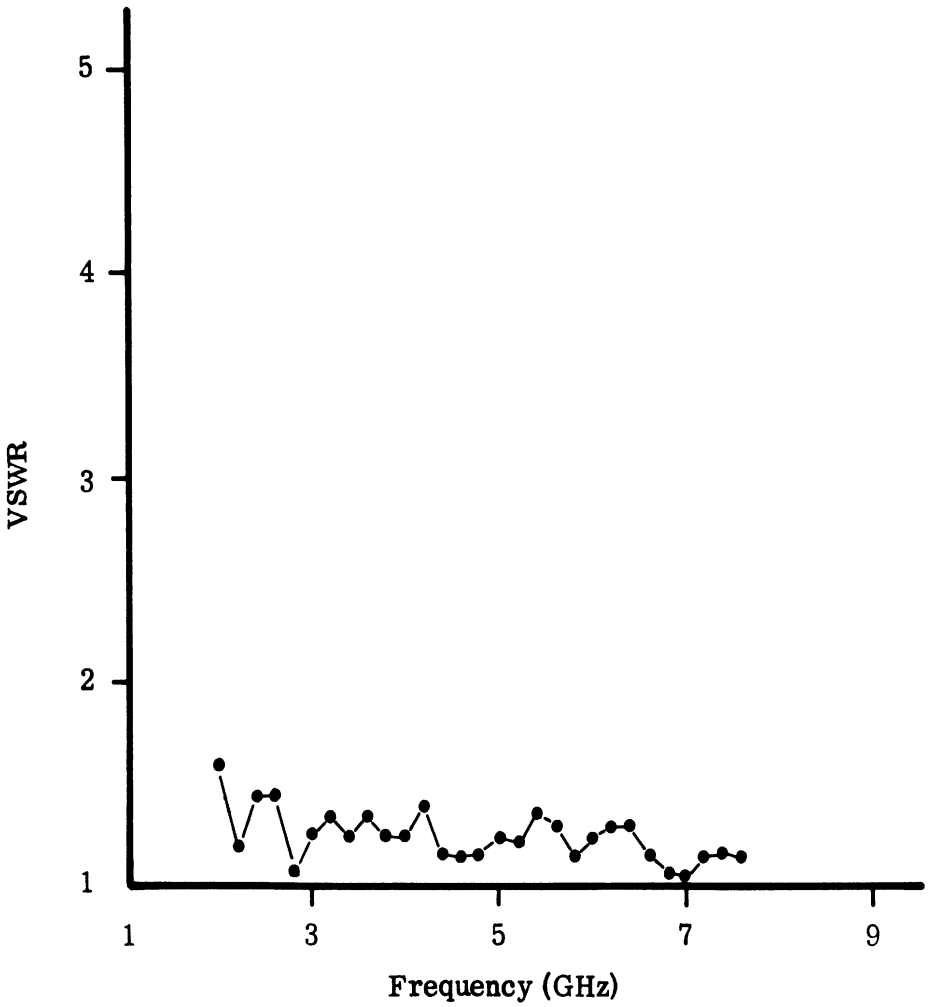

FIG. 2-12: VSWR CHARACTERISTICS OF RUDIMENTARY HORN NO. 7C.

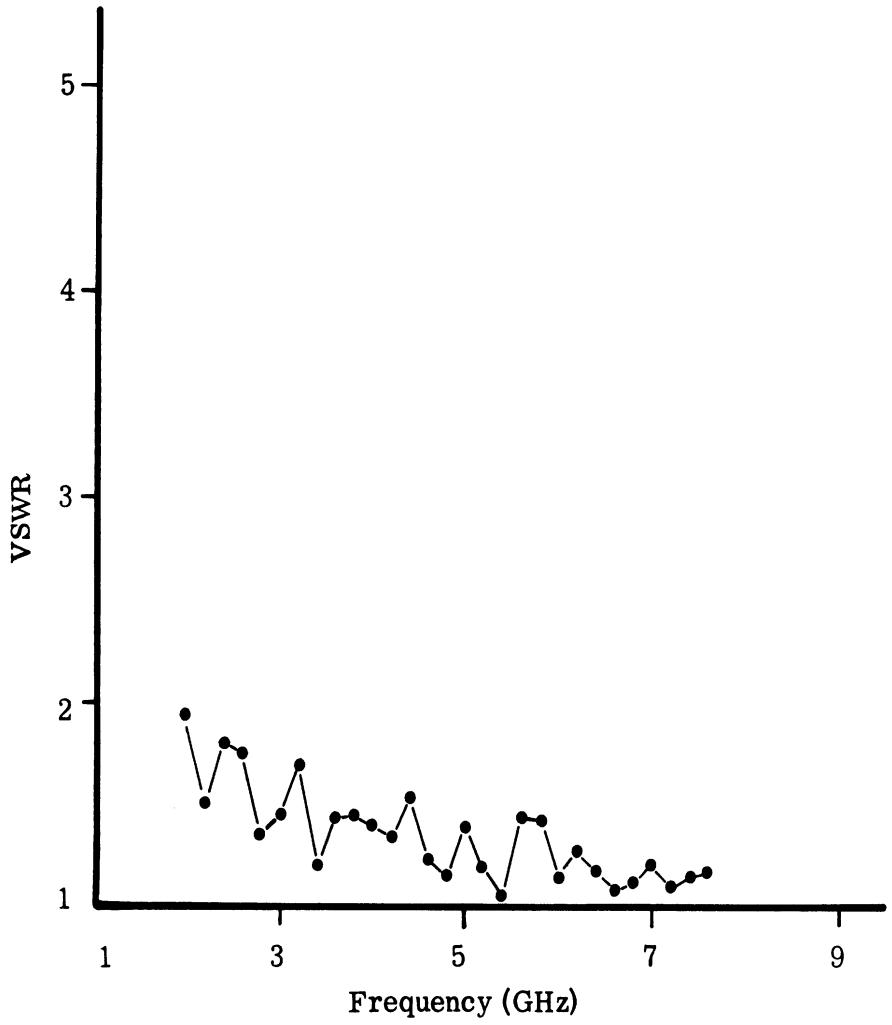

FIG. 2-13: VSWR CHARACTERISTICS OF RUDIMENTARY HORN NO. 7D.

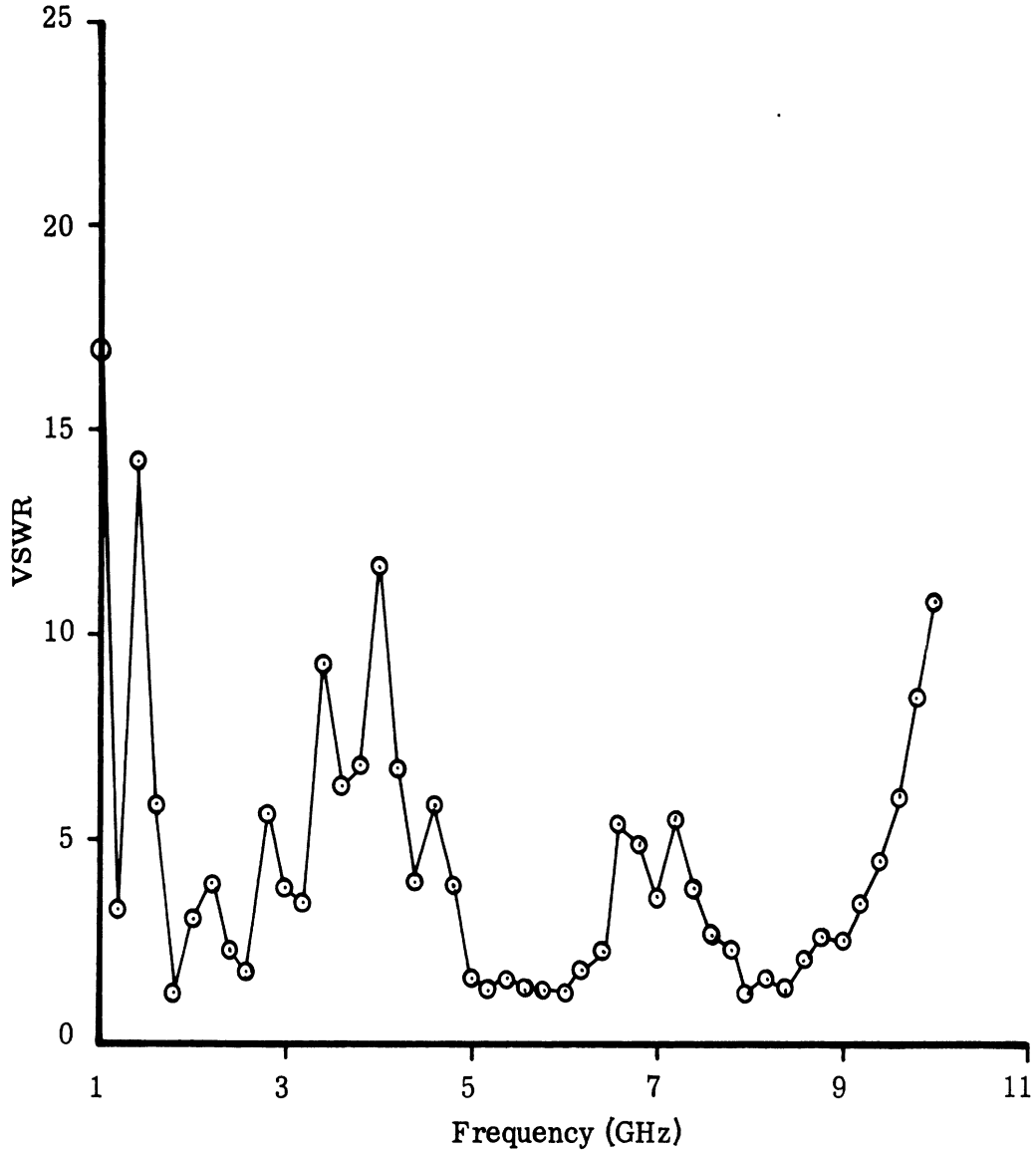

FIG. 2-14: VSWR CHARACTERISTICS OF RUDIMENTARY HORN NO. 4.

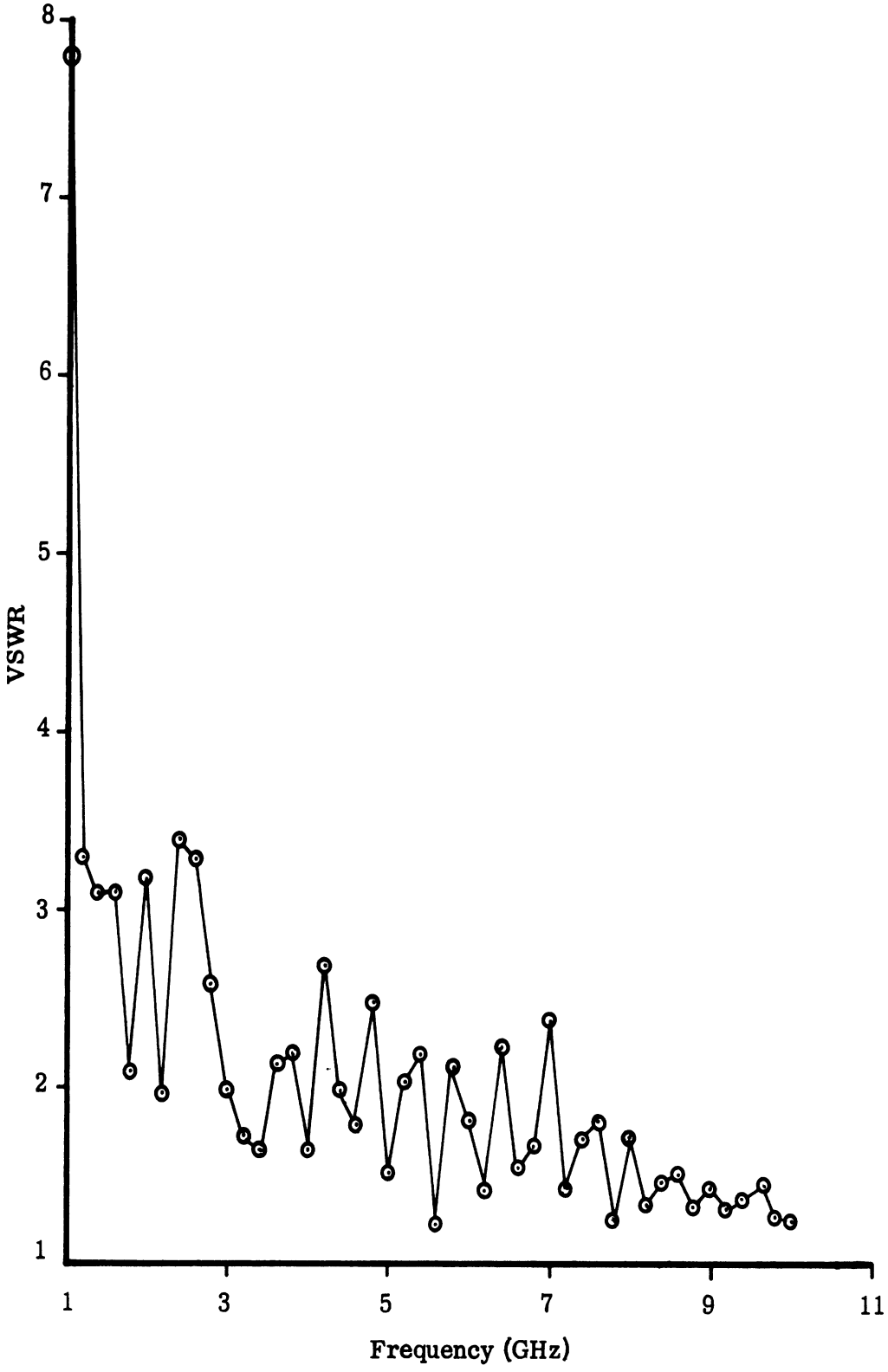

FIG. 2-15: VSWR CHARACTERISTICS OF RUDIMENTARY HORN NO. 5A.

As mentioned before all the VSWR results discussed above pertain to cases where the conducting ground plane size was 36" x 14.5" . In order to study the influence of the ground plane size on the VSWR characteristics, a series of measurements were taken with a specific antenna model for successivly reduced ground plane. The smallest size ground plane used was 10" x 10" . These results indicated that within this range of variation of the ground plane size the overall VSWR characteristics did not change appreciably.

2.4.3 Discussion

In this section we make the following observations on the basis of the VSWR results reported above:

(i) With a rudimentary horn having L = 18" (symmetrical or asymmetrical) connected to a 50 Ω input line it is possible to maintain a VSWR at a level $\leq 3:1$ within most of the frequency range between 1 - 10 GHz. Increase of L improved the performance further.

(ii) By using wider radiating strips or by linearly increasing the widths of the radiating strips towards the open end of the antenna it is possible to improve considerably the VSWR characteristics over the entire band of frequencies of interest.

(iii) With the asymmetrical antennas a reduction of the ground plane size from 36" x 14.5" to 10" x 10" does not change the VSWR characteristics appreciably. For satisfactory VSWR characteristics the minimum size ground plane used should be 10" x 10" .

(iv) The VSWR characteristics of rudimentary horns are in general better than conventional V-antennas of comparable size.

2.5 Impedance Characteristics

Limited amounts of information regarding the impedance variation of rudimentary horn antenna may be obtained from the VSWR results given in the previous sections. In this section we discuss the impedance properties of the asymmetrical configuration model 9-5C over the frequency band 1 - 10 GHz. This particular model has been chosen for the present investigation because of the fact that the full scale dimensions of the antenna in the HF range correspond favorably with commonly used rhombic antennas for long range HF communication. The test antenna model 9-5C has the following dimensions (Fig. 2-1).

L = 24"
D = 5" .

The curvature of the radiating element is as given in Table II-1. The width of the radiating strip is 0.25" at the input end and it increases linearly to a value of 2" at the open end of the antenna For convenience the ground plane size has been chosen to be 11 1/2" x 24" .

The measured normalized impedance variation with frequency of the above rudimentary horn is given in the Smith Chart shown in Fig. 2-16. The reactive and resistive parts of the impedance of the antenna are shown as functions of frequency in Figs. 2-17 and 2-18 respectively. It has been found that the average impedance behavior of the antenna is a function of the particular transition section used in the feed system. A high frequency antenna used for long range communication purposes is the TAHA antenna (Tapered Aperture Horn Antenna) (Clark et al, 1959). The measured impedance variation of the TAHA antenna in the HF range is shown in Fig. 2-19. This result is included here for the purpose of comparison with the rudimentary horn results.

2.6 Radiation Characteristics

In this section the results of an experimental investigation of the radiation patterns of several rudimentary horn antenna configurations are discussed. All the patterns have been obtained by following the principle of model measurement, the model frequency being in the range 1 - 10 GHz. Following the usual practice the test models were used as receiving antennas during the measurement. Other important radiation characteristics like gain, sidelobe level, etc., have been obtained from the measured patterns and are also discussed below. As in the case of VSWR study here also more emphasis has been given to asymmetrical antennas.

2.6.1 Symmetrical Configurations

The only symmetrical rudimentary horn antenna to be considered here is the model 3, as shown in Figs. 2-1 and 2-3, whose design parameters are as given in Table II-2. The far field radiation patterns of the antenna in the E- and H-planes are shown in Figs. 2-20(a), (b), (c) for three selected frequencies. The 3 dB beamwidths of the E- and H-plane patterns of the rudimentary horn 3, as obtained from the measured patterns, are shown in Figs. 2-21(a) and (b) . It is found from these figures that the pattern is more directive in the H-plane. From the measured patterns the directive gain of the antenna has been calculated by using the following expression (Kraus, 1950):

$$D = 41,253/\theta_E \phi_H \quad ,$$

where θ_E and ϕ_H are the half-power beamwidths in degrees in the E- and H-planes respectively. The directive gain as a function of frequency for the rudimentary horn 3 is shown in Table II-4 . The actual gain of the antenna has also been measured by subsitution method and the results are shown in Table II-5.

2.6.2 Asymmetrical Configurations

The first asymmetrical rudimentary horn to be considered is the model 3G which uses a 36" x 14.5" ground plane and whose other design parameters are as given in Table II-2. The measured E- and H-plane patterns as a function of frequency in the range 1 - 10 GHz are shown in Fig. 2-22

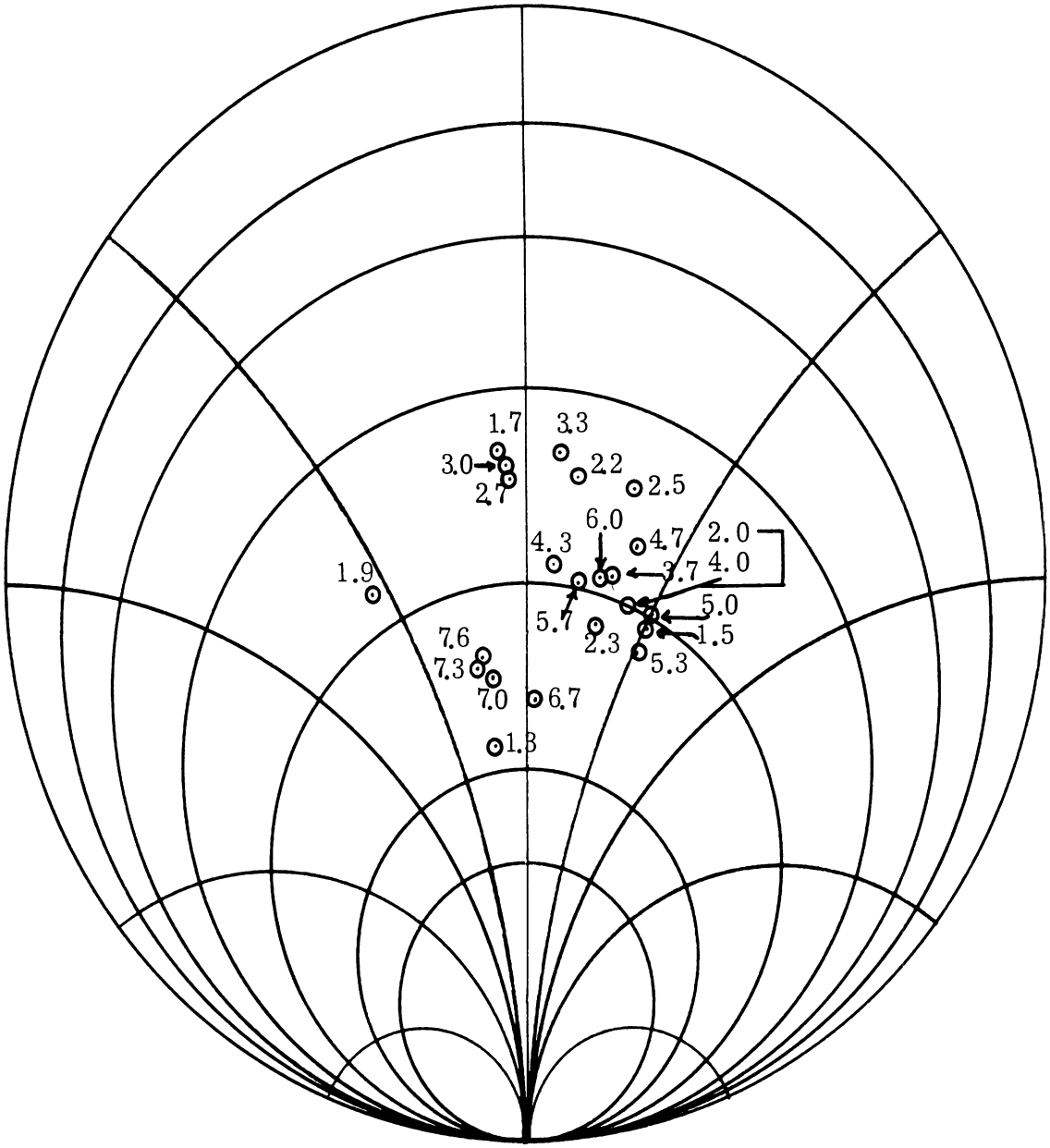

FIG. 2-16: NORMALIZED IMPEDANCE CHARACTERISTICS OF RUDIMENTARY HORN NO. 9-5C (Freq. = GHz).

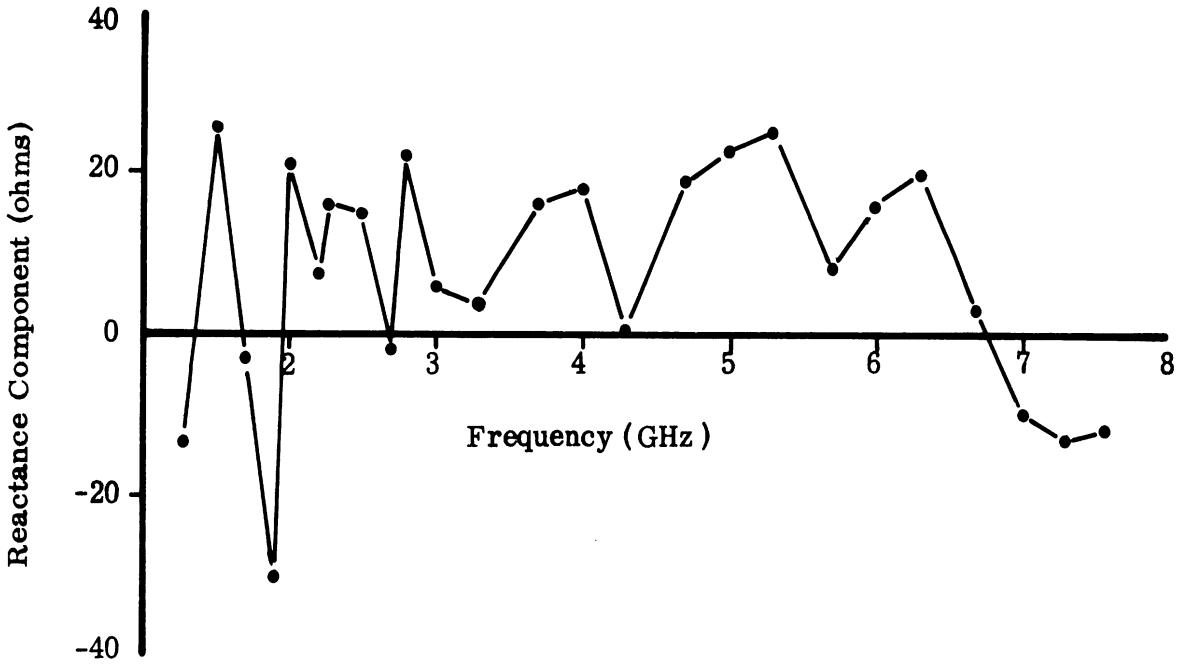

FIG. 2-17: INPUT REACTANCE OF RUDIMENTARY HORN NO. 9-5C AS A FUNCTION OF FREQUENCY.

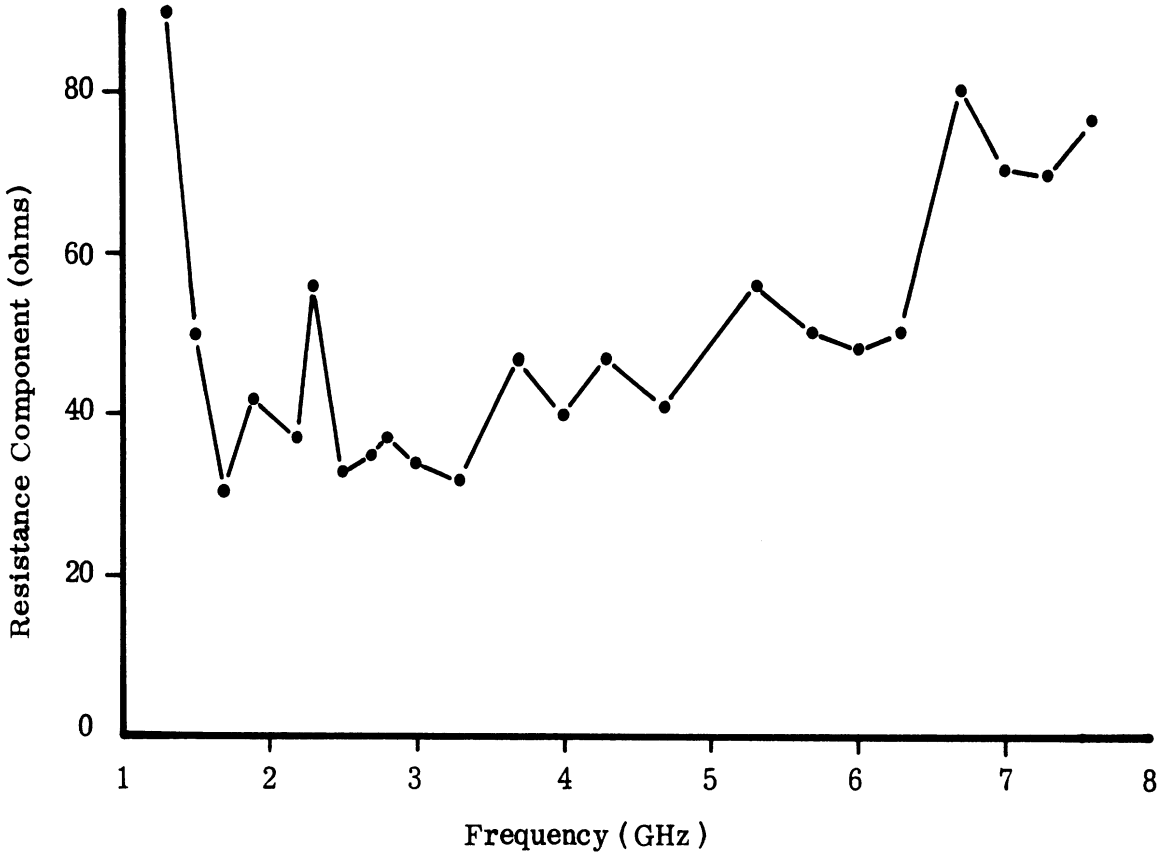

FIG. 2-18: INPUT RESISTANCE OF RUDIMENTARY HORN NO. 9-5C AS A FUNCTION OF FREQUENCY.

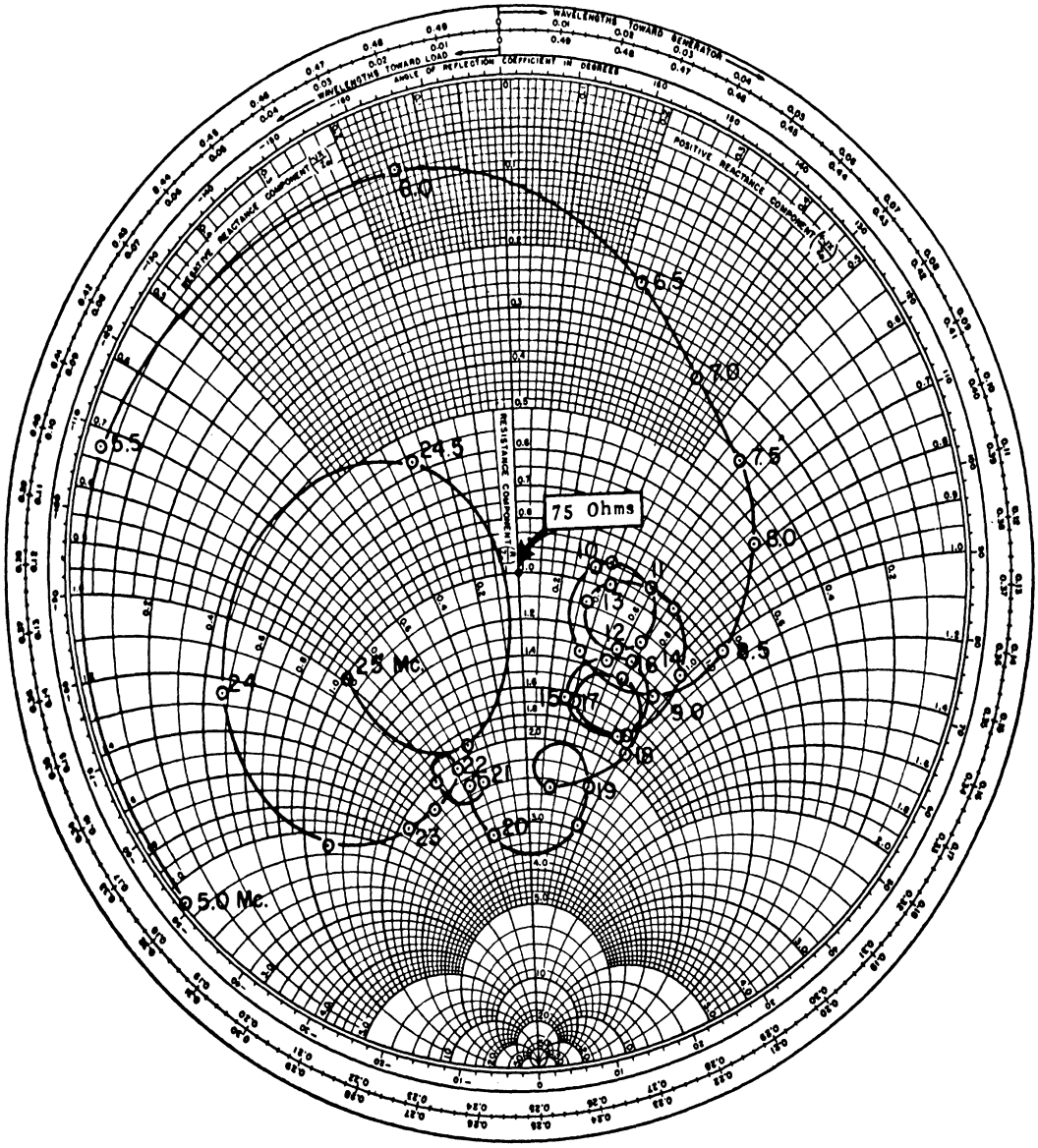

FIG. 2-19: MEASURED INPUT IMPEDANCE OF TAHA.

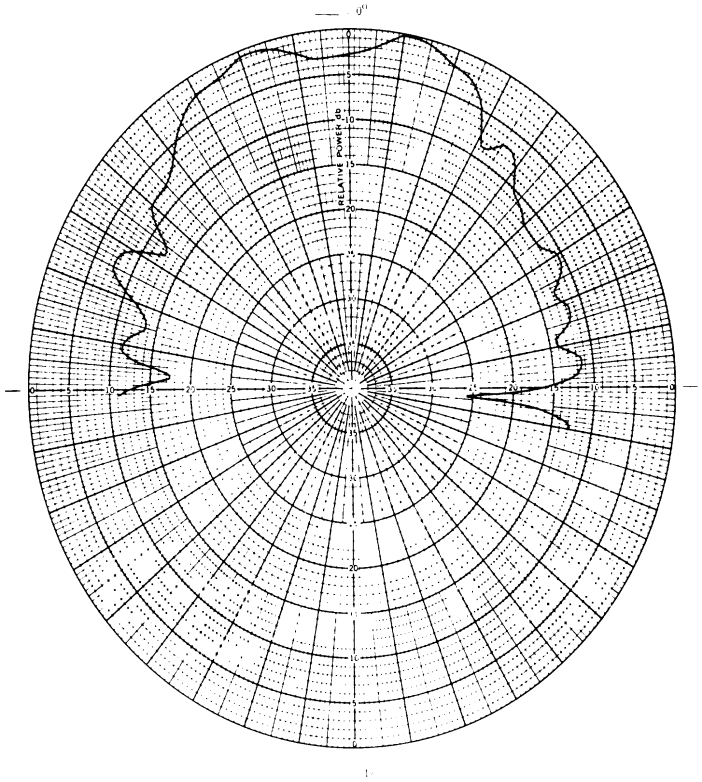

E-Plane

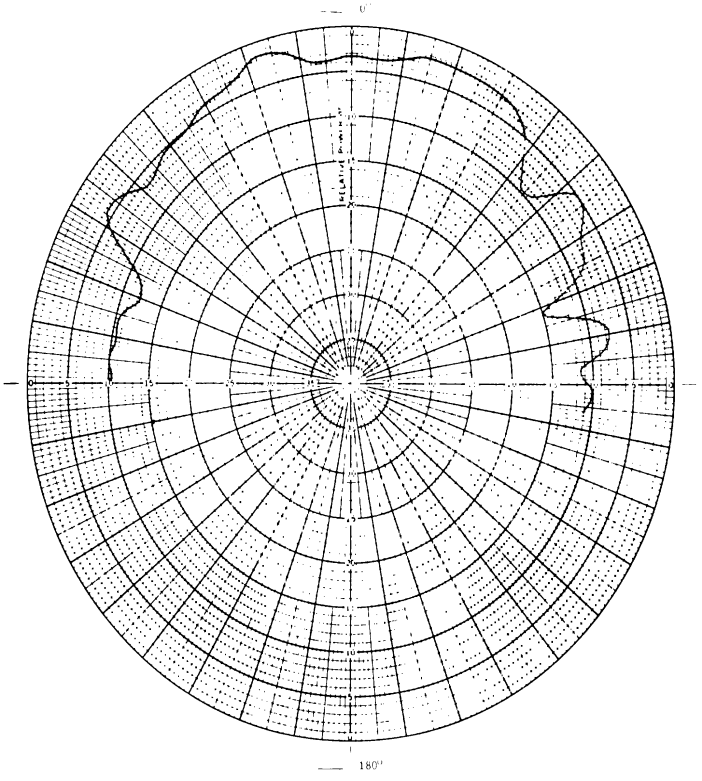

H-Plane

FIG. 2-20a: THE E- and H-PLANE RADIATION PATTERNS OF RUDIMENTARY HORN NO. 3 AT 1.0 GHz.

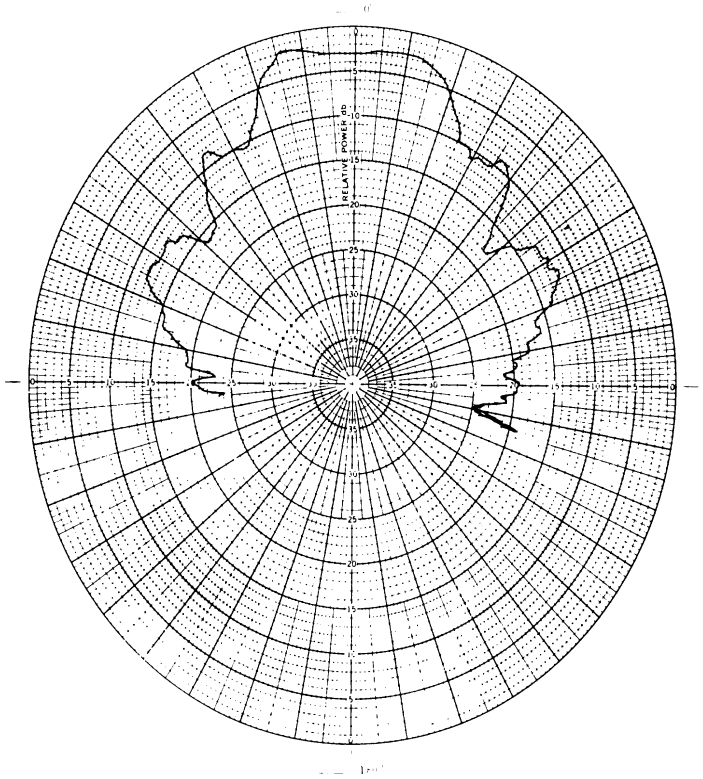

E-Plane

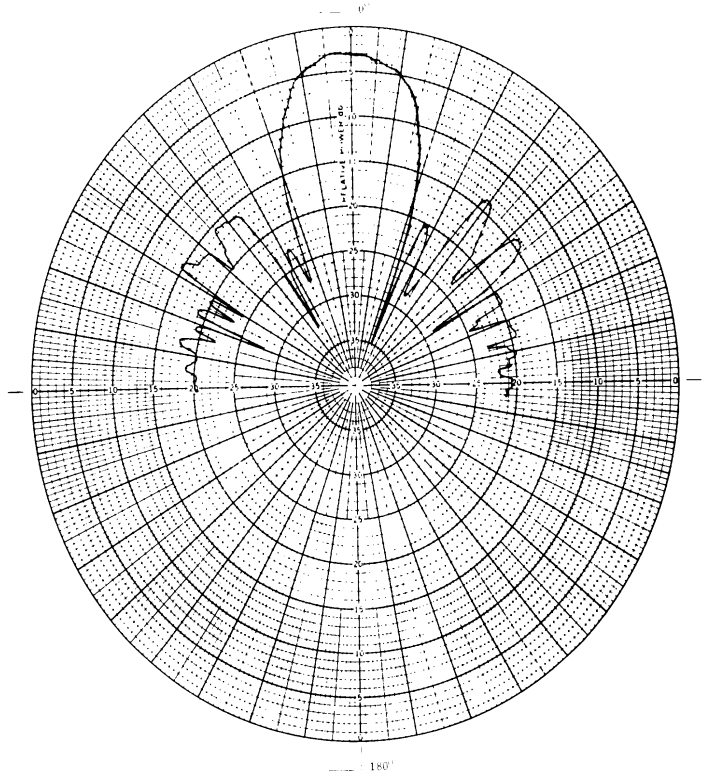

H-Plane

FIG. 2-20b: THE E- and H-PLANE RADIATION PATTERNS OF RUDIMENTARY HORN NO. 3 AT 4.0 GHz.

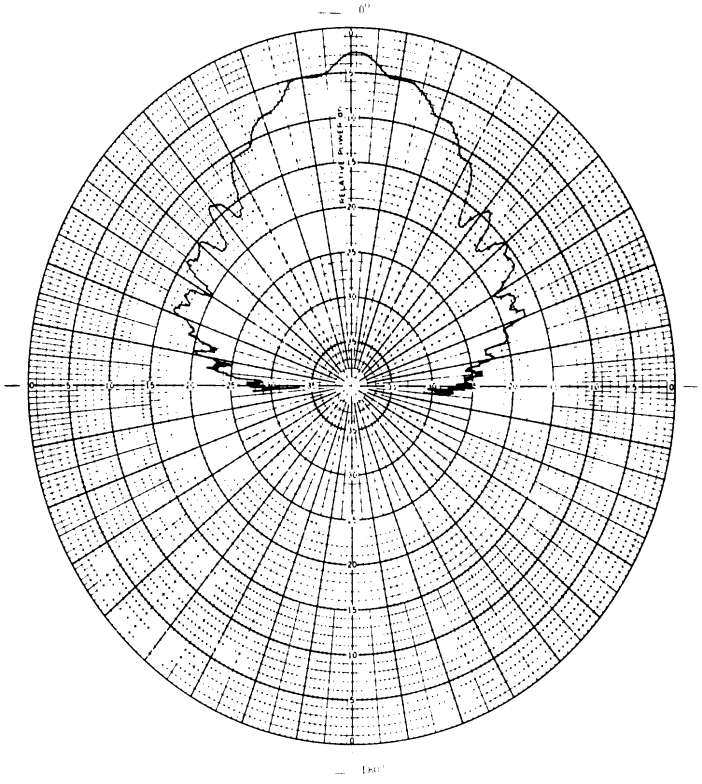

E-Plane

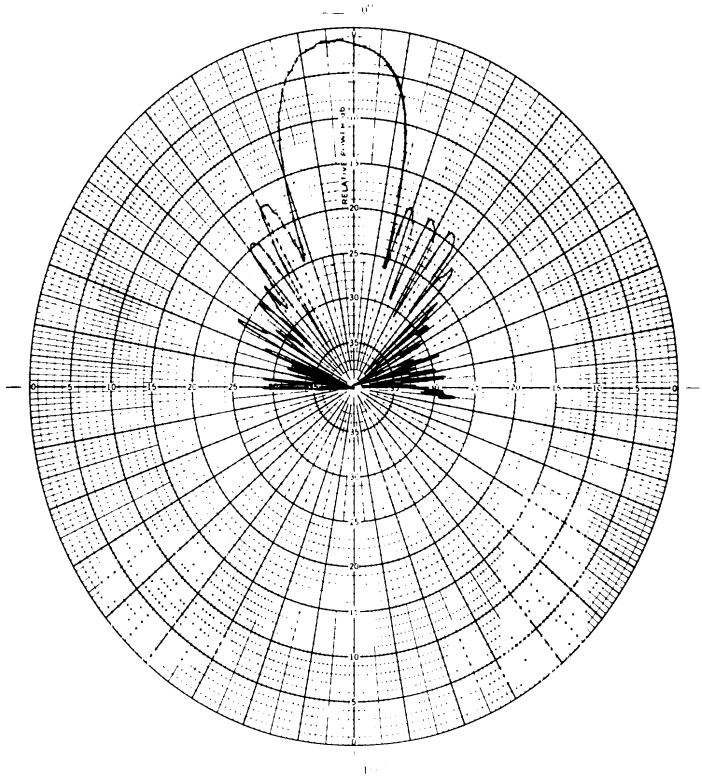

H-Plane

FIG. 2-20c: THE E- and H-PLANE RADIATION PATTERNS OF RUDIMENTARY HORN NO. 3 AT 8.0 GHz.

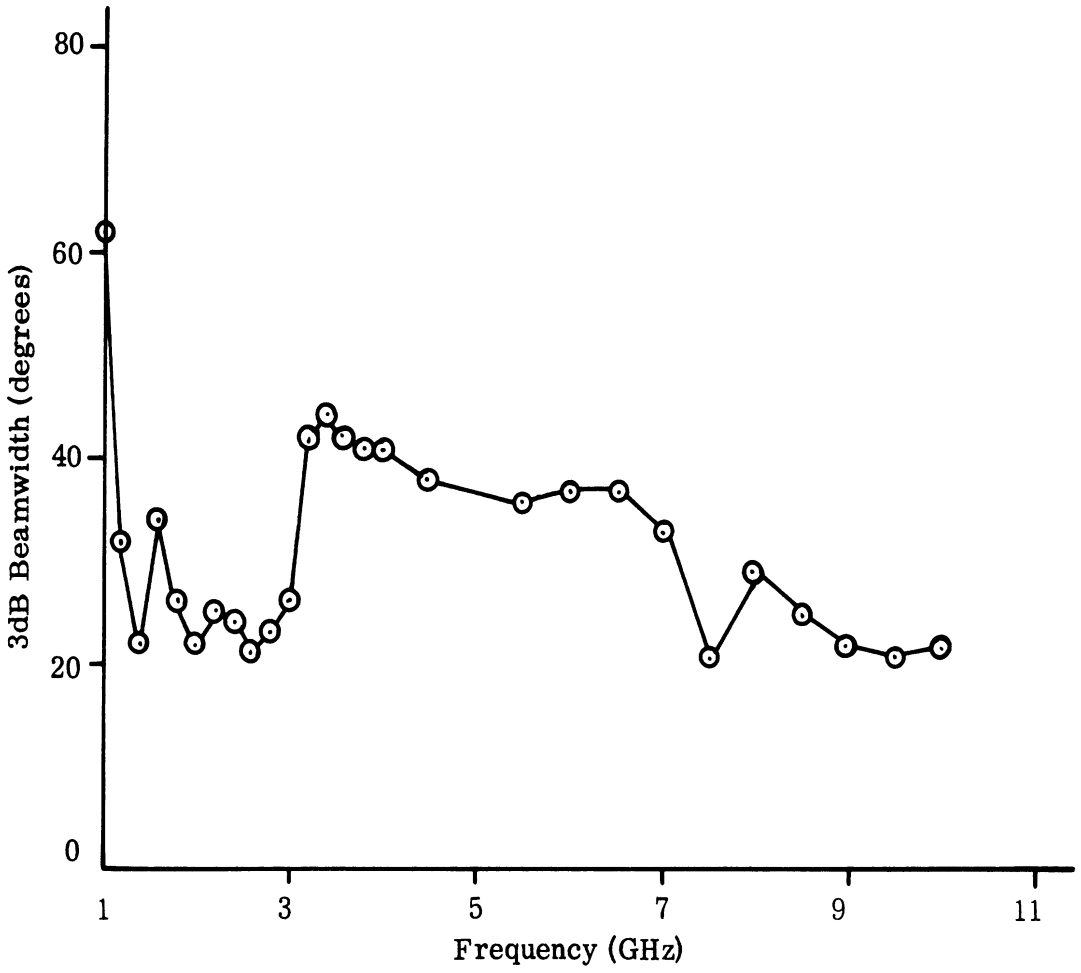

FIG. 2-21a: E-PLANE HALF POWER BEAMWIDTH (θ_3) AS A FUNCTION OF FREQUENCY FOR RUDIMENTARY HORN NO. 3.

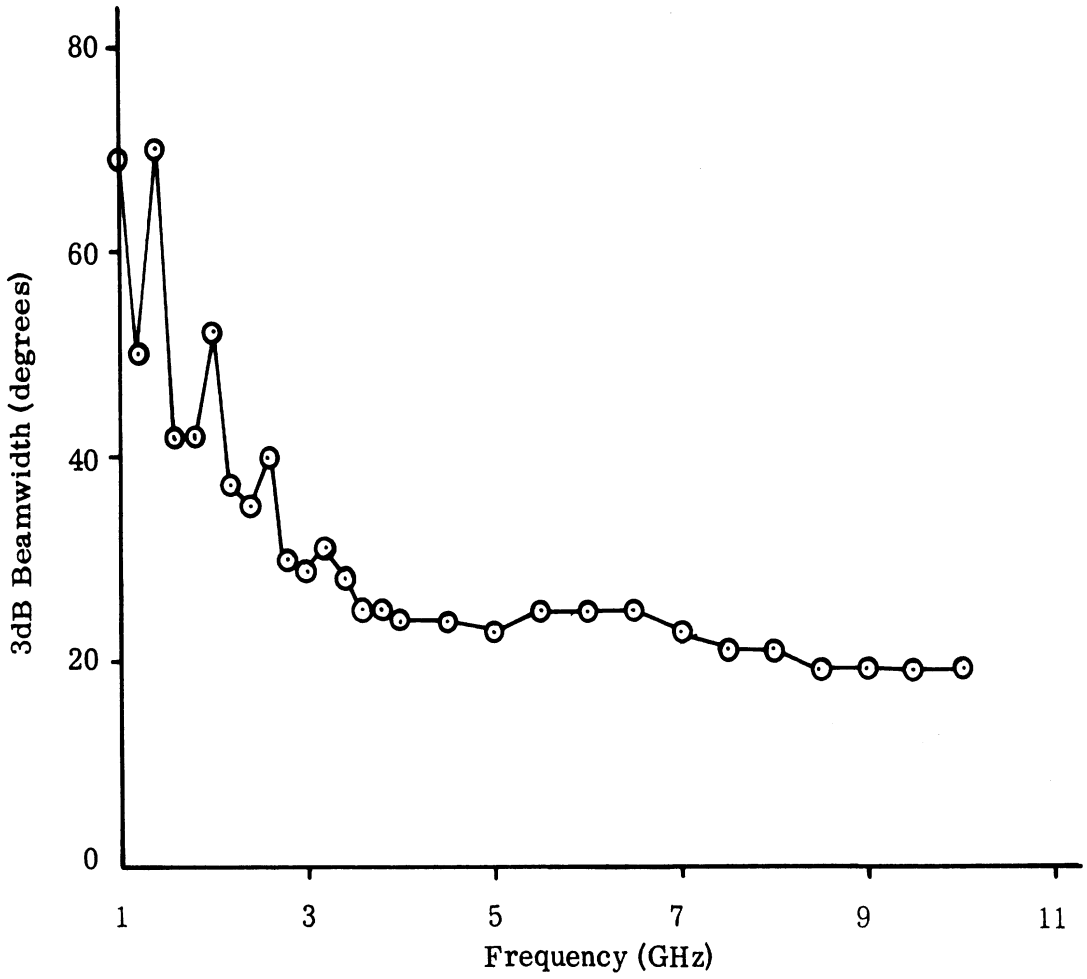

FIG. 2-21b: H-PLANE HALF POWER BEAMWIDTH (ϕ_3) AS A FUNCTION OF FREQUENCY FOR RUDIMENTARY HORN NO. 3.

TABLE II-4: RUDIMENTARY HORN NO. 3 DIRECTIVITY RELATIVE TO AN ISOTROPIC SOURCE

Frequency (GHz)	Directivity (dB)
1.0	9.8
2.0	17.6
3.0	17.2
4.0	16.1
5.0	16.8
6.0	16.5
7.0	17.3
8.0	18.5
9.0	20.1
10.0	19.9

$\text{Dir} = 10 \log \frac{41,253}{\theta_3 \phi_3}$, where θ_3 is from Fig. 2-21(a) and ϕ_3 from Fig. 2-21(b) .

TABLE II-5: RUDIMENTARY HORN NO. 3 GAIN RELATIVE TO AN ISOTROPIC SOURCE

Frequency (GHz)	Gain (dB)
1.2	7.0
2.2	12.3
3.0	10.8
4.0	10.6
5.0	12.6
6.0	12.5
7.0	14.4
8.0	14.6
9.0	16.2
10.0	15.5

The patterns shown in Fig. 2-22 are plotted in dB. Although the details of the patterns are lost, the results given here may be found useful in studying the general behavior of the patterns as the frequency is varied. Table II-6 gives the directive gain of the antennas as obtained from the measured patterns shown in Fig. 2-22. The variations of the E- and H-plane half-power beamwidths as a function of frequency are shown in Figs. 2-23 and 2-24 respectively.

Because of its potential interest to the sponsor, the effects of the ground plane size in the E-plane radiation patterns of antenna 3G have been studied in more detail. Ideally with an infinite ground plane the maximum in the pattern should be directed in the forward direction along the ground plane, i.e. in the direction of positive x-axis in Fig. 2-2. However, due to the finiteness of the gound plane the beam is tilted upward. The E-plane half-power beamwidth and the beam tilt of the antenna model 3G as functions of frequency and the ground plane size are shown in Table II-7. The two circular ground planes used have 4' and 15' diameters. In general it can be concluded from a study of Table II-7 that larger ground plane produces narrower beam and lowers the beam tilt.

The E- and H-plane radiation patterns of rudimentary horn model 5A as a function of frequency are shown in Fig. 2-25. The general behavior of the pattern is found to be similar to that of model 3G.

It was mentioned in section 2.4.2 that two sets of measurements were taken with antenna models 7 and 7C in order to ascertain the effects of constant and variable width radiating elements on the VSWR characteristics. Similar measurements have been performed to determine their effects on the radiation patterns. It has been found that tapering the radiating element width does not appreciably change the beamwidths of the patterns. However, it effects the front-to-back ratio of the pattern considerably. To study this effect, the rudimentary horn model 7 has been investigated more carefully. For this purpose model 7 was modified by linearly increasing the width of the radiation strip towards the open end. These models are numbered 7A, 7B, 7C and 7D depending on the amount of such tapering used. All these models have the width of the radiating element w = 0.250" at the input end and the following widths at the open end:

7A	6"
7B	4"
7C	2"
7D	1"

The front-to-back ratio in dB as obtained from the measured E-plane patterns of the above models are shown in Table II-8 which clearly indicates that the back radiation from the antenna can be considerably reduced by following this technique.

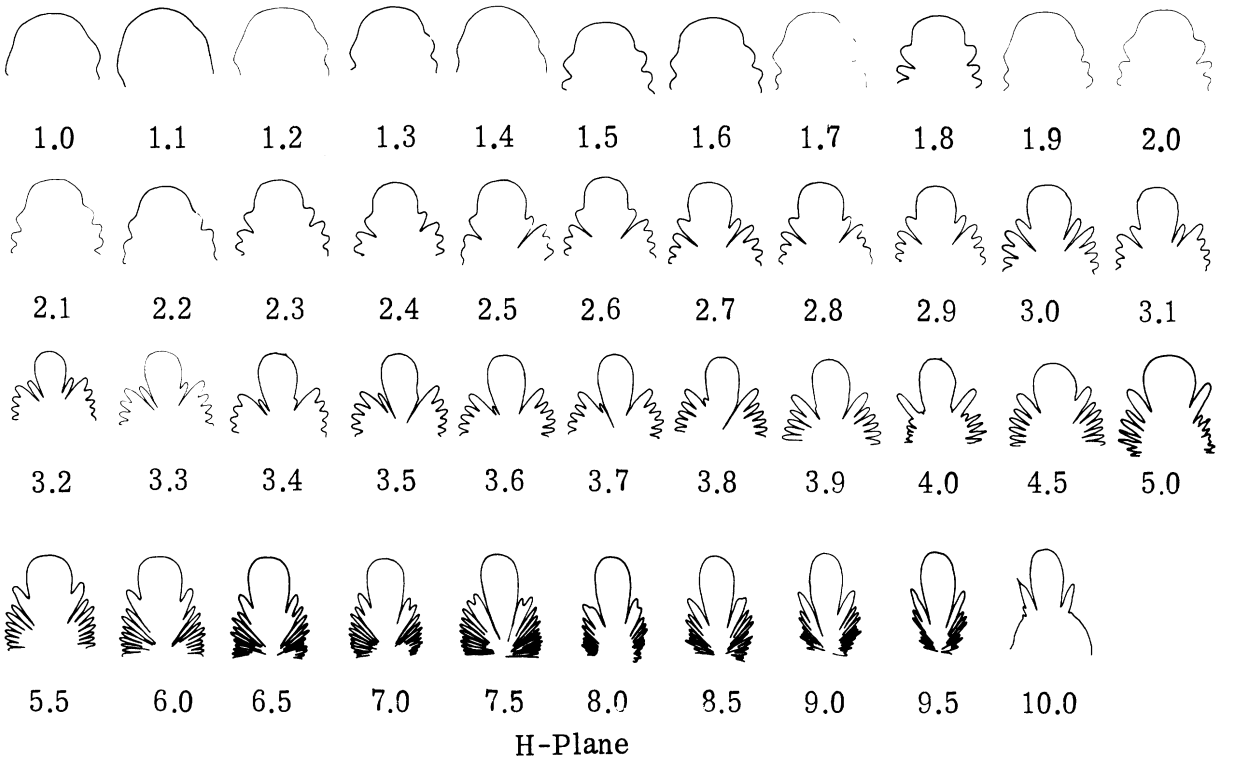

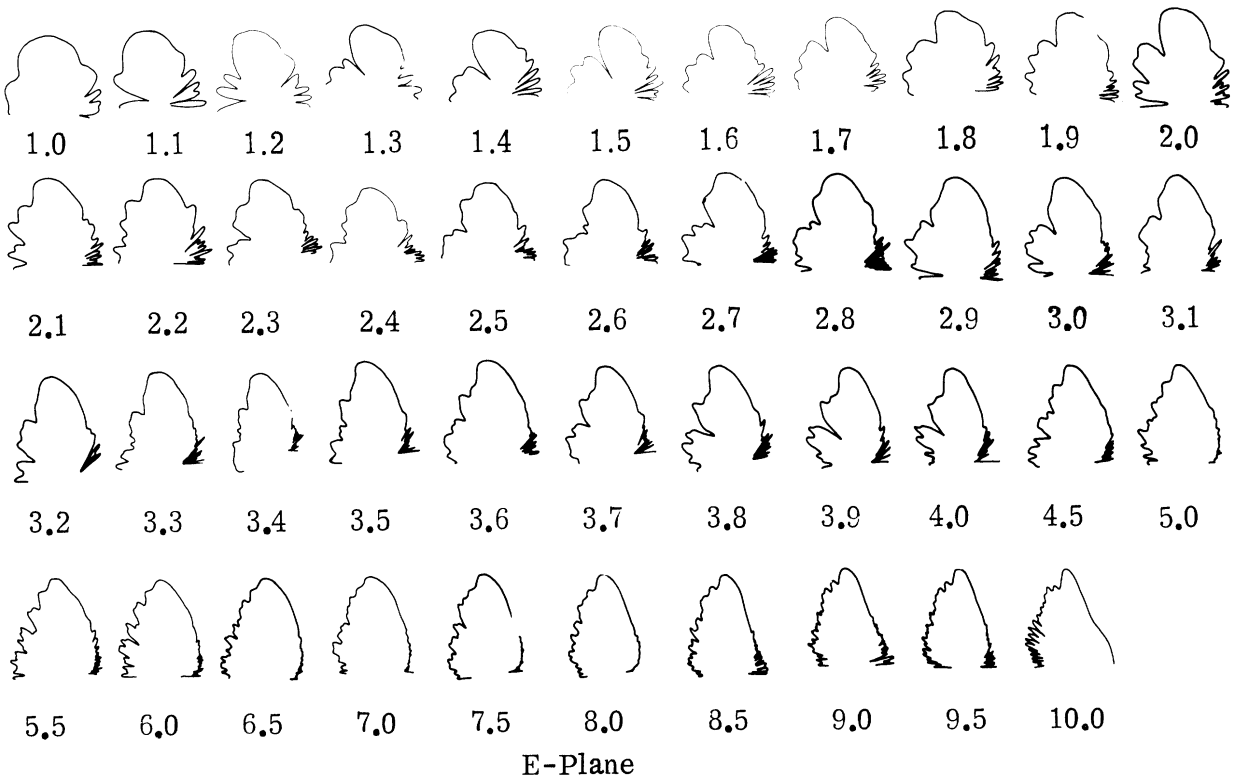

FIG. 2-22: THE RADIATION PATTERN CHARACTERISTICS OF RUDIMENTARY HORN NO. 3G AS A FUNCTION OF FREQUENCY.

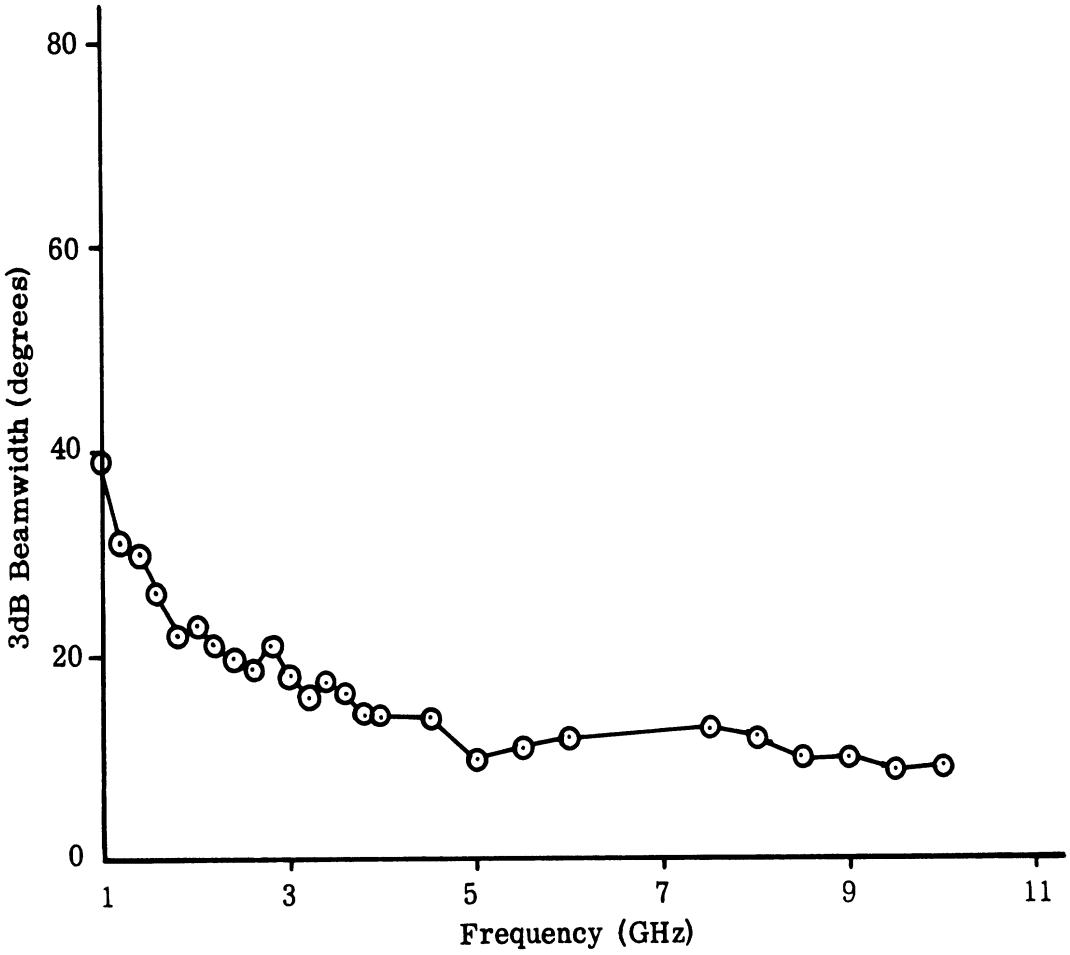

FIG. 2-23: E-PLANE HALF POWER BEAMWIDTH (θ_3) AS A FUNCTION OF FREQUENCY FOR RUDIMENTARY HORN NO. 3G.

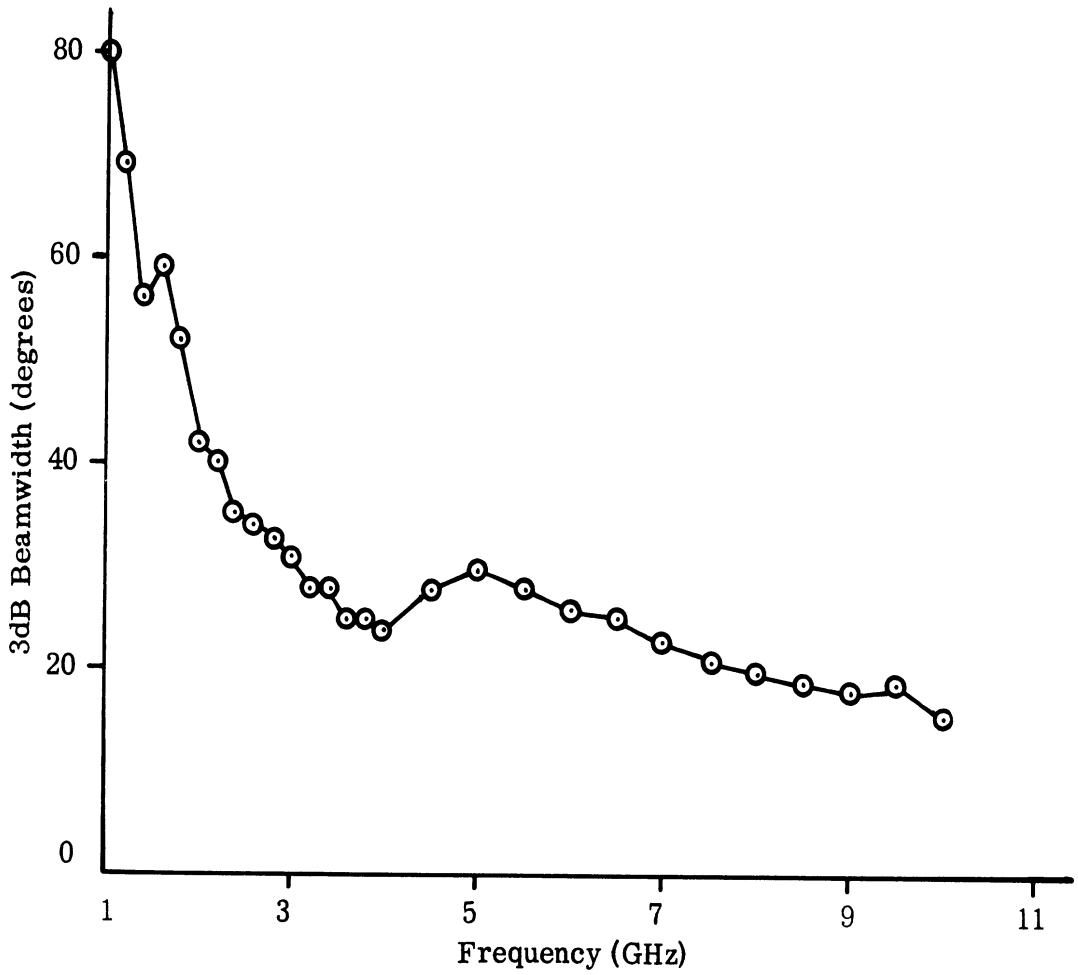

FIG. 2-24: H-PLANE HALF POWER BEAMWIDTH (ϕ_3) AS A FUNCTION OF FREQUENCY FOR RUDIMENTARY HORN NO. 3G.

TABLE II-6: RUDIMENTARY HORN NO. 3G DIRECTIVITY RELATIVE TO AN ISOTROPIC SOURCE

Frequency (GHz)	Directivity (dB)
1.0	11.1
2.0	16.9
3.0	18.5
4.0	20.9
5.0	21.3
6.0	21.2
7.0	21.7
8.0	22.3
9.0	23.3
10.0	24.5

$\text{Dir} = 10 \log \frac{41,253}{\theta_3 \phi_3}$, where θ_3 is from Fig. 2-23 and ϕ_3 from Fig. 2-24 .

TABLE II-7: E-PLANE HALF-POWER BEAMWIDTH AND BEAM TILT AS FUNCTIONS OF GROUND PLANE SIZE AND FREQUENCY FOR ANTENNA No. 3G.

Frequency GHz	3 dB Beamwidth (deg.)		Beam Tilt (deg.)	
	4' Ground Plane	15' Ground Plane	4' Ground Plane	15' Ground Plane
1.3	27	17	25	16
1.5	26	16	18	15
1.7	23	15	18	14
1.9	24	13	18	13
2.0	24	12	16	13
2.2	22	12	17	12
2.3	19	11	16	12
2.5	19	11	17	12
2.7	18	11	17	11
2.8	20	10	16	11
3.0	17	11	16	12
3.5	-	17	-	12
5.0	10	-	14	-
6.0	13	-	13	-
7.0	15	-	13	-
7.5	13	-	12	-
8.0	12	-	11	-

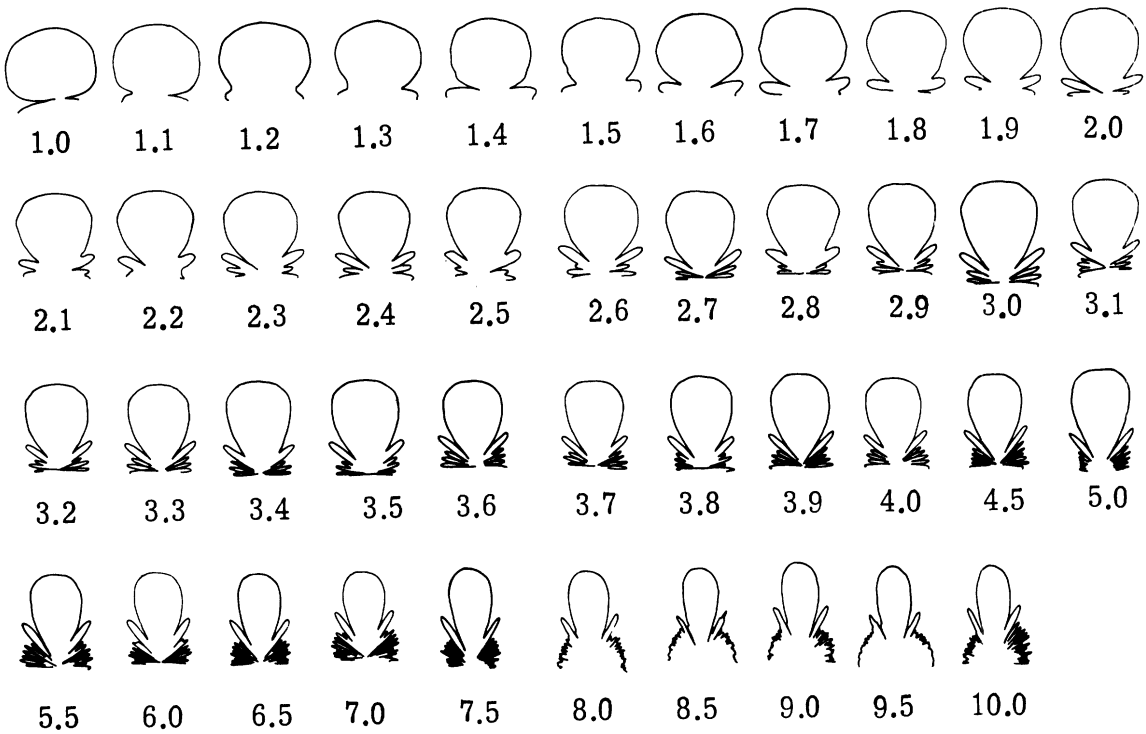

(H-Plane)

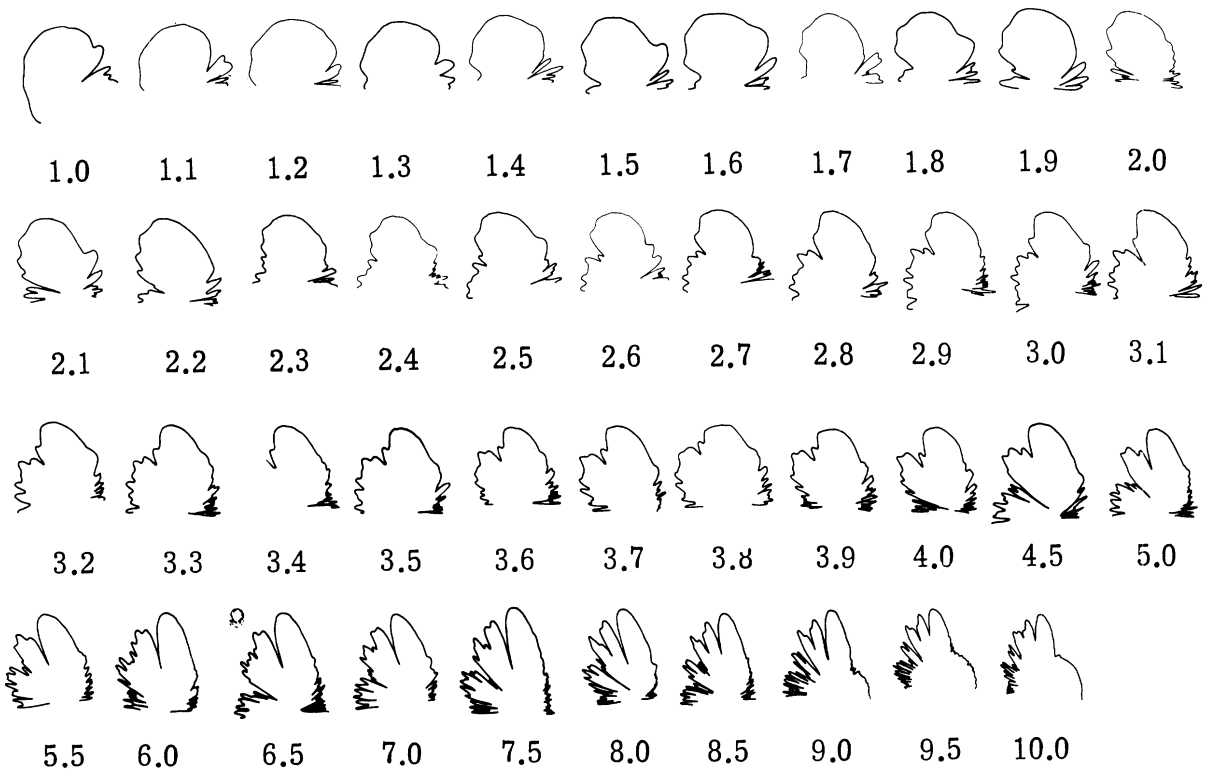

(E-Plane)

FIG. 2-25: THE RADIATION PATTERN CHARACTERISTICS OF RUDIMENTARY HORN NO. 5A AS A FUNCTION OF FREQUENCY.

TABLE II-8: FRONT-TO-BACK RATIO IN THE E-PLANE PATTERNS OF RUDIMENTARY HORN NO. 7 AS FUNCTIONS OF FREQUENCY AND ELEMENT WIDTH TAPERING . Values are expressed in dB.

Frequency (GHz)	7	7D	7C	7B	7A
1.3	2.5	4.7	6.3	8.8	14
1.5	3.0	5.2	7.3	10.4	11
1.7	4.5	5.3	7.7	10.1	10
1.9	5.5	7.5	9.6	-	12
2.0	4.0	6.5	9.1	12.0	12
2.2	3.5	6.8	9.1	17.0	14
2.3	4.5	8.0	11.4	16.4	14
2.5	3.5	6.0	10.1	11.0	9
2.7	6.0	10.4	14.8	19.1	16
2.8	6.0	11.0	13.1	14.8	14
3.0	6.5	12.0	16.4	16.4	20
3.3	-	12.0	18.4	16.4	20
3.5	7.5	-	-	-	-
3.7	-	11.7	18.4	14.8	14
4.0	5.3	10.4	12.0	17.7	18

TABLE II-9: E-PLANE FIRST AND SECOND SIDELOBE LEVELS IN THE PATTERNS OF ANTENNAS 9C AND 7C .

	9C				7C			
	1st Sidelobe		2nd Sidelobe		1st Sidelobe		2nd Sidelobe	
Freq. (GHz)	Ampl. (dB)	Pos. (°)	Ampl. (dB)	Pos. (°)	Ampl. (dB)	Pos. (°)	Ampl. (dB)	Pos. (°)
1.3	3.0	37	5.1	75	5.3	35	8.1	90
1.5	4.8	35	5.1	75	6.9	33	5.6	80
1.7	7.3	32	3.0	60	7.5	30	4.5	70
1.9	7.9	30	2.8	57	7.9	29	5.3	56
2.0	9.3	29	2.6	50	8.4	28	5.3	50
2.2	12.0	29	2.7	42	9.1	25	5.1	45
2.3	11.0	28	3.6	46	7.7	25	4.8	40
2.5	13.9	28	2.8	39	6.0	24	2.9	38
2.7	13.1	25	2.8	37	5.4	24	4.1	37
2.8	12.0	24	2.3	36	5.1	23	5.1	30
3.0	7.7	23	3.0	36	4.0	22	4.0	29
3.3	6.1	21	3.0	29	2.4	20	3.0	27
3.7	4.2	19	3.0	26	1.2	19	3.7	25
4.0	3.0	18	3.0	37	1.4	18	4.0	24

The first and second sidelobe levels in the E-plane patterns of antennas 7C and 9C as obtained from the measured patterns are shown in Table II-9. Test antenna model 9C consists of a compound structure whose radiating strip has exponential curvature up to a length of 10" and the rest of the length is linear. From a study of Table II-9 it may be concluded that the compound curvature tends to improve the first sidelobe characteristics but deteriorates slightly the second sidelobe characteristics. Over the frequency band 1.3 - 10 GHz the half-power beamwidths of the E-plane patterns of model 7C have been found to be slightly larger than those of model 7C. This is attributed to the larger length of model 9C.

2.6.3 Cross-Polarization Characteristics

Cross-polarization characteristics of the rudimentary horn model 5A have been investigated over the frequency band 1 - 10 GHz. The design parameters of the antenna are as shown in Table II-3 and the ground plane used has the dimensions 4' x 17.5" . Figures 2-26 through 2-28 show the H-plane patterns and the corresponding cross-polarized radiation patterns of the antenna at three selected frequencies. It has been found in general that the cross-polarized response is better than 30 dB down in the forward direction at all frequencies except at 1 GHz where the cross-polarized response is about 19 dB down. In other directions the maximum cross-polarized response has been found to be 5 dB down at 1 GHz and better than 10 dB down at other frequencies within the band.

2.6.4 Discussion

On the basis of the radiation pattern results given above we make the following observations:

(i) The antenna maintains its main beam shape over the band of frequencies 1 - 10 GHz. The H-plane patterns are sharper than the E-plane patterns.

(ii) The first sidelobe level and the front-to-back ratio in the E-plane patterns can be improved considerably by linearly increasing the width of the radiating strip toward the open end of the antenna.

(iii) The cross-polarization response is minimum in the forward direction and is about 30 dB down. In all other directions the response is higher and is about 10 dB down.

2.7 Measurement of the Antenna Current Distribution

In this section we give the results of an investigation performed to measure the amplitude distribution of currents on the radiating elements of a few selected rudimentary horn antennas. The measurements have been carried out by making use of the facility developed and designed previously at the Radiation Laboratory for the purpose of measuring the surface field on scattering bodies (Knott et al, 1965; Knott, 1965). A block diagram of the equipment for amplitude measurements is shown in Fig. 2-29. Descriptions of the complete experimental arrangement may

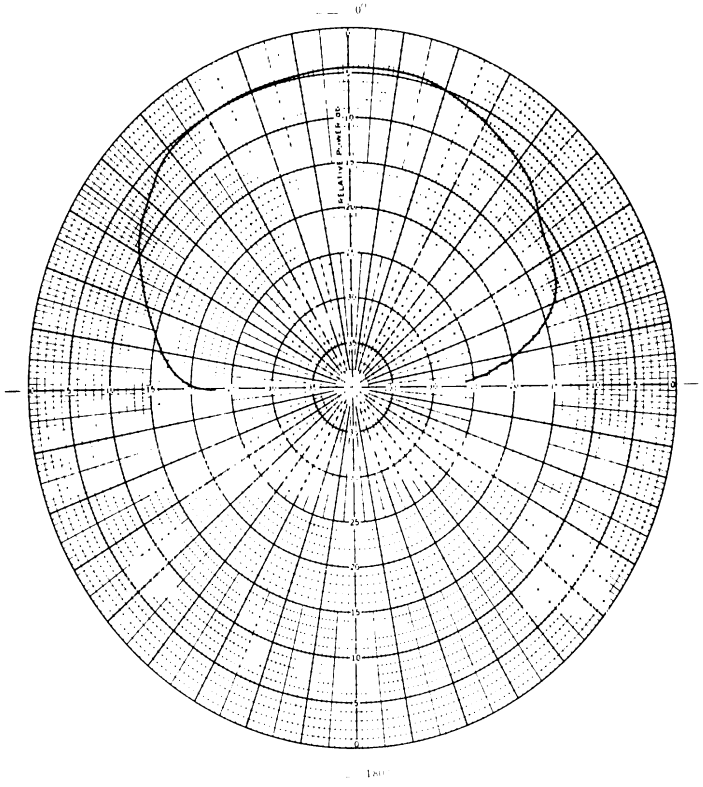

H-Plane

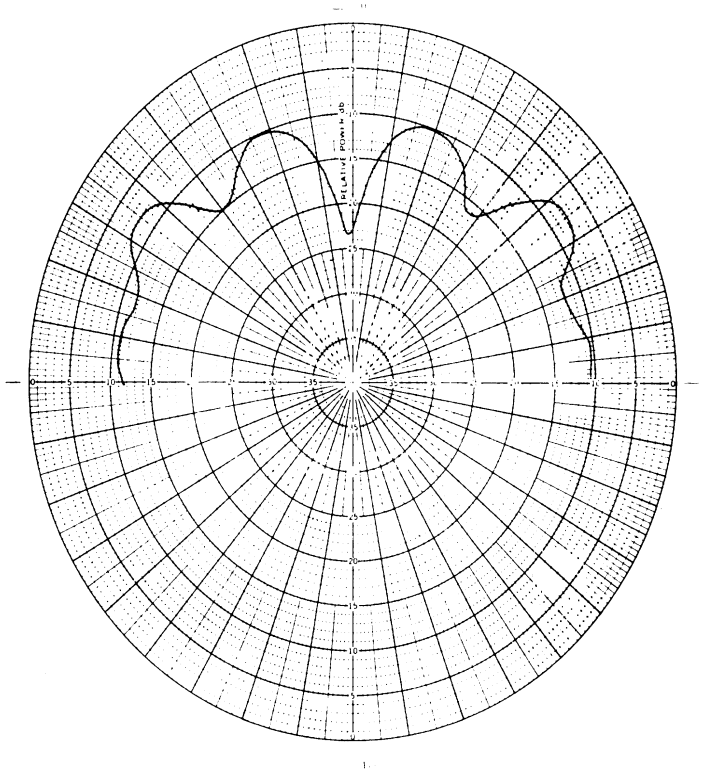

Cross-Polarized

FIG. 2-26: THE H-PLANE RADIATION PATTERN AND THE CORRESPONDING CROSS-POLARIZED PATTERN FOR ANTENNA NO. 3 AT 1 GHz.

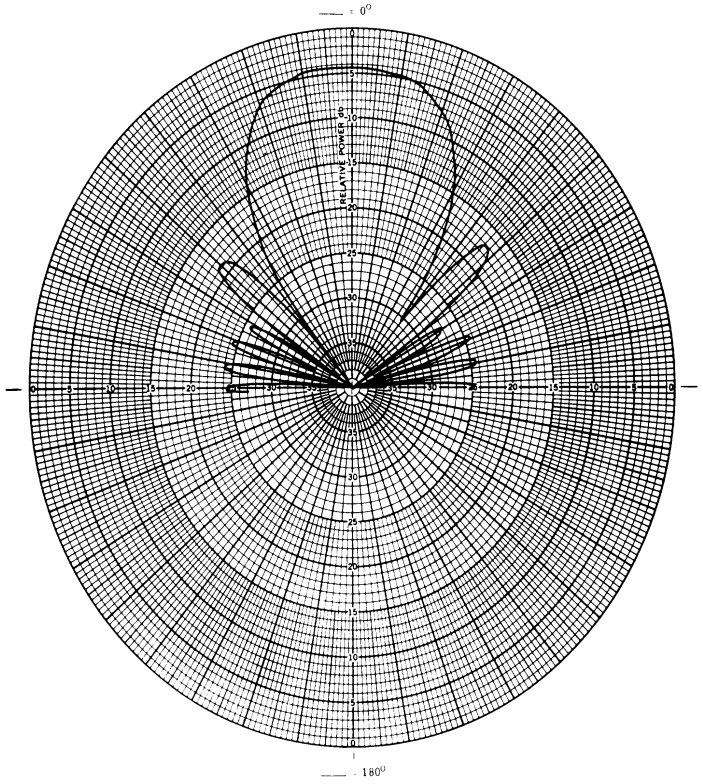

H-Plane

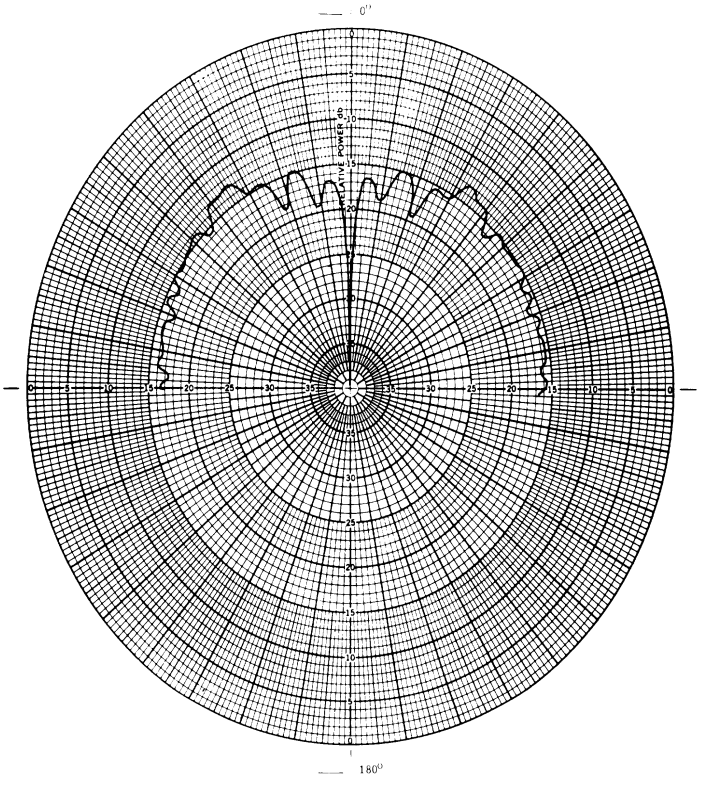

Cross-Polarized

FIG. 2-27: THE H-PLANE RADIATION PATTERN AND THE CORRESPONDING CROSS-POLARIZED PATTERN FOR ANTENNA NO. 3 AT 4.0 GHz.

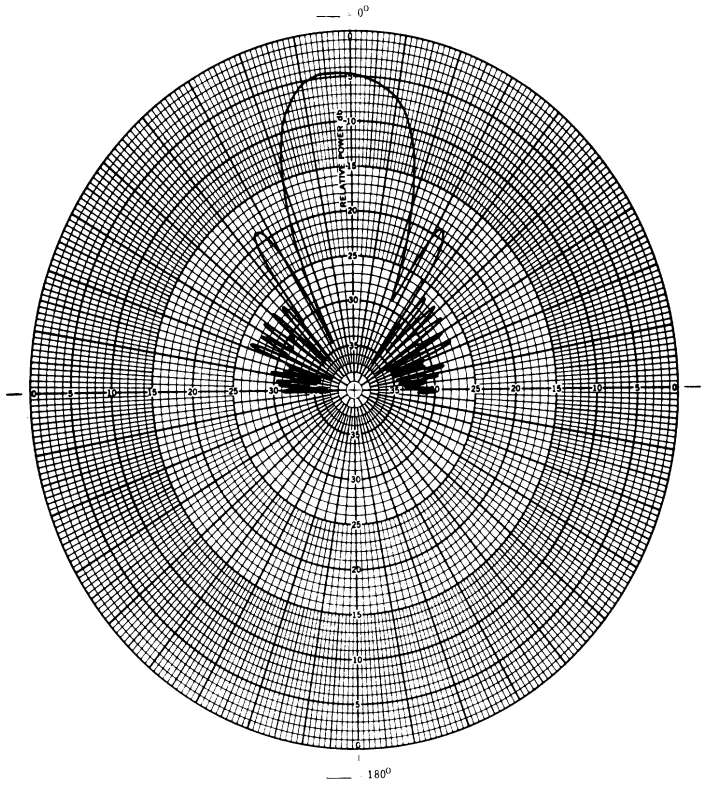

H-Plane

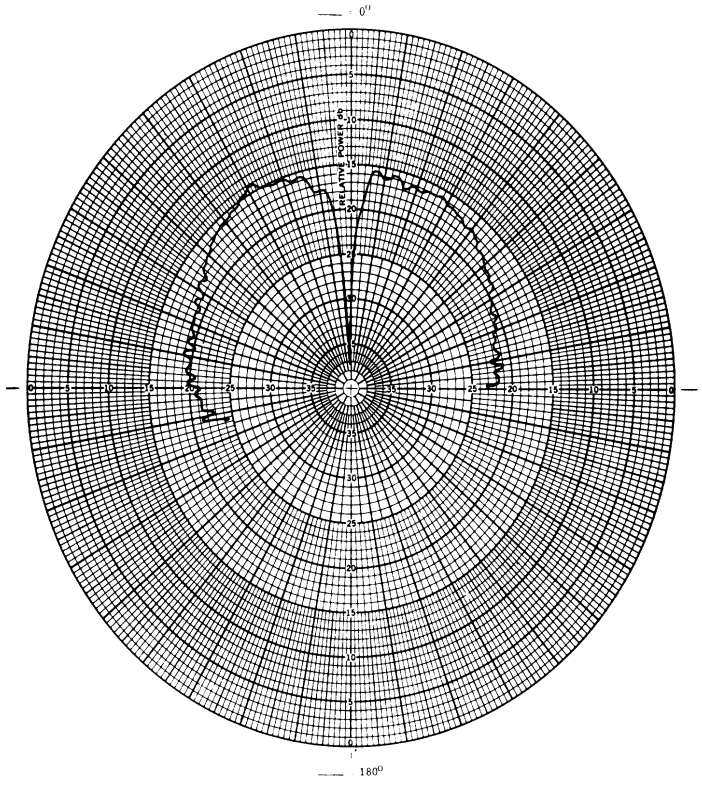

Cross-Polarized

FIG. 2-28: THE H-PLANE RADIATION PATTERN AND THE CORRESPONDING CROSS-POLARIZED PATTERN FOR ANTENNA NO. 3 AT 7.5 GHz.

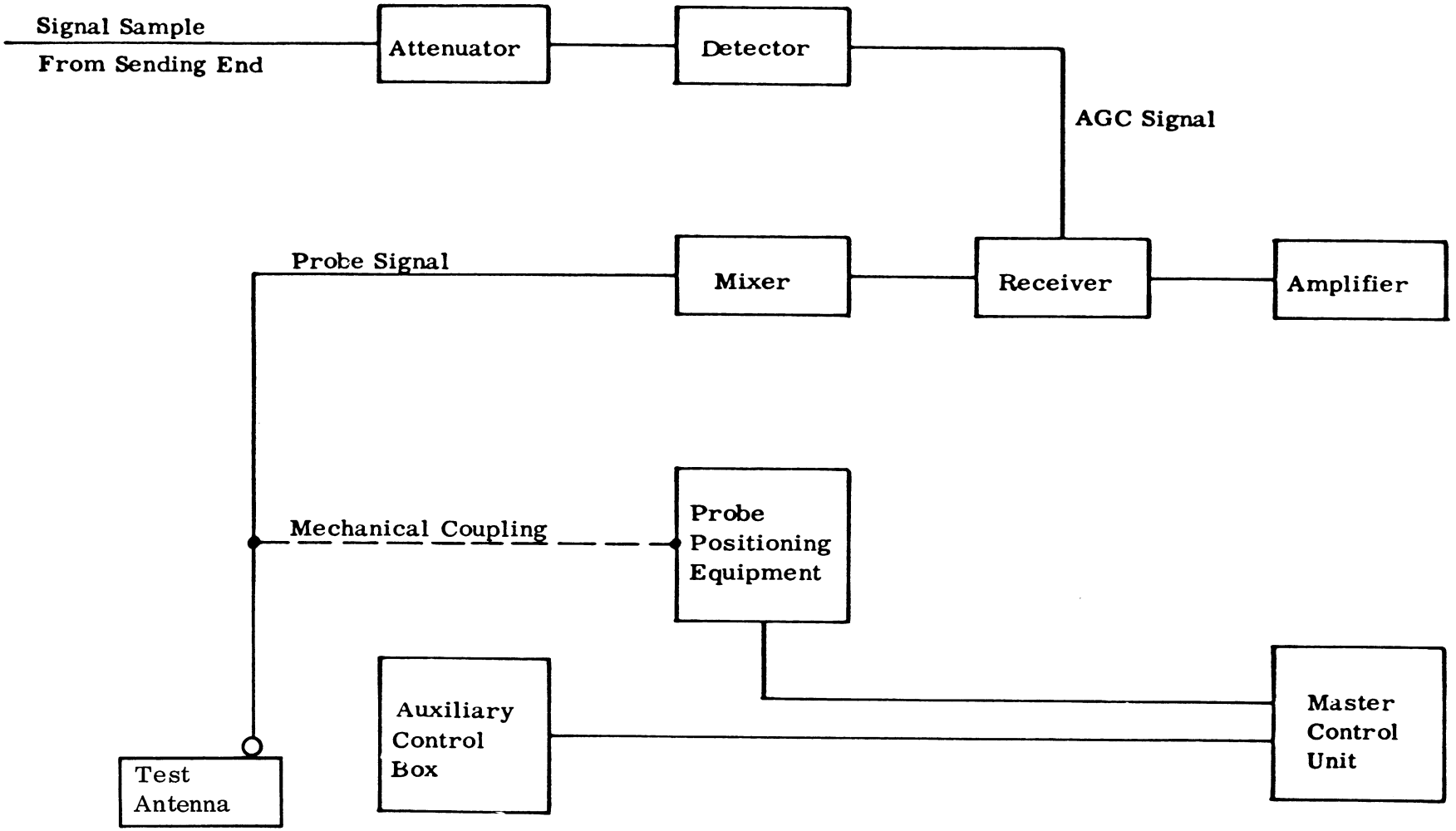

FIG. 2-29: BLOCK DIAGRAM OF THE EQUIPMENT FOR SURFACE CURRENT AMPLITUDE MEASUREMENTS.

be found in the report by Knott (1965) and will not be repeated here. With the help of this facility the amplitude of the current along a radiating element of a rudimentary horn has been measured at discrete points. The results presented here pertain to the relative amplitude distribution of currents at discrete points a distance ℓ from the input of the antenna and measured along the length of the radiating element.

Figures 2-30(a) - 2-30(d) show the measured amplitude distribution of current on the radiating element of the rudimentary horn model 3G for four selected frequencies. Similar results for the test antenna model 7 are shown in Figs. 2-31(a) and (b) .

The measured current distributions indicate the existence of standing waves. However, from a study of the amplitudes of the standing waves in Figs. 2-30 and 2-31 it may be seen that the reflected wave existing on the radiating element is of much lower amplitude than the forward traveling wave. The measurement has also been carried out with antennas having different length L and it has been found that for smaller L or towards the lower end of the frequency band (i. e. near 1 GHz), the standing waves become stronger in amplitude.

2.8 Concluding Remarks

In the present chapter we have discussed the results of elaborate experimental investigation of the VSWR and the radiation pattern characteristics of rudimentary horns having various configurations. The most important finding of this investigation is that the antenna appears to be capable of maintaining satisfactory performance over a wide band of frequencies both with respect to VSWR and radiation pattern performance. Many configurations of symmetrical and asymmetrical rudimentary horns have been considered in the above. The choice of a particular antenna will depend on the specific application for which they are considered. The antenna appears to be comparable in performance with other antennas commonly used for HF communication. More will be discussed about this in a later section.

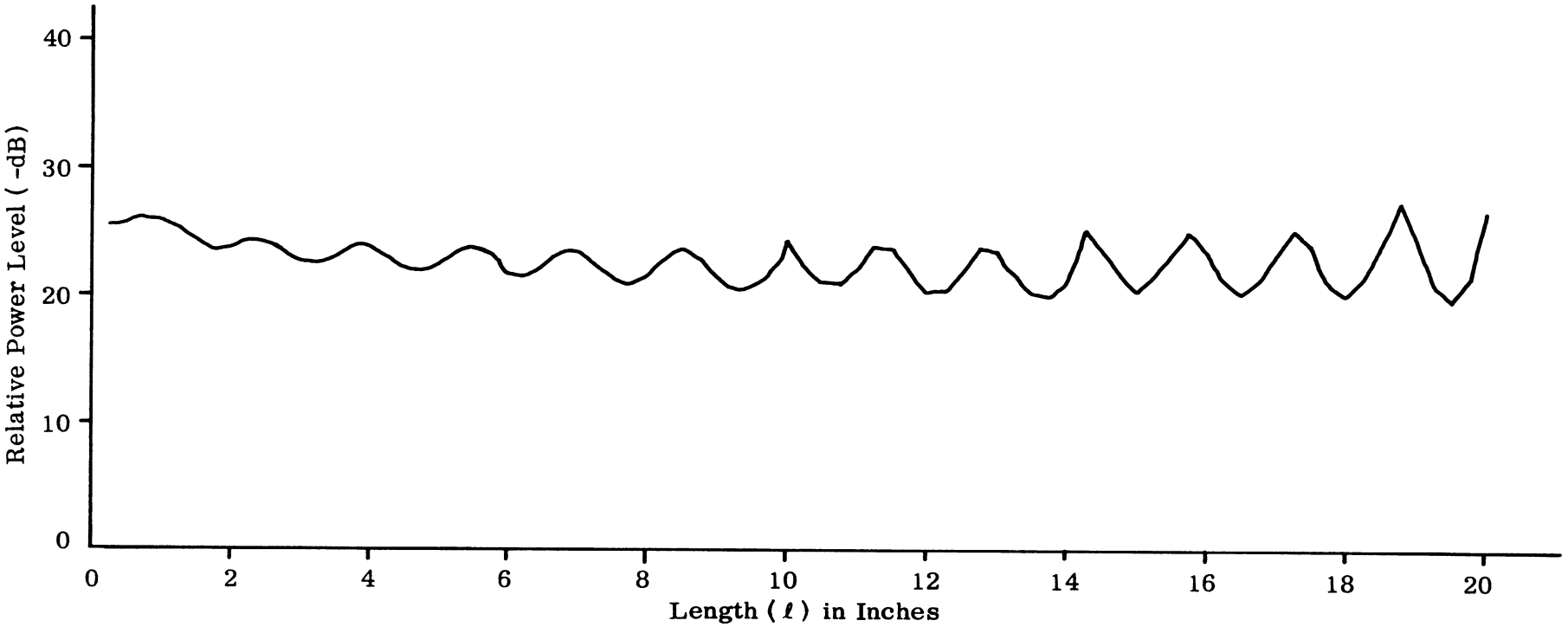

FIG. 2-30a: ELEMENT SURFACE CURRENT AMPLITUDE DISTRIBITION OF RUDIMENTARY HORN NO. 3G (4.0 GHz).

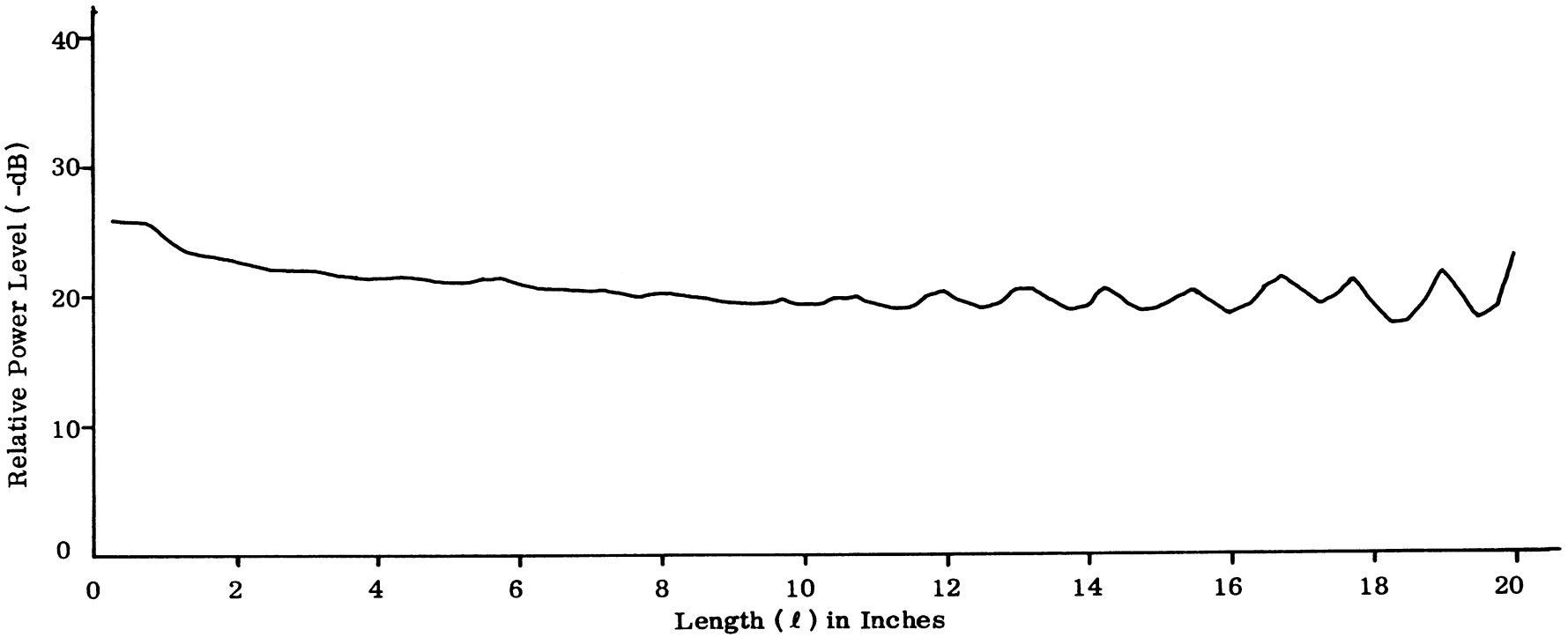

FIG. 2-30b: ELEMENT SURFACE CURRENT AMPLITUDE DISTRIBUTION OF RUDIMENTARY HORN NO. 3G (5.0 GHz).

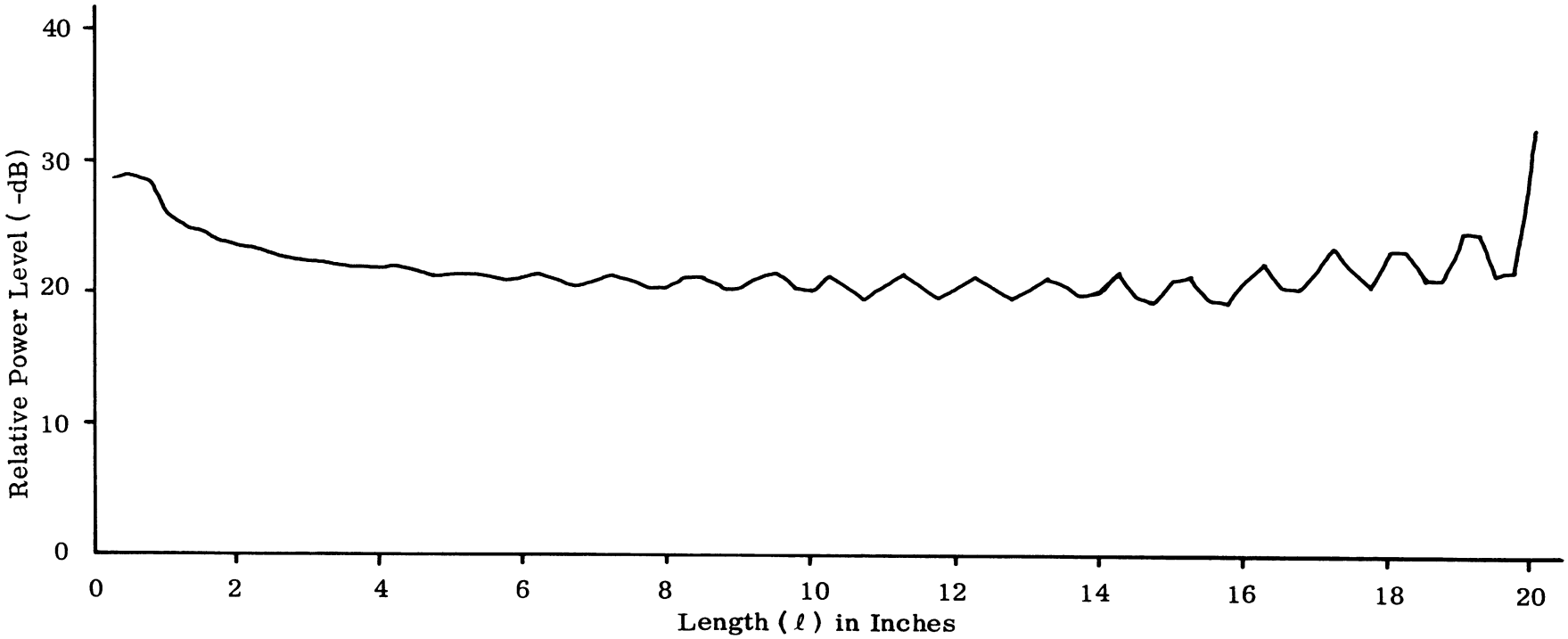

FIG. 2-30c: ELEMENT SURFACE CURRENT AMPLITUDE DISTRIBUTION OF RUDIMENTARY HORN NO. 3G (6.0 GHz).

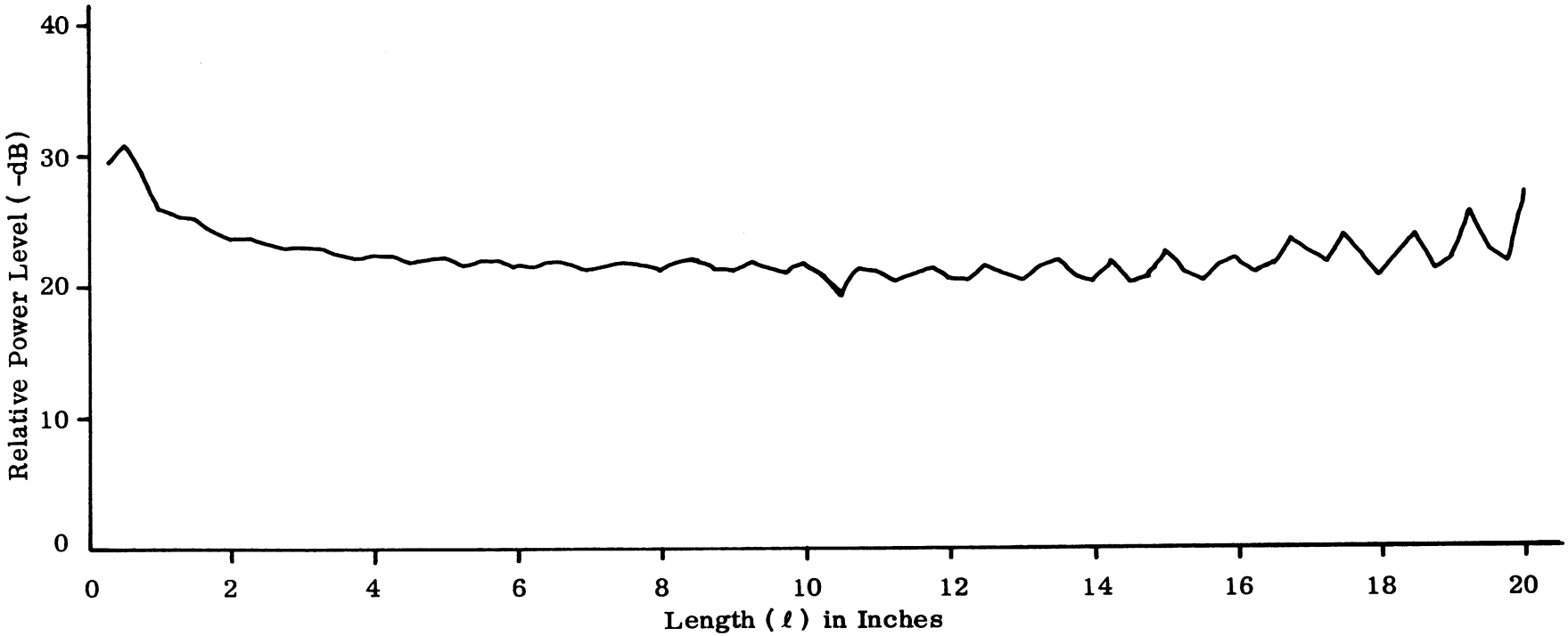

FIG. 2-30d: ELEMENT SURFACE CURRENT AMPLITUDE DISTRIBUTION OF RUDIMENTARY HORN NO. 3G (7.0 GHz).

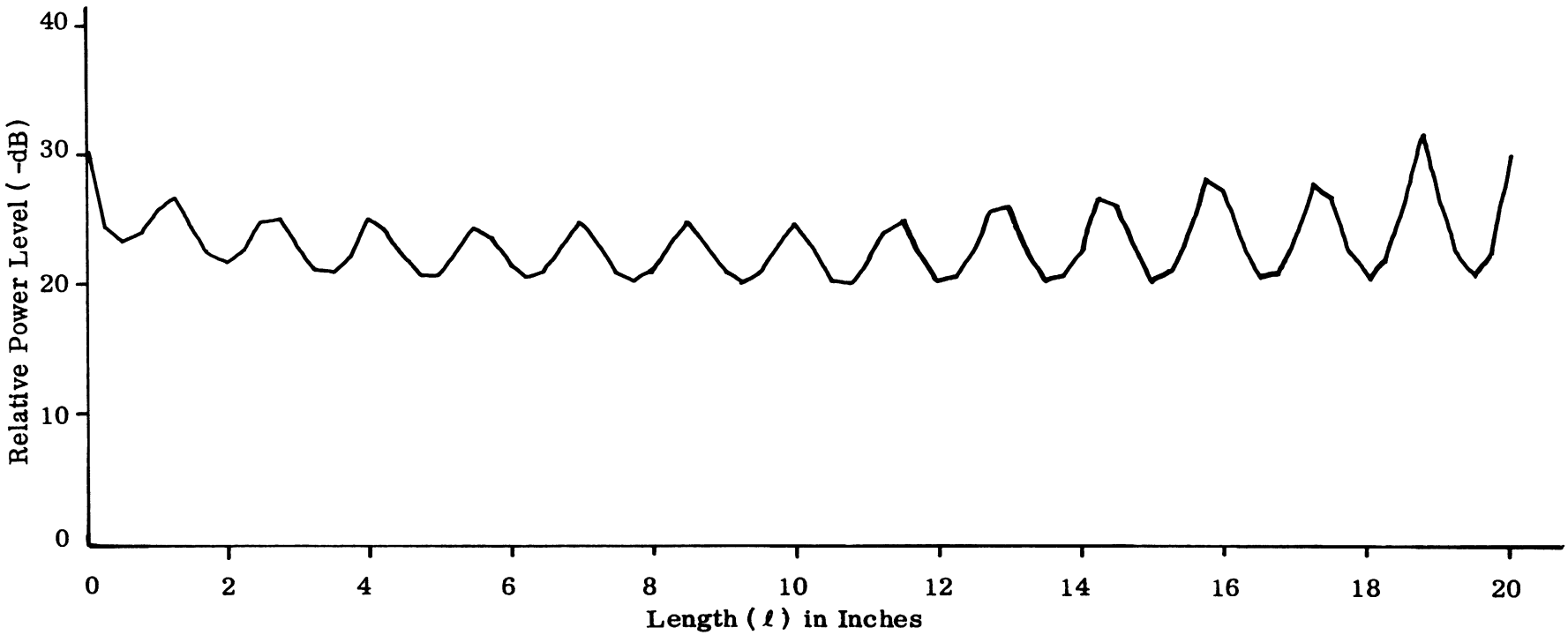

FIG. 2-31a: ELEMENT SURFACE CURRENT AMPLITUDE DISTRIBUTION OF RUDIMENTARY HORN NO. 7 (4.0 GHz).

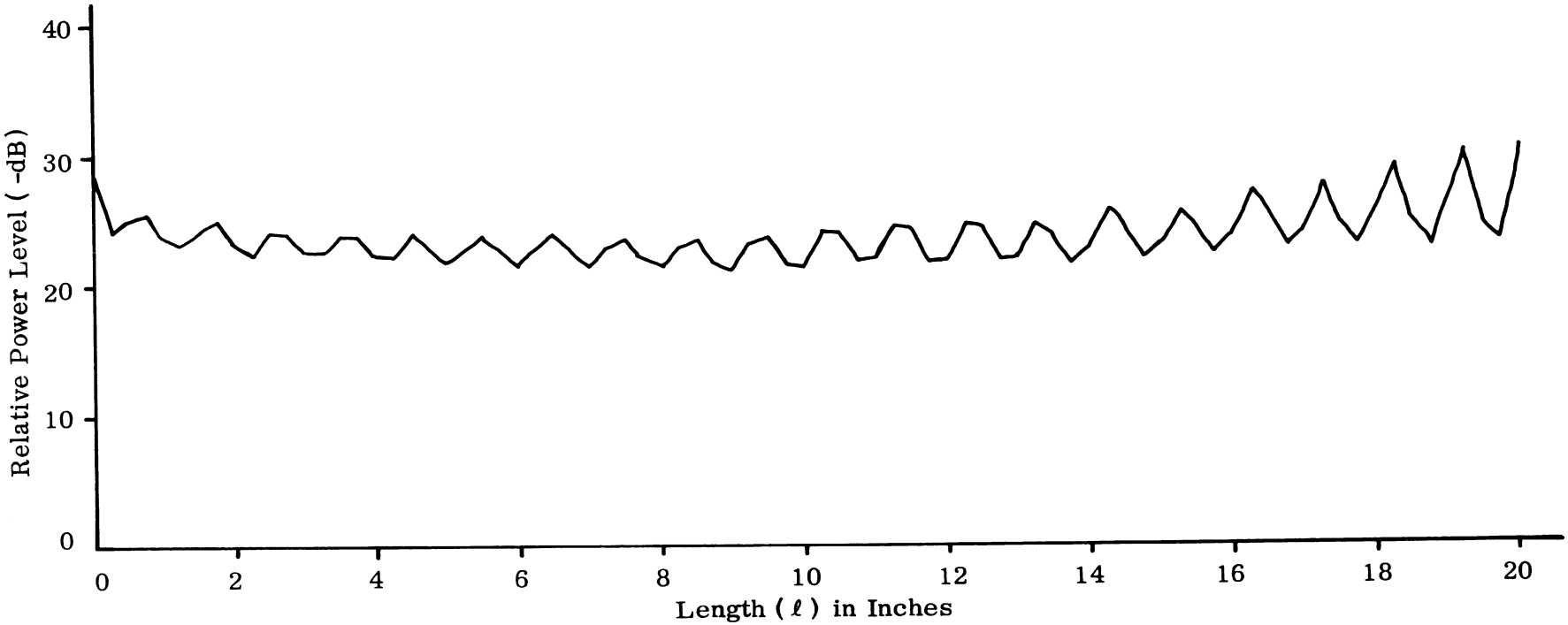

FIG. 2-31b: ELEMENT SURFACE CURRENT AMPLITUDE DISTRIBUTION OF RUDIMENTARY HORN NO. 7 (6.0 GHz).

III

THEORETICAL ANALYSIS

3.1 Introduction

In the present chapter an attempt is made to analyze theoretically the radiation field produced by a rudimentary horn antenna. Only the symmetrical configuration of the antenna has been considered for this purpose. The theory developed can be easily applied to the corresponding asymmetrical configuration having an infinite ground plane. The analysis for the case with a finite ground plane is quite difficult and will not be considered at this stage.

The theoretical investigation is carried out in two steps. In the first step we develop theoretical expressions for the radiation field of an exponentially tapered rudimentary horn when each arm carried a constant amplitude traveling wave of current. The propagation constant of the traveling wave is kept arbitrary at this stage of the analysis. The initial part of the analysis is kept general enough so that it may be applied to antennas having a more general type of curvature for its radiating elements. The exponential curvature has been considered here because it is believed to be of practical importance and also because it simplifies the analysis a great deal.

In the second step we analyze the propagation characteristics of a variable cross section strip transmission line and obtain an approximate expression for the propagation constant of the dominant traveling wave in the antenna.

Finally, the two results are combined to obtain the radiation field of a rudimentary horn antenna.

3.2 General Expressions for the Radiation Field

The first logical step in the analysis of the radiation field of a rudimentary horn antenna should be the determination of the current distribution on the radiating arms of the antenna. At this stage no attempt will be made to solve such a boundary value problem. In the following sections we derive general expressions for the radiation field of an exponentially tapered rudimentary horn carrying an assumed current distribution. It is assumed that the two arms of the antenna are made of round and perfectly conducting wires and that they are suitably tapered exponentially. As far as the far field radiation pattern of the antenna is concerned, the assumption of round wire for the radiating element is equivalent to that of strip as long as the diameter of the wire and the width of the strip are both much smaller than a wavelength. Our radiation pattern analysis is based on this assumption which is partially justified on the basis of the experimental results discussed in Section 2.6.

3.2.1 Method of Analysis

The determination of the far field produced by a given current distribution is discussed in many antenna textbooks (see, for example, Wolff, 1966). In this section we quote a few of the basic expressions without giving their derivations.

Let a wire AB carry a current $\bar{I} = \hat{i}_\ell \, I(\ell) \, e^{i\omega t}$ where ℓ is measured from along the wire the $\hat{i}_\ell$ is a unit vector in the direction of the current flow (see Fig. 3-1). The vector potential $\bar{A}$ produced at the far field point $P(R, \theta, \phi)$ by the above current is given by

$$\bar{A} = \frac{\mu_o}{4\pi} \frac{e^{-ikR}}{R} \bar{N} \quad , \tag{1}$$

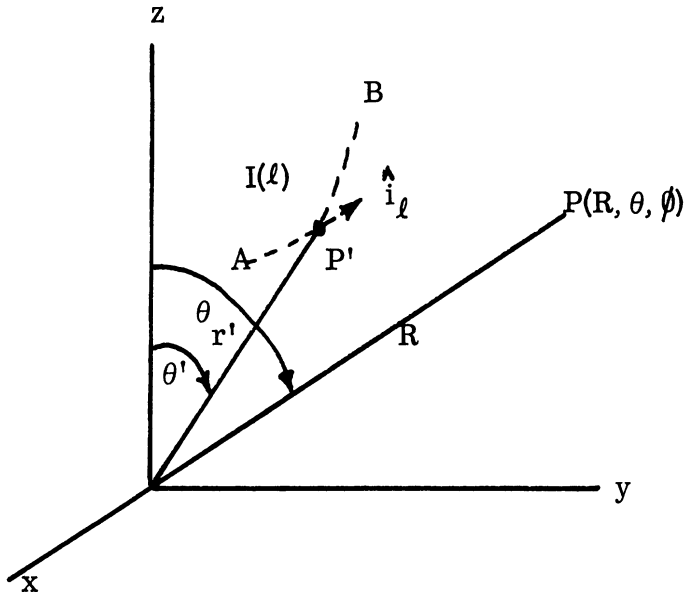

FIG. 3-1: GENERAL COORDINATE SYSTEM FOR AN ARBITRARY CURRENT ELEMENT.

where

μ_o is the permeability of free space,

$k = \frac{2\pi}{\lambda}$ is the propagation constant in free space,

$e^{i\omega t}$ is the assumed time dependence,

and $\bar{N}$ is the radiation vector produced at the far field point $P(R,\theta,\phi)$ by the current flowing in the wire AB and is given by

$$\bar{N} = \int_L \hat{i}_\ell \, I(\ell) e^{ikr'\cos\psi} \, d\ell \, , \tag{2}$$

where

(r', θ', ϕ') are the coordinates of a point P' on the wire (Fig. 3-1),

$$\cos\psi = \sin\theta \sin\theta' \cos(\phi - \phi') + \cos\theta\cos\theta' \, , \tag{3}$$

$\int_L$ means the integration over the length L of the wire.

In general $\bar{N}$ has rectangular components N_x, N_y and N_z and it is simpler to obtain the rectangular components of the radiation vector separately. The spherical components of $\bar{N}$ can then be obtained by using the following equations:

$$\left.\begin{aligned} N_r &= N_x \sin\theta\cos\phi + N_y \sin\theta\sin\phi + N_z\cos\theta \\ N_\theta &= N_x \cos\theta\cos\phi + N_y \cos\theta\sin\phi - N_z\sin\theta \\ N_\phi &= -N_x \sin\phi + N_y \cos\phi \end{aligned}\right\} \, . \tag{4}$$

It can be shown that the far fields produced by the wire AB carrying a current $I(\ell)$ are given by

$$E_\theta = K \eta_o N_\theta \tag{5}$$

$$E_\phi = K \eta_o N_\phi \tag{6}$$

where

$$K = -\frac{ike^{-ikR}}{4\pi R} \, , \tag{7}$$

N_θ, N_ϕ are the θ and ϕ-components of the radiation vector,

and

η_o is the intrinsic impedance of free space.

3.2.2 Determination of the Radiation Vector $\bar{N}$

In this section we determine the radiation vector produced by the rudimentary horn. The geometry and the coordinate system used are shown in Fig. 3-2. It is assumed that the rudimentary horn lies in the y-z plane ($\phi' = \pi/2$). The wires AB and CD are assumed to be tapered such that

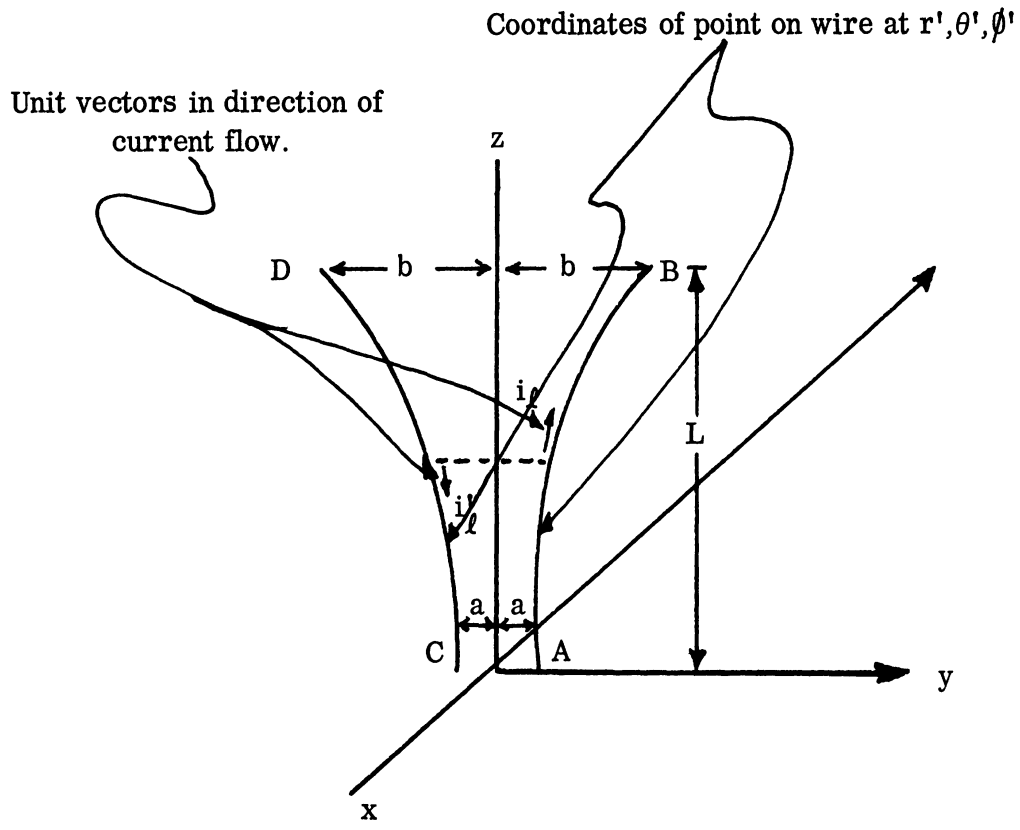

FIG. 3-2: RUDIMENTARY HORN AND COORDINATE SYSTEM USED.

$$y' = ae^{\alpha z'/L} \quad \text{for AB}$$
$$= -ae^{\alpha z'/L} \quad \text{for CD} \tag{8}$$

where a and α are positive constants. The parameter α will be called the tapering factor and is related to the other physical parameters of the antenna by the following relation,

$$\alpha = \ell n \left(\frac{b}{a} \right) . \tag{9}$$

Thus the parameters b and a are related to each other by the relation

$$b = a\, e^{\alpha} . \tag{10}$$

Let us assume that the current in the arm AB is of the form

$$\bar{I}(\ell) = \hat{i}_{\ell} I_o\, e^{-i\beta z'} , \tag{11}$$

where β is the propagation constant in the z-direction. The assumption of this form of current is questionable and we do not give any justification for it here except that a non-uniform transmission line (e. g. exponential line) can support such a current wave under certain conditions. The measured current distributions on an actual rudimentary horn antenna discussed in Section 2. 7, indicate the existence of a reflected wave whose amplitude is much smaller than the forward traveling wave. For the purpose of the present analysis we neglect this reflected wave. In a later section we shall discuss more about the current distribution $\bar{I}(\ell)$ on the rudimentary horn antenna. Similarly, the current in the wire CD is:

$$\bar{I}(\ell) = \hat{i}'_{\ell} I_o e^{-i\beta z'} , \tag{12}$$

where $\hat{i}'_{\ell}$ is directed as shown in Fig. 3-2.

It can be shown that the rectangular components of the radiation vector produced by the current in AB are given by the following:

$$N_{y_{AB}} = i_o\left(\frac{\alpha a}{L}\right)\int_0^L e^{-i(\beta - k\cos\theta + i\frac{\alpha}{L})z'}\, e^{ikae^{\alpha z'/L}\sin\theta\sin\phi}\, dz' \tag{13}$$

$$N_{z_{AB}} = I_o \int_0^L e^{-i(\beta - k\cos\theta)z'}\, e^{ikae^{\alpha z'/L}\sin\theta\sin\phi}\, dz' . \tag{14}$$

Note that both the integrals in (13) and (14) are expressed in terms of z' by using (8). Similarly, the radiation vector components produced at a point P by the current in CD are:

$$N_{y_{CD}} = I_o\left(\frac{\alpha a}{L}\right)\int_0^L e^{-i(\beta - k\cos\theta + i\frac{\alpha}{L})z'}\, e^{-ikae^{\alpha z'/L}\sin\theta\sin\phi}\, dz' , \tag{15}$$

$$N_{z_{CD}} = -I_o \int_0^L e^{-i(\beta - k\cos\theta)z'}\, e^{-ikae^{\alpha z'/L}\sin\theta\sin\phi}\, dz' . \tag{16}$$

The total y-component of the radiation vector produced at P by the rudimentary horn is obtained by adding (13) and (15) and is given by

$$N_y = N_{y_{AB}} + N_{y_{CD}} = 2I_o\left(\frac{\alpha a}{L}\right)\int_0^L e^{-i(\beta - k\cos\theta + i\frac{\alpha}{L})z'} \cdot \cos\left(kae^{\alpha z'/L}\sin\theta\sin\phi\right) dz' \tag{17}$$

Similarly the total z-component of the radiation vector is

$$N_z = N_{z_{AB}} + N_{z_{CD}} = 2iI_o \int_0^L e^{-i(\beta - k\cos\theta)z'} \sin\left\{ka e^{\alpha a'/L} \sin\theta\sin\phi\right\} dz' . \quad (18)$$

The integrals in (17) and (18) cannot be performed in closed form. However, assuming

$$ka e^{\alpha z'/L} \ll 1,$$

the cosine and sine terms in the integrands may be expended into infinite series and then the integrations can be carried out term by term. The final expressions for N_y and N_z can be shown to be given by the following:

$$N_y = 2I_o a\alpha e^{\alpha/2} e^{-i(\beta - k\cos\theta)L/2} \cdot \left[\frac{\sin\left\{(\beta - k\cos\theta)\frac{L}{2} + i\alpha/2\right\}}{\left\{(\beta - k\cos\theta)\frac{L}{2} + i\alpha/2\right\}} + \right.$$

$$\left. + \sum_{n=1}^{\infty} (-1)^n \frac{(ka e^{\alpha/2} \sin\theta\sin\phi)^{2n}}{(2n)!} \cdot \frac{\sin\left\{(\beta - k\cos\theta)\frac{L}{2} + i(2n+1)\alpha/2\right\}}{\left\{(\beta - k\cos\theta)\frac{L}{2} + i(2n+1)\alpha/2\right\}} \right], \quad (19)$$

$$N_z = i2LI_o e^{\alpha/2} e^{-i(\beta - k\cos\theta)\frac{L}{2}} \cdot \left[(ka\sin\theta\sin\phi) \frac{\sin\left\{(\beta - k\cos\theta)\frac{L}{2} + i\alpha/2\right\}}{\left\{(\beta - k\cos\theta)\frac{L}{2} + i\alpha/2\right\}} + \right.$$

$$\left. + \sum_{n=1}^{\infty} (-1)^n \frac{(ka\sin\theta\sin\phi)^{2n+1}}{(2n+1)} e^{i2n\alpha/2} \cdot \frac{\sin\left\{(\beta - k\cos\theta)\frac{L}{2} + i(2n+1)\alpha/2\right\}}{\left\{(\beta - k\cos\theta)\frac{L}{2} + i(2n+1)\alpha/2\right\}} \right] . \quad (20)$$

3.2.3 Far Field Expressions

The complete expressions for the far field produced by a rudimentary horn can be obtained by using Eqs. (4) - (6) along with (19) and (20). Using (4, 5, 19 and 20) and after considerable algebraic manipulation it can be shown that the far electric field component E_θ is given by the following:

$$E_\theta = K\eta_o 2I_o L e^{\alpha/2} e^{-i(\beta - k\cos\theta)L/2} S_\theta(\theta, \phi) , \quad (21)$$

where

$$S_\theta(\theta,\phi)=\left[\left(\frac{a\alpha}{L}\cos\theta-ika\sin^2\theta\right)f_o(\theta)+\sum_{n=1}^{\infty}(-1)^n\left(\frac{a\alpha}{L}\cos\theta-i\frac{ka\sin^2\theta}{2n+1}\right)\cdot\right.$$

$$\left.\cdot\frac{(kb_1\sin\theta\sin\phi)^{2n}}{(2n)!}f_n(\theta)\right]\sin\phi\ , \tag{22}$$

$$b_1=ae^{\alpha/2}\ , \tag{23}$$

$$f_o(\theta)=\frac{\sin\left[(\beta-k\cos\theta)\frac{L}{2}+i\frac{\alpha}{2}\right]}{\left[(\beta-k\cos\theta)\frac{L}{2}+i\frac{\alpha}{2}\right]}\ , \tag{24}$$

$$f_n(\theta)=\frac{\sin\left[(\beta-k\cos\theta)\frac{L}{2}+i(2n+1)\frac{\alpha}{2}\right]}{\left[(\beta-k\cos\theta)\frac{L}{2}+i(2n+1)\frac{\alpha}{2}\right]}\ , \tag{25}$$

and

K is given by Eq. (7).

Similarly, using (4), (6) and (19) it can be shown that the E_ϕ component of the far electric field is given by the following:

$$E_\phi=K\eta_o 2I_oLe^{\alpha/2}\,e^{-i(\beta-k\cos\theta)L/2}\,S_\phi(\theta,\phi)\ , \tag{26}$$

where

$$S_\phi(\theta,\phi)=\left[f_o(\theta)+\sum_{n=1}^{\infty}(-1)^n\,\frac{(kb_1\sin\theta\sin\phi)^{2n}}{(2n)!}\,f_n(\theta)\right]\frac{a\alpha}{L}\,dos\phi\ . \tag{27}$$

The quantities $S_\theta(\theta,\phi)$ and $S_\phi(\theta,\phi)$ in (21) and (26) may be identified with the complex far field radiation patterns produced by the antenna. In the two principal planes of the antenna defined as $\phi=0^o$ (H-plane) and $\phi=\pi/2$ (E-plane) the radiation field expressions simplify considerably. Thus in the E-plane:

$$E_\theta=K\eta_o 2I_oLe^{\alpha/2}\,e^{-i(\beta-k\cos\theta)L/2}\,S_\theta(\theta,\pi/2)\ , \tag{28}$$

where

$$S_\theta(\theta,\pi/2)=\left(\frac{a\alpha}{L}\cos\theta-ika\sin^2\theta\right)f_o(\theta)+$$

$$+\sum_{n=1}^{\infty}(-1)^n\left(\frac{a\alpha}{L}\cos\theta-i\frac{ka\sin^2\theta}{2n+1}\right)\frac{(kb_1\sin\theta)^{2n}}{(2n)!}\,f_n(\theta), \tag{29}$$

and $E_\phi \equiv 0$, because $S_\phi(\theta, \pi/2) \equiv 0$ as can be seen from (27).

In the H-plane we obtain:

$E_\theta \equiv 0$, because $S_\theta(\theta, 0^o) \equiv 0$

$$E_\phi = K\eta_o \; 2I_o L e^{\alpha/2} \; e^{-i(\beta - k\cos\theta)L/2} \; S_\phi(\theta, 0^o) \tag{30}$$

where

$$S_\phi(\theta, 0^o) = \frac{a\alpha}{L} f_o(\theta) \; . \tag{31}$$

It is found that in the two principal planes there is no cross-polarized field. However, cross-polarized components of the field will appear in other planes.

3.2.4 Principal Plane Patterns

It can be seen from the previous section that the H-plane far field produced by the rudimentary horn is given by the simple expression (31). After introducing (24) into (31) and taking the magnitude of the resulting expression the far field radiation pattern in the H-plane is obtained in the following form.

$$\left|S_\phi(\theta, 0^o)\right| = \frac{a\alpha}{L} \left[\frac{\sin^2\left\{(\beta - k\cos\theta)\frac{L}{2}\right\} + \sinh^2\left(\frac{\alpha}{2}\right)}{\left\{(\beta - k\cos)\frac{L}{2}\right\}^2 + \left(\frac{\alpha}{2}\right)^2} \right]^{1/2} \; . \tag{32}$$

The E-plane radiation pattern can be obtained by taking the magnitude of (29). As it stands, (29) is rather complicated. In some practical situations the parameter $kb_1 \ll 1$ and under this condition Eq. (29) may be approximated as follows:

$$S_\theta(\theta, \frac{\pi}{2}) \simeq \left(\frac{a\alpha}{L}\cos\theta - ika\sin^2\theta\right) f_o(\theta) \; . \tag{33}$$

The approximate E-plane radiation pattern is then given by

$$\left|S_\theta(\theta, \frac{\pi}{2})\right| \simeq \left[\frac{a^2\alpha^2}{L^2}\cos^2\theta + (ka)^2\sin^4\theta\right]^{1/2} \times \left[\frac{\sin^2\left\{(\beta - k\cos\theta)\frac{L}{2}\right\} + \sinh^2\frac{\alpha}{2}}{\left\{(\beta - k\cos\theta)\frac{L}{2}\right\}^2 + \left(\frac{\alpha}{2}\right)^2} \right]^{1/2} \; . \tag{34}$$

If necessary $\left|S_\theta(\theta, \pi/2)\right|$ may be improved by including more terms in (29).

On the basis of the patterns given by (32) and (34), the back-to-front ratio ρ, of the pattern produced by the antenna is given by

$$\rho^2 = \frac{\sin^2(\beta+k)\frac{L}{2} + \sinh^2\frac{\alpha}{2}}{\sin^2(\beta-k)\frac{L}{2} + \sinh^2\frac{\alpha}{2}} \cdot \frac{(\beta-k)^2L^2+\alpha^2}{(\beta+k)^2L^2+\alpha^2} \quad . \tag{35}$$

If $\beta = k$,

$$\rho^2 = \frac{\sin^2 kL + \sinh^2\frac{\alpha}{2}}{\sin^2\frac{\alpha}{2}} \cdot \frac{\alpha^2}{4k^2L^2+\alpha^2} \quad . \tag{36}$$

3.2.5 Discussion

In the above, theoretical expressions have been developed for the radiation field produced by a rudimentary horn carrying a traveling wave of current. The expressions derived above are based on the assumption that the propagation constant of the assumed current wave is known. In the following section the propagation characteristics of a rudimentary horn structure are analyzed with the goal of obtaining an expression for β.

The assumption of exponential taper for the radiating elements enabled us to carry out the integrations involved in the radiation field expressions. For more general type of tapering, the above analysis will still apply but it appears that numerical techniques must be used to carry out the integrations involved in this case.

3.3 Propagation Characteristics

In the present section the propagation characteristics of a variable cross section strip transmission line are analyzed. A rudimentary horn antenna may be looked upon as a section of such a transmission line and hence the results of such an analysis can be applied to the former case.

The analysis of the propagation characteristics of such a transmission line makes use of the work of Schelkunoff (1955) on the conversion of Maxwell's equations into generalized telegraphist's equations. First of all we obtain the most general form of the transmission line type of equations for the structure. In this form the equations take into account the infinitely many possible modes that can propagate along the line. Then we consider only the principal mode and obtain an expression for the principal mode propagation constant β.

3.3.1 Basic Equations

Let us consider a variable cross section strip transmission line as shown in Fig. 3-3. The line is made of conducting strips of width w and its orientation and other dimensions are as shown in the figure. In the absence of nonuniformity, i.e. $a(z)=a_0$, the dominant mode in the line is the TEM having only the field components E_x, H_y. Depending on the separation between the strips it can support

higher order modes, which can be analyzed by standard methods. The basic principle involved here is to obtain the transmission line type of equations for the nonuniform line in terms of the modes existing in the line when it is uniform. In the following we discuss the transverse magnetic (TM) modes which are of more direct importance in the present case.

We consider the symmetric modes only , i. e. the modes whose field configurations are symmetric with respect to the plane y 0 z (Fig. 3-3). Since the line is symmetric, in the present case we can insert a perfectly conducting plane y 0 z in the middle of the line without disturbing the field configuration. All the field quantities are assumed to be independent of tye y-coordinate and the assumed time dependence is $e^{i\omega t}$. Under these conditions the source-free Maxwell's equations are:

$$\frac{\partial E_x}{\partial z} = -j\omega\mu H_y + \frac{\partial E_z}{\partial x} \tag{37}$$

$$\frac{\partial H_y}{\partial z} = -j\omega\epsilon E_x \tag{38}$$

$$E_z = \frac{1}{j\omega\epsilon}\frac{\partial H_x}{\partial x} \quad . \tag{39}$$

The boundary conditions are

$$E_z(0, z) \equiv 0 \, , \tag{40}$$

$$E_t(a, z) \equiv 0 \, , \tag{41}$$

where $E_t(a, z)$ is the component of the electric field tangential to the strip. Since

$$E_t = E_z \cos\gamma + E_x \sin\gamma \, , \tag{42}$$

where γ (z) is the angle between the axial plane and the plane tangent to the strip, the second boundary condition given by (41) can be written in the following manner

$$E_z(a, z) = -E_x \tan\gamma \, . \tag{43}$$

The fields E_x, H_y in the present configuration can be expressed in terms of the modes appropriate to the case of the uniform transmission line. Thus we can write:

$$E_x = \frac{V_o(z)}{a} + \sum_1^{\infty} N_n^{-1} V_n(z) \cos\frac{n\pi x}{a} \, , \tag{44}$$

$$H_y = \frac{I_o(z)}{w} + \sum_1^{\infty} N_n^{-1} I_n(z) \cos\frac{n\pi x}{a} \, , \tag{45}$$

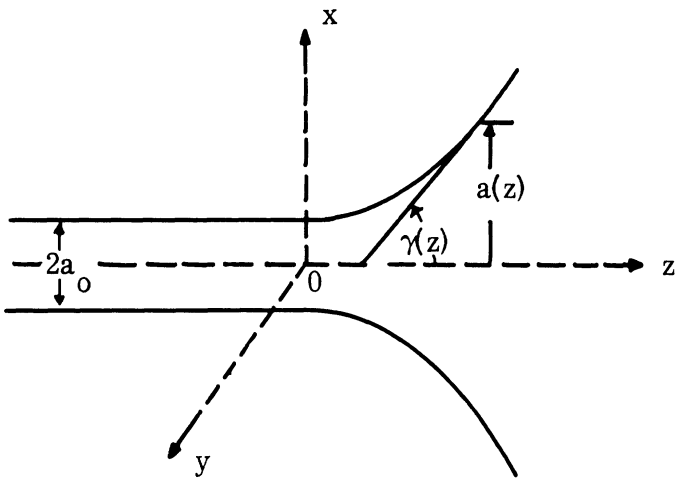

FIG. 3-3: A VARIABLE CROSS-SECTION STRIP TRANSMISSION LINE.

where the normalizing constant N_n is given by

$$N_n^2 = \int_0^a \int_0^w \cos^2 \frac{n\pi x}{a}\, dx\, dy = \frac{1}{2} aw \quad . \tag{46}$$

The quantities V_o, I_o, V_n and I_n in (44) and (45) may be identified with the mode voltages and currents of proper mode number. They are defined as follows

$$V_o(z) = \int_0^a E_x dx \, , \tag{47}$$

$$I_o(z) = \frac{w}{a} \int_0^a H_y dx \, , \tag{48}$$

$$V_n(z) = \int_0^a E_x \cos \frac{n\pi x}{a}\, dx \, , \tag{49}$$

$$I_n(z) = \frac{w}{a} \int_0^a H_y \cos \frac{n\pi x}{a}\, dx \quad . \tag{50}$$

From (43) and (44) we obtain when x=a ,

$$E_z(a, z) = -E_x \tan\gamma = -\frac{\tan\gamma}{a} V_o(z) - \sum_1^\infty (-1)^n N_n^{-1} \tan\gamma V_n(z) \quad . \tag{51}$$

To obtain the telegraphist's equations corresponding to the lowest order mode quantities V_o, I_o, we integrate Eq. (37) with respect to n and make use of (47) and (48) to obtain the following:

$$\frac{dV_o(z)}{dz} = -\frac{j\omega\mu a}{w} I_o(z) + E_z(a, z) - E_z(0, z) \quad . \tag{52}$$

After using (40) and (51), Eq. (52) may be written as follows:

$$\frac{dV_o(z)}{dz} = -\frac{j\omega\mu a}{w} I_o(z) - \frac{\tan\gamma}{a} V_o(z) - \sum_1^\infty (-1)^n N_n^{-1} \tan\gamma V_n(z) \quad . \tag{53}$$

Similarly, by integrating (38) with respect to x and following a similar procedure we obtain the following equation:

$$\frac{dI_o(z)}{dz} = -\frac{j\omega \epsilon w}{a} V_o(z) \quad . \tag{54}$$

Note that in Eq. (53) the effects of higher order modes appear in the expression through the voltage transfer coefficients. We shall not show the details of obtaining the transmission line type of equations for the higher ofder mode quantities $V_n(z)$, $I_n(z)$. They can be obtained by multiplying (37) and (38) by

$$N_m^{-1} \cos \frac{m\pi x}{a}$$

and integrating over the cross section of the line. Only the final results are given below:

$$\frac{dV_m(z)}{dz} = -Z_{mn} I_m(z) - \sum_{n=o}^{\infty} V_{T_{mn}} V_n(z) \tag{55}$$

$$Z_{mm} = j\omega\mu + \frac{m^2\pi^2}{j\omega\epsilon a^2} \tag{56}$$

$$V_{T_{mn}} = (-1)^{m+n} N_m^{-1} N_n^{-1} w \tan\gamma - \frac{n\pi a'}{N_m N_n a^2} \int_0^a \int_0^w n \cos\frac{m\pi x}{a} \sin\frac{n\pi x}{a} dxdy$$

$$\text{for } m \neq n,\ m \neq 0,\ n \neq 0, \tag{57}$$

$$V_{T_{mm}} = N_m^{-2} w \tan\gamma + N_m' N_m^{-1} - \frac{m\pi a' w}{2N_m^2 a^2} \int_0^a x \sin\frac{2m\pi x}{a} dy \tag{58}$$

$$V_{T_{mo}} = \frac{(-1)^m w \tan\gamma}{N_m a} \quad . \tag{59}$$

In the above equations the prime above a quantity refers to the derivative with respect to z. The corresponding equation for $I_m(z)$ is:

$$\frac{dI_m(z)}{dz} = -j\omega\epsilon V_m(z) - \sum_{n=o}^{\infty} I_{T_{mn}} I_n(z) \ , \tag{60}$$

where

$$I_{T_{mn}} = -\frac{n\pi a'}{a^2 N_m N_n} \int_0^a \int_0^w x \cos\frac{m\pi x}{a} \sin\frac{n\pi x}{a} dx\, dy$$

$$m \neq n,\ m \neq 0,\ n \neq 0, \tag{61}$$

$$I_{T_{mm}} = N_m' N_m^{-1} - \frac{m\pi a'}{2a^2 N_m^2} \int_0^a \int_0^w x \sin\frac{2m\pi x}{a} dx dy \tag{62}$$

$$I_{T_{mo}} = 0 \ . \tag{63}$$

In the above we have given the telegraphist's equations corresponding to all the modes of TM type that can exist in a variable cross section strip transmission line.

3.3.2 Principal Mode Analysis

In this section we discuss the telegraphist's equations for the quantities V_o, I_o which we call the principal mode equations. Neglecting the effects of the higher order modes on the principal mode we obtain the following two fundamental equations:

$$\frac{dV_o(z)}{dz} = -\frac{j\omega\mu a}{w} I_o(z) - \frac{\tan\gamma}{a} V_o(z) \tag{64}$$

$$\frac{dI_o(z)}{dz} = -\frac{j\omega\epsilon w}{a} V_o(z) . \tag{65}$$

It should be noted that in (64) and (65) the quantities a and γ are functions of z. It can be shown now that $V_o(z)$ and $I_o(z)$ satisfy the following two equations:

$$\frac{d^2V_o(z)}{dz^2} + \left[k^2 - 2\left(\frac{a'}{a}\right)^2 + \frac{a''}{a}\right] V_o(z) = 0 , \tag{66}$$

$$\frac{d^2I_o(z)}{dz^2} + 2\left(\frac{a'}{a}\right)\frac{dI_o(z)}{dz} + k^2 I_o(z) = 0 , \tag{67}$$

where the prime over a signifies differentiation with respect to z and $k^2=\omega^2\mu\epsilon$ = free space propagation constant.

It is now necessary to assume some functional form for a(z) in order to obtain the solutions of (66) and (67). From the nature of the differential equations it can be said that only for some specific types of functional form for a(z) they will have simple solutions. The exponential variation of the cross section of the line is such a function. For this particular case we assume:

$$a(z) = a_o e^{\alpha/L\, z} , \tag{68}$$

where $\alpha = \ln(b/a_o)$ is the tapering coefficient. For such a line (66) and (67) can be written as follows:

$$\frac{d^2V_o(z)}{dz^2} + \left[k^2 - \left(\frac{\alpha}{L}\right)^2\right] V_o(z) = 0 \tag{69}$$

$$\frac{d^2 I_o(z)}{dz^2} + 2\frac{\alpha}{L}\frac{dI_o(z)}{dz} + k^2 I_o(z) = 0 \quad . \tag{70}$$

Equation (70) has the following solution:

$$I_o(z) = I_{o1} e^{\left(-\frac{\alpha}{L} - \sqrt{\frac{\alpha^2}{L^2} - k^2}\right)z} + I_{o2} e^{\left(-\frac{\alpha}{L} + \sqrt{\frac{\alpha^2}{L^2} - k^2}\right)z} \tag{71}$$

where the I_{o1} and I_{o2} are two constants. In a practical case, $\alpha/kL \ll 1$, thus (71) can be written as:

$$I_o(z) = I_{o1} e^{\left(-\frac{\alpha}{L} - ik\sqrt{1 - \frac{\alpha^2}{k^2 L^2}}\right)z} + I_{o2} e^{\left(-\frac{\alpha}{L} + ik\sqrt{1 - \frac{\alpha^2}{k^2 L^2}}\right)z} \quad . \tag{72}$$

Equation (72) is the general solution; the forward traveling wave of current in the strip transmission line under consideration is:

$$I_o(z) = I_{o1} e^{-\frac{\alpha}{L} z - ik\sqrt{1 - \frac{\alpha^2}{k^2 L^2}}\, z} \quad . \tag{73}$$

Thus the propagation constant in this case is given by:

$$\beta = -i\frac{\alpha}{L} + k\sqrt{1 - \frac{\alpha^2}{k^2 L^2}} \quad . \tag{74}$$

3.4 Radiation Patterns of Rudimentary Horn Antennas

In the present section we apply the results given above to obtain the far field radiation pattern produced by a rudimentary horn antenna. It is assumed that the antenna is made of conducting strips (as shown in Fig. 3-3) and having a variable cross section of the form given by Eq. (68). We also assume that the antenna supports a traveling wave of current as given by Eq. (72). Thus we obtain here the radiation field produced by a single traveling wave of current in the antenna caused by the principal mode of wave only. The results given in this section are based on the analysis discussed previously.

With reference to Section 3.2 the principal plane radiation patterns of a rudimentary horn carrying a current of the form $I = I_o e^{-i\beta z}$ are given by the following:

$$S_{\phi}(\theta, 0^{o}) = \frac{a\alpha}{L} f_{o}(\theta) , \tag{75}$$

$$S_{\theta}(\theta, \pi/2) = \left(\frac{a\alpha}{L} \cos\theta - ika \sin^{2}\theta\right) f_{o}(\theta) + \sum_{n=1}^{\infty} (-1)^{n} \left(\frac{a\alpha}{L} \cos\theta - i \frac{ka \sin^{2}\theta}{2n+1}\right) \frac{(kb_{1} \sin\theta)^{2n}}{(2n)!} f_{n}(\theta) , \tag{76}$$

where

$$f_{o}(\theta) = \frac{\sin\left[(\beta - k\cos\theta)\frac{L}{2} + i\frac{\alpha}{2}\right]}{\left[(\beta - k\cos\theta)\frac{L}{2} + i\frac{\alpha}{2}\right]} , \tag{77}$$

$$f_{n}(\theta) = \frac{\sin\left[(\beta - k\cos\theta)\frac{L}{2} + i(2n+1)\frac{\alpha}{2}\right]}{\left[(\beta - k\cos\theta)\frac{L}{2} + i(2n+1)\frac{\alpha}{2}\right]} , \tag{78}$$

$$b_{1} = a_{o} e^{\alpha/2} . \tag{79}$$

With the current distribution given by (72), the propagation constant β in the above equations should be modieifed as follows:

$$\beta = -i\frac{\alpha}{L} + k\sqrt{1 - \frac{\alpha^{2}}{k^{2}L^{2}}} . \tag{80}$$

Thus, introducing (80) into (77) and (79) we obtain the following:

$$f_{o}(\theta) = \frac{\sin\left[\left(\sqrt{1 - \frac{\alpha^{2}}{k^{2}L^{2}}} - \cos\theta\right)\frac{kL}{2}\right]}{\left[\sqrt{1 - \frac{\alpha^{2}}{k^{2}L^{2}}} - \cos\theta\ \frac{kL}{2}\right]} , \tag{81}$$

$$f_{n}(\theta) = \frac{\sin\left[\left(\sqrt{1 - \frac{\alpha^{2}}{k^{2}L^{2}}} - \cos\theta\right)\frac{kL}{2} + in\alpha\right]}{\left[\left(\sqrt{1 - \frac{\alpha^{2}}{k^{2}L^{2}}} - \cos\theta\right)\frac{kL}{2} + in\alpha\right]} . \tag{82}$$

The far field radiation pattern of the antenna in the $\phi = 0^{o}$ plane is given by

$$\left|S_{\phi}(\theta, 0^{o})\right| = \frac{a\alpha}{L} \left|f_{o}(\theta)\right| = \frac{a\alpha}{L} \frac{\sin\left[\left(\sqrt{1 - \frac{\alpha^{2}}{k^{2}L^{2}}} - \cos\theta\right)\frac{kL}{2}\right]}{\left[\left(\sqrt{1 - \frac{\alpha^{2}}{k^{2}L^{2}}} - \cos\theta\right)\frac{kL}{2}\right]} . \tag{83}$$

The far field radiation pattern in the $\phi=\pi/2$ plane as given by (76) is in the form of infinite series. We shall give the complete expressions for the zero'th and first order approximations only. The zero'th order approximation to $S_\theta(\theta,\pi/2)$ is obtained by retaining only the first term in (76) and thus we obtain:

$$S_\theta(\theta,\pi/2) \simeq \frac{a\alpha}{L}\left(\cos\theta - i\frac{kL}{\alpha}\sin^2\theta\right) f_o(\theta) \tag{84}$$

from which we obtain the following for the zero'th order radiation field:

$$\left|S_\theta(\theta,\pi/2)\right|_o = \frac{a\alpha}{L}\left(\cos^2\theta + \frac{k^2L^2}{\alpha^2}\sin^4\theta\right)^{1/2} f_o(\theta)\ . \tag{85}$$

The first order approximation to $S_\theta(\theta,\pi/2)$ is obtained as:

$$S_\theta(\theta,\pi/2)_1 = \frac{a\alpha}{L}\left(\cos\theta - i\frac{kL}{\alpha}\sin^2\theta\right) f_o(\theta) - \frac{a\alpha}{L}\left(\cos\theta - i\frac{kL}{\alpha}\frac{\sin^2\theta}{3}\right)\frac{(kb_1\sin\theta)^2}{2} f_1(\theta), \tag{86}$$

where

$$f_1(\theta) = \frac{\sin\left[\left(\sqrt{1-\frac{\alpha^2}{k^2L^2}} - \cos\theta\right)\frac{kL}{2} + i\,\alpha\right]}{\left[\left(\sqrt{1-\frac{\alpha^2}{k^2L^2}} - \cos\theta\right)\frac{kL}{2} + i\,\alpha\right]}\ . \tag{87}$$

The first order approximation to the radiation pattern in the $\phi=\pi/2$ plane is obtained by taking the magnitude of Eq. (86).

3.5 Comparison Between Theory and Experiment

The normalized H-plane patterns of a symmetrical rudimentary horn antenna as obtained numerically from Eq. (83) are shown in Figs. 3-4(a) — 3-4(c) for thrre selected frequencies. The corresponding measured pattern of the same antenna (obtained from Fig. 2-20a) is also superposed on Fig. 3-4(a) for direct comparison. As can be seen from Fig. 3-4(a), the general agreement between theory and experiment over most of the region of the main beam may be considered to be fair. Because of the restrictions imposed by the experimental equipment, the measured pattern shown in Fig. 3-4(a) has been terminated at $\theta = \pm 95^0$. Only the main beam of the measured H-plane pattern of the antenna at 8 GHz (obtained from Fig. 2-20(c)) is shown in Fig. 3-4(c). The agreement between theory and experiment, as found in Fig. 3-4(c), can again be considered to be fair. The minor lobe details of the theoretical and experimental patterns of the antenna are given in Table III-1 so that they can be compared with each other. Table III-1 indicates that the theory needs to be improved to provide better agreement with experiment. Considering the nature of approximations made in obtaining the theoretical patterns, it may be concluded on the basis of the results shown in Fig. 3-4 that the first order theory can explain fairly well the H-plane patterns of a symmetrical rudimentary horn antenna.

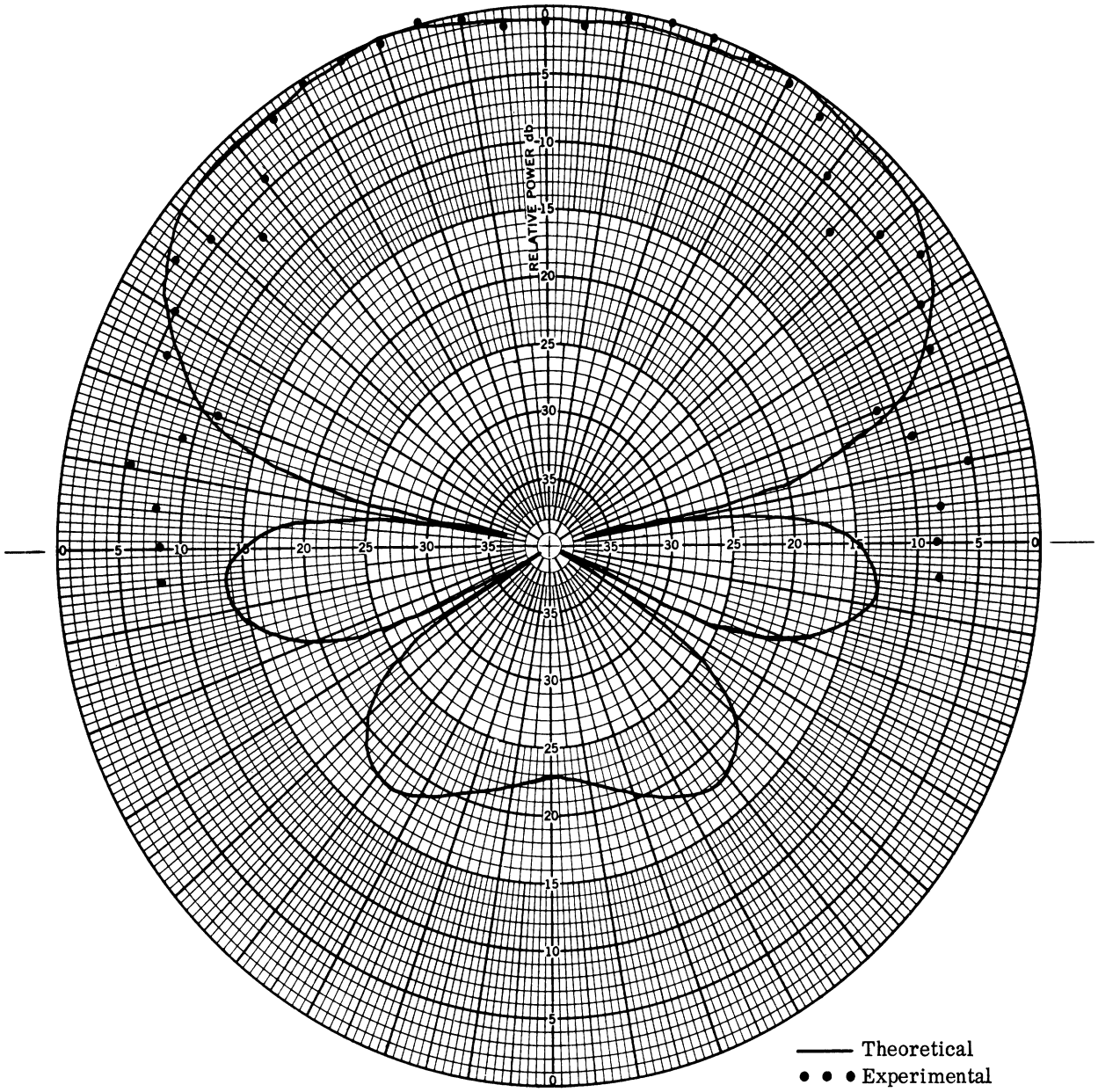

FIG. 3-4a: H-PLANE FREE SPACE RADIATION PATTERN OF A SYMMETRICAL RUDIMENTARY HORN ANTENNA.
a = 0.025", b = 6.00", L = 18.00", α = 5.48, f = 1 GHz.

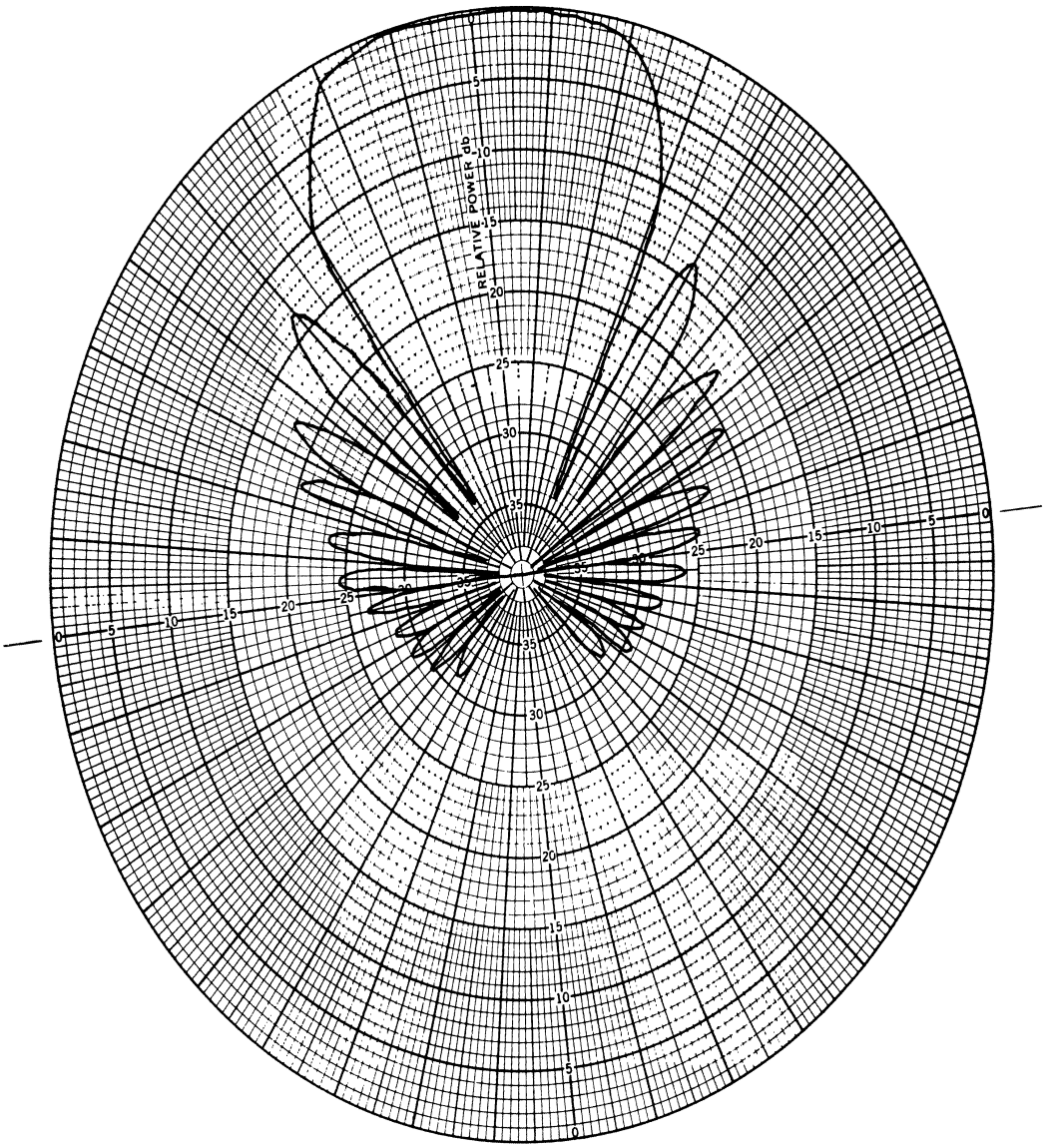

FIG. 3-4b: THEORETICAL H-PLANE FREE SPACE PATTERN OF A SYMMETRICAL RUDIMENTARY HORN ANTENNA. a = 0.025", b = 6.00", L = 18.00", α = 5.48, f = 4 GHz.

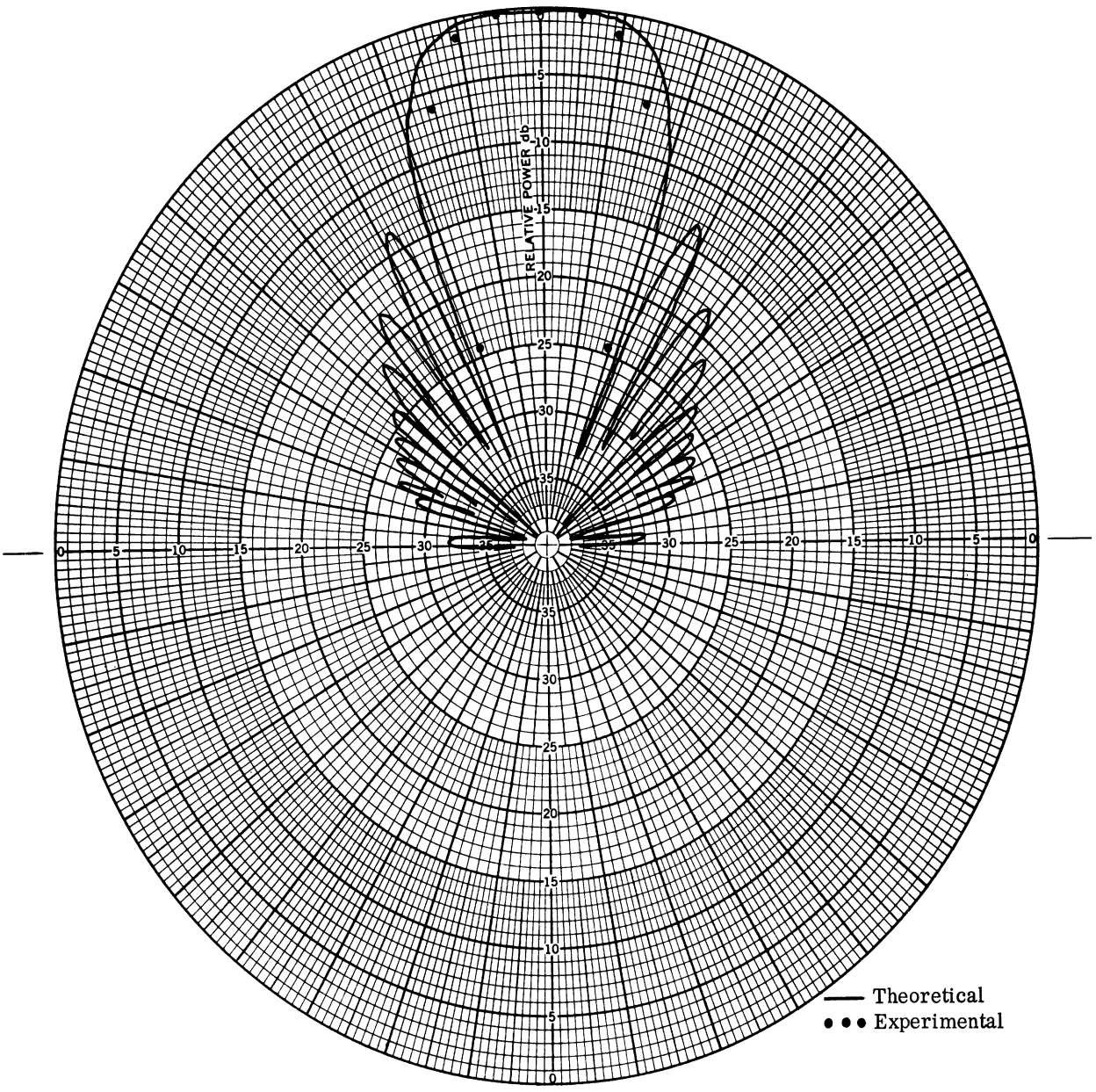

FIG. 3-4c: H-PLANE FREE SPACE RADIATION PATTERN OF A SYMMETRICAL RUDIMENTARY HORN ANTENNA.
a = 0.025", b = 6.00", L = 18.00", α = 5.48, f = 8 GHz.

TABLE III-1: MINOR LOBE CHARACTERISTICS OF THE H-PLANE PATTERN OF A SYMMETRICAL RUDIMENTARY HORN AT 8 GHZ.

	Position		Amplitude in dB	
Pattern Detail	Theoretical	Experimental (avg)	Theoretical	Experimental (avg)
First Minimum	23°	21°	-33.0	-23.9
First Sidelobe Maximum	28°	25°	-13.2	-15.3
Second Minimum	34°	29°	-31.5	-30.0
Second Sidelobe Maximum	38°	33°	-18.0	-17.9

The normalized E-plane patterns of the above symmetrical rudimentary horn antenna as obtained numerically from Eq. (85) are shown in Figs. 3-5(a) — 3-5(c) for three selected frequencies. The corresponding measured patterns (obtained from Figs. 2-20(a) and 2-20(c)) are also superposed on Figs. 3-5(a) and 3-5(c) for comparison. The general agreement between theory and experiment in this case is found to be worse than that shown in Fig. 3-4. This is attributed to the fact that the theoretical E-plane patterns have been computed from the first term of the E-plane pattern expression given by Eq. (76). It is anticipated that by including more terms in the expression during computation, better agreement with experiment can be obtained. However, this procedure involves more elaborate computational procedures; we have not done this due to lack of funds and time.

The first order theory used here for pattern analysis takes into account only the principal mode of the TM type that may exist in the antenna structure. It is conceivable that higher order TM modes as well as modes of TE-type may exist in the rudimentary horn structure. Theoretical pattern expressions obtained by considering the effects of these modes will certainly improve the agreement between theory and experiment. This conclusion is based on the nature of the agreement between the first order theory and experiment discussed above.

3.6 Discussion

In the above we have discussed the theory of radiation fields of a rudimentary horn antenna. In general, the antenna structure is capable of supporting both TM and TE modes of propagation. We have discussed only the TM case because it is believed that this mode is of importance here. However, the effect of TE mode on the antenna performance should also be investigated. In deriving the current distribution only the lowest order mode of propagation has been considered. The effects of higher order TM modes on the propagation constant β and the current distribution I(z) should be studied in order to improve the theory. This will involve solving a set of simultaneous ordinary differential equations. The number

of equations will depend on the number of modes considered. The theoretical analysis given above should be considered as a first step towards the development of a theory for the rudimentary horn antenna. Even with the simplifying assumptions made, the H-plane pattern expressions given above can explain the general pattern behavior fairly well. It is felt that further investigation is necessary to improve the present theory. This can be done as follows:

1) Investigate the effects of higher order TM modes on the propagation constant β and the current distribution I(z). This can be done by using the general expressions given in Section 3.3.1.

2) Study numerically the effects of taking more terms in the E-plane radiation patterns as given by Eq. (76).

3) Study the effects of the existence of the standing wave of current in the antenna.

4) Investigate the importance of TE modes in the antenna.

5) If the above procedure fails to yield a dependable theory then a slightly different approach may be followed. This consists of analyzing the antenna in curvilinear coordinates. The general method outlined by Schelkunoff (1955) appears to be applicable to the present problem.

6) The modal analysis given above should be used to determine the input reflection coefficient or the VSWR of the antenna.

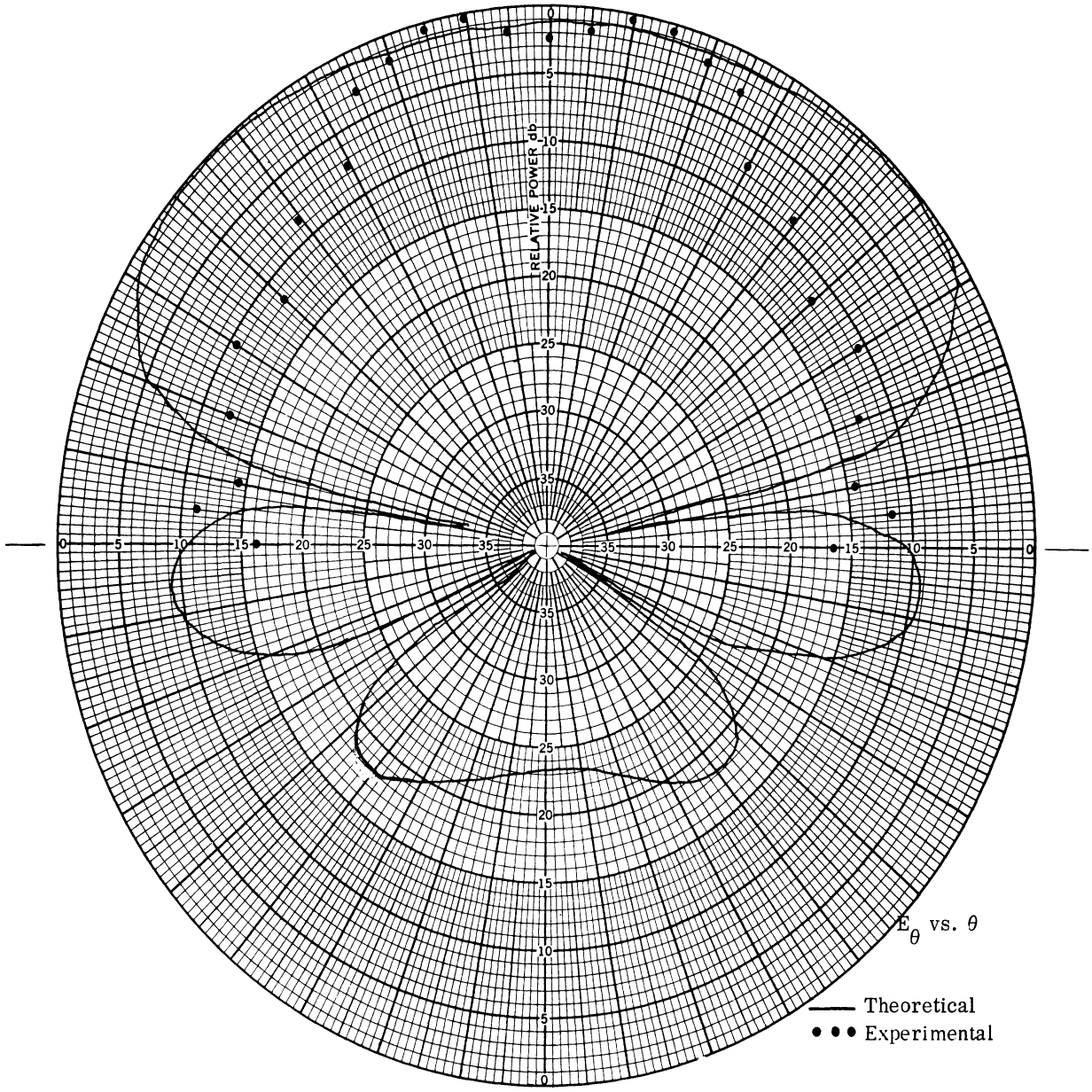

FIG. 3-5a: E-PLANE FREE SPACE RADIATION PATTERN OF A SYMMETRICAL RUDIMENTARY HORN ANTENNA.
a = 0.025", b = 6.00", L = 18.00", α = 5.48, f = 1 GHz.

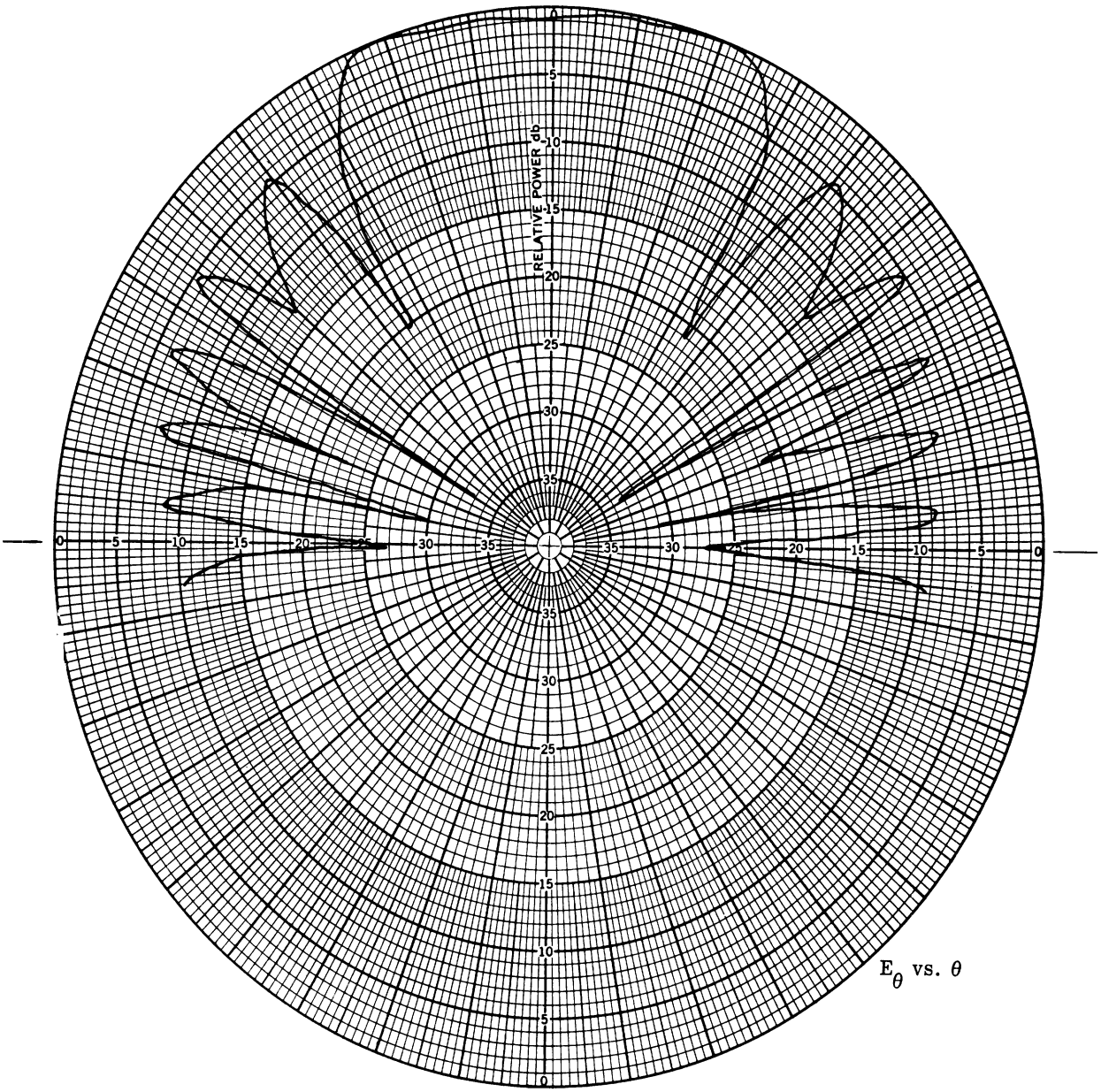

FIG. 3-5b: THEORETICAL E-PLANE FREE SPACE RADIATION PATTERN OF A SYMMETRICAL RUDIMENTARY HORN ANTENNA.
a = 0.025", b = 6.00", L = 18.00", α = 5.48, f = 4 GHz.

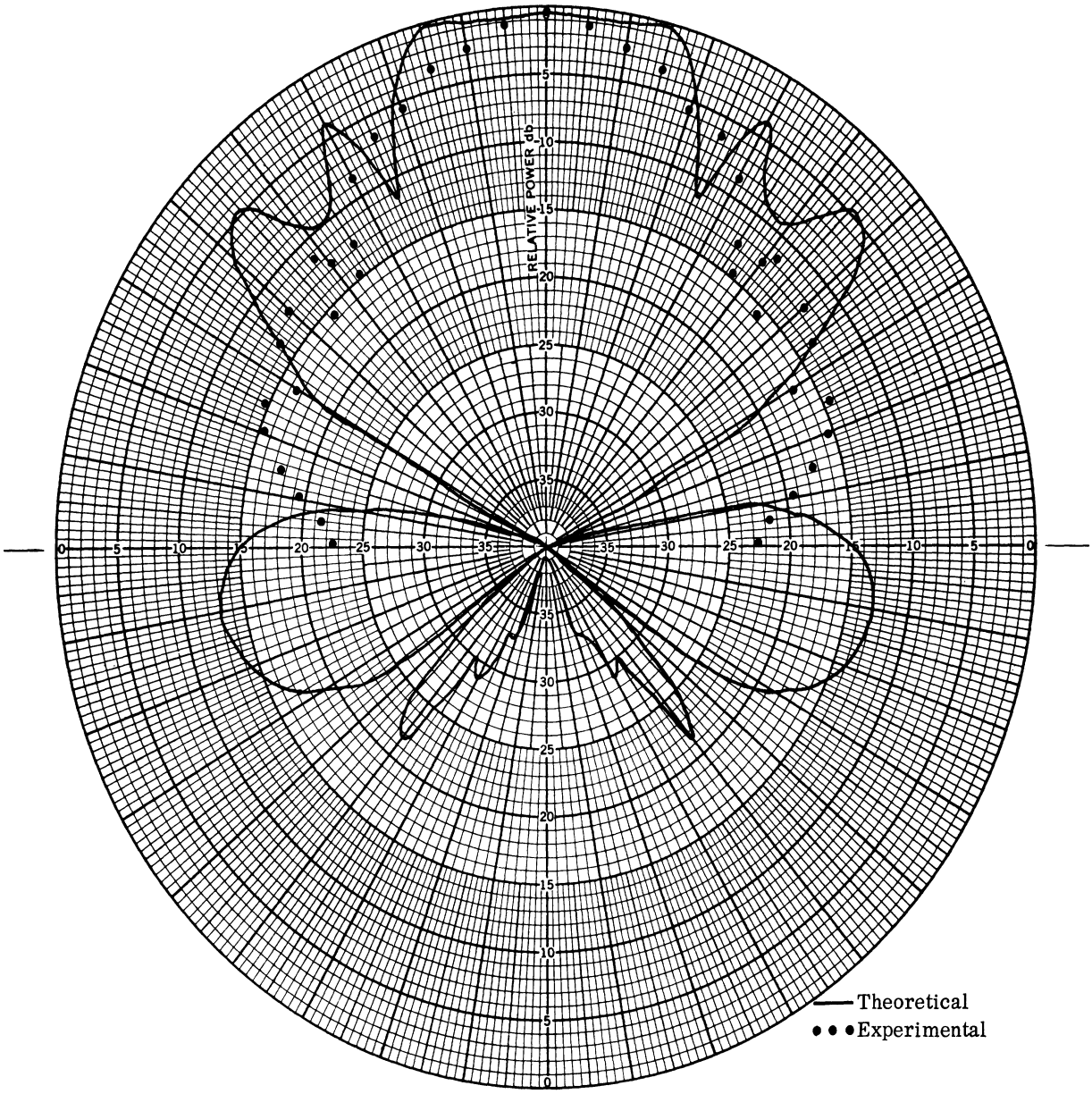

FIG. 3-5c: E-PLANE FREE SPACE RADIATION PATTERN OF A SYMMETRICAL RUDIMENTARY HORN ANTENNA.
a = 0.025", b = 6.00", L = 18.00", α = 5.48, f = 8 GHz.

IV

COMPARISON BETWEEN RUDIMENTARY HORNS AND OTHER SIMILAR ANTENNAS

4.1 Introduction

It was mentioned in Section 1.1 that the primary purpose of the present study has been to investigate the potential application of rudimentary horn antennas to long range HF communication systems. In the previous chapters we have given the detailed results obtained from our investigation of various properties of such antennas. It is appropriate now to make a comparative study of rudimentary horn and other antennas which are currently in use in the HF range.

The antennas which are commonly used for long range HF communications are Log Periodic (TCI, 1968), Rhombic-RD-4 (Clark et al, 1959) and the Tapered Aperture Horn Antenna, TAHA (Clark et al, 1959). The detailed description of mechanical and electrical characteristics of these antenna may be found in the references cited. The performance of these three antennas are compared below with two rudimentary horn models 9-5C and 7-5C whose dimensions are as given in Table II-2. These two specific rudimentary horns are chosen because they have comparable mechanical dimensions with those of Rhombic RD-4 and antenna at the full scale high frequency range.

4.2 Comparative Discussion

The important design parameters and the various parameters indicative of the electrical performance of all these antennas are grouped together and shown in Table IV-1 for direct comparison.

The directive gain of the rhombic antenna has been obtained from the published literature (Jasik, 1961; Harper, 1941; Christensen, 1947; Brueckmann, 1957). The data for the L-P antenna are obtained from the information published by the manufacturer of the L-P antenna for use in the frequency range 3 - 30 GHz (TCI, [illegible]). The data for the TAHA have been obtained from the TAHA report (Clark et al, 1959). The rudimentary horn data have been obtained from our investigation reported in earlier chapters.

The directive gain of Rhombic RD-4 and the rudimentary horn 9-5C as a function of frequency are shown in Fig. 4-1. It is found from Fig. 4-1 that the Rhombic RD-4 has slightly higher gain than the rudimentary horn over the entire band of frequencies of interest. An important parameter of interest for HF communication purposes is the beam tilt which is defined as the angle above the horizon at which the maximum of the main beam occurs. The beam tilt angle as

a function of frequency is shown in Fig. 4-2, for the two antennas. It can be seen from Fig. 4-2 that the rudimentary horn produces lower beam tilt toward the lower end of the frequency band. In some cases this may be found to be an advantage.

From the results given above it may be concluded that the rudimentary horn antenna is competitive with three other commonly used HF antennas in all respects. An added advantage of the rudimentary horn may be its simplicity of mechanical design.

TABLE IV-1: ELECTRICAL AND MECHANICAL CHARACTERISTICS OF SOME HF ANTENNAS

	TCI 503-2LP	Rhombic RD-4	TAHA	Rudimentary 9-5C	Rudimentary 7-5C
Frequency	3.4 - 20 MHz	5 - 20 MHz	6.75 - 24 MHz	4 - 24 MHz	4 - 24 MHz
VSWR	< 2.0 : 1	-	< 4.0 : 1	< 3.0 : 1	< 3.0 : 1
Avg. Impedance	50 Ω	-	75 Ω	50 Ω	50 Ω
Azimuth Beamwidth	120°	16°	15°	30°	28°
Elevation Beamwidth	18°	10°	10°	10°	10°
Beam Tilt	12°	8°	10°	10°	10°
Directive Gain	12 dB	25 dB*	25 dB*	21 dB*	21 dB*
Height	145'	130'	253'	138'	138'
Length	351'	756'	924'	638'	500'
Width	208'	260'	506'	200'	200'
Polarization	Vertical	Horizontal	Horizontal	Vertical	Vertical

*Midband

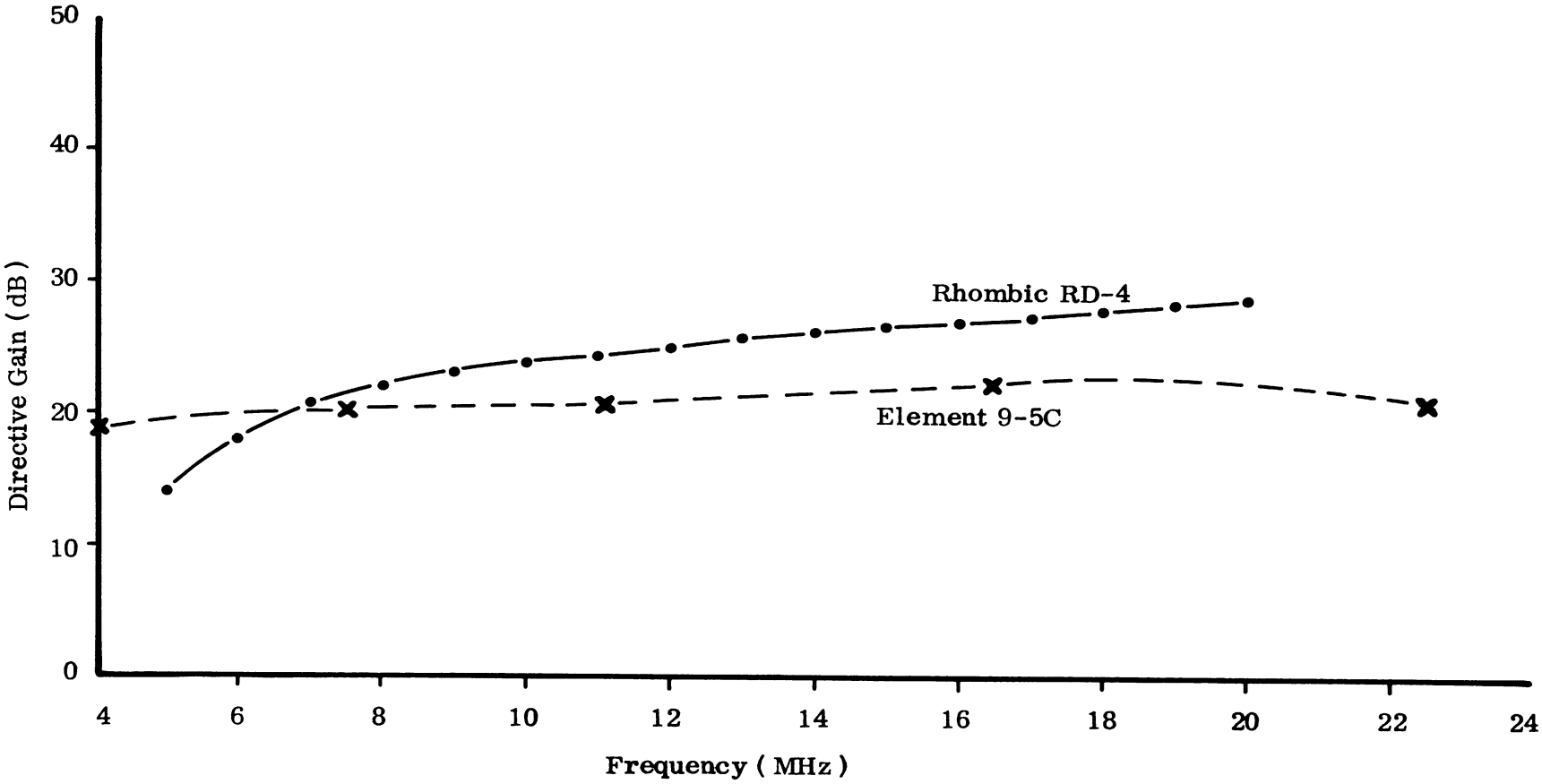

FIG. 4-1: DIRECTIVE GAIN AS A FUNCTION OF FREQUENCY FOR THE RHOMBIC RD-4 AND THE RUDIMENTARY HORN 9-5C.

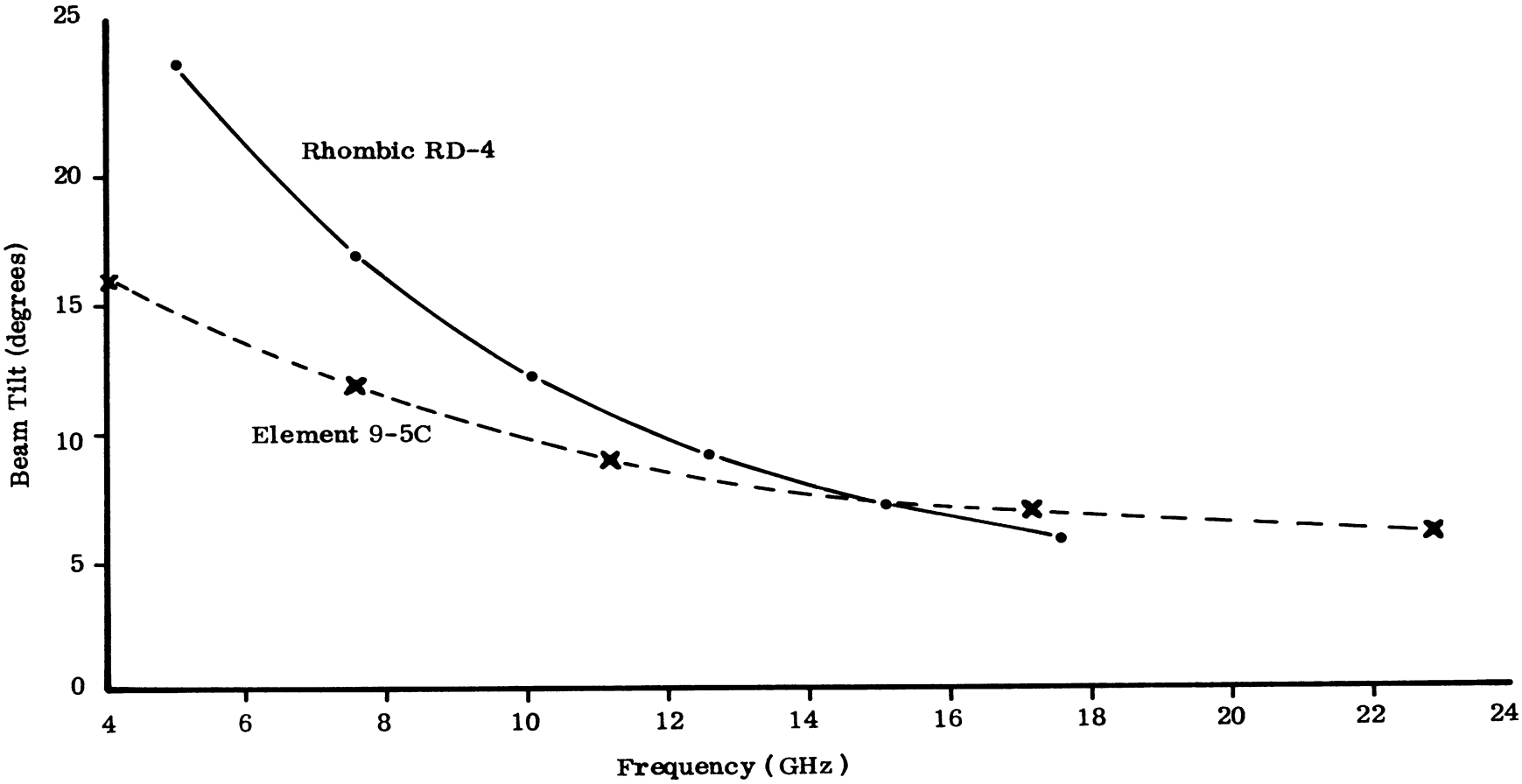

FIG. 4-2: BEAM TILT AS A FUNCTION OF FREQUENCY FOR THE RHOMBIC RD-4 AND THE RUDIMENTARY HORN 9-5C.

V

POSSIBLE APPLICATIONS

5.1 Introduction

From the results given in the previous chapters it appears that the rudimentary horn antenna may be considered to be a broadband antenna having satisfactory VSWR and radiation pattern characteristics over at least 1:5 band of frequencies; with less stringent requirements the bandwidth may be considered to be 1:10. The antenna is linearly polarized; its cross-polarization response in the direction of the main beam maximum is better than 30 dB down. It is directional in both the principal planes but the gain in the H-plane is slightly higher. With these characteristics in mind, the following section presents some of the areas where the rudimentary horn antenna may be found useful.

5.2 Possible Applications

Usually rhombic antennas are used in long range point-to-point communication in the HF range. These antennas are horizontally polarized. From the results given in Chapter IV it is found that the Rhombic RD-4 and the rudimentary horns are comparable in mechanical dimensions as well as in electrical performance. Because of its simple mechanical properties the rudimentary horn can be easily used as a vertically polarized antenna. Thus it appears that a rudimentary horn is quite compatible with the Rhombic RD-4, and the two antennas could be used as a pair for polarization diversity type of reception in tactical long range point-to-point communication.

Both symmetrical and asymmetrical rudimentary horns can be used singly for HF communication purposes. Their performance has been found to be ompetetive with others.

Although the primary purpose of our investigation has been to determine the potential application of the rudimentary horn to the HF communication system, it is believed the antenna may find applications in other systems and in other frequency ranges. We enumerate the following possible uses of the antenna:

i) It may be employed as a broadband feed for reflector type antennas operating in any range from UHF or EHF. Its simplicity along with physical shape and size may well be found advantageous.

ii) It can be designed to operate as a single receiving antenna in the VHF range with good broadband properties.

iii) Because of its physical characteristics and its short H-plane dimensions, it may be employed to an advantage as an element in a phased array in the HF region.

VI

CONCLUSIONS AND RECOMMENDATIONS

6.1 Introduction

As outlined in the technical guidelines of the project, "The main objective of this investigation is to establish the design criteria for the choice of the various parameters in order to obtain optimum performance from the antenna in each of a variety of possible applications. Emphasis shall be placed on the application as a vertically polarized, ground based receiving antenna in long range communication circuits at frequencies between 3 and 30 MHz." From the results reported in the earlier chapters it can be said that the main objective of the present project has been accomplished. In the following sections, we give a general discussion of the antenna along with our conclusions and recommendations for further work to be done.

6.2 General Discussion

Our investigation has shown that the rudimentary horn is an extremely broad band linearly polarized antenna. The antenna maintains its desirable radiation pattern and VSWR characteristics over a wide range of frequencies. The mechanical design of the antenna is quite simple. The symmetrical configuration is more suitable for being used as a vertically polarized antenna. As a vertically polarized antenna it may provide considerably more directivity than other antennas such as the log periodic.

Although the exponential tapering of the radiating element has been found useful, the results of our investigation have shown that it is desirable to employ a complex curvature for the radiating elements, i.e. one that has an exponential taper near the feed point and linear taper near the open end. The exponential taper helps in maintaining a good impedance match. The linear taper has the advantage of simplicity and it seems to reduce the sidelobe amplitudes in the elevation patterns. Such a radiating element should be designed so that there is a smooth transition from the exponential into the linear taper and that the slope of the linear section is of the order of 20^{o} or less .

It has been found preferable to fabricate the radiating element with conducting strips rather than round wires. The latter seem to produce poor VSWR performance. The back radiation from the antenna can be considerably reduced by increasing the width of the radiating strip. The strip can be triangular in shape such that its width is narrow at the feed point and increases linearly toward the open end.

The minimum size of the ground plane necessary for satisfactory impedance performance of a rudimentary horn should be at least $3\lambda \times 3\lambda$ at the center frequency.

6.3 Design of the Rudimentary Horn Antenna

In this section a short discussion is given regarding the choice of the important design parameters for the rudimentary horn antenna so that it may be used effectively in the HF range. The important design parameters are the length L, the radiating aperture 2b (b in the case of asymmetrical antenna), the tapering ratio α and the width w of the radiating strip. In the case of the asymmetrical configuration another additional parameter is the size of the ground plane. General considerations guiding the choice of these parameters are enumerated below:

i) To obtain a directive gain or comparable or better than other commonly used HF antennas, the length L of the rudimentary should be chosen to be at least six wavelengths long at the center of the frequency band. The tapering of the radiating element should be such that $b \gtrsim 2\lambda$. The gain is more sensitive to the parameter b.

ii) For a given combination of L and b various values of the tapering coefficient α may be used. The value of α should be kept as small as possible. The specific value of α will depend on the input impedance of the feed. It should be noted that the VSWR performance is more dependent on α than the pattern main beam.

iii) The width of the radiating strip can be increased from a small value ($w = \lambda/16$) at the input end to a larger value ($w \sim \lambda/6$ at the center frequency) at the open end of the antenna. This technique considerably reduces the back radiation from the antenna.

iv) In the case of asymmetrical configuration the minimum size of the ground plane should be about $3\lambda \times 3\lambda$ at the center frequency for satisfactory VSWR performance.

6.4 Conclusions

On the basis of our investigation we arrive at the conclusion that the rudimentary horn antenna is found to be competitive with commonly used HF antennas in all aspects of electrical performance. It has the added advantage that it can be used as a horizontally or vertically polarized antenna. It has a simple geometrical configuration and its mechanical design is quite simple.

6.5 Recommendations for Further Work

Although we have discussed in detail the characteristics of the rudimentary horn antenna, we feel that further theoretical and experimental work is necessary before the antenna can be brought into some definite practical use and also the potentialities of the antenna can be ascertained completely. Therefore, we recommend that further work be done along the following lines:

1) The first order theory developed for the radiation field should be improved further by taking into account the higher order modes.

2) Theoretical expressions should be developed for the input reflection coefficient for a rudimentary horn antenna.

3) Optimization of the pattern characteristics should be investigated so that the proper choice of the design parameters may be made for a desirable performance of the antenna.

4) With regard to the application of the antenna for HF communication, the pattern characteristics of the antenna should be investigated by modeling the actual ground constants.

5) Investigate the performance of a full scale rudimentary horn antenna in the HF range.

REFERENCES

Brueckmann, H. (January 1957), "Analysis of Measured Radiation Patterns of Two HF Antenna Arrays and one Rhombic - Engineering Report" Signal Corps Engineering Laboratories Report E-1198, Ft. Monmouth, N. J.

Christiansen, W. M. (1947), "Rhombic Antenna Arrays, " A. W. A. Technical Review, 7, No. 4, pp. 361-383.

Clark, F. C., R. D. Guhne and B. G. Hagaman (30 June 1959), ""Tapered Aperture Horn Antenna - Final Technical Report", Developmental Engineering Corporation Report No. 14-F, Washington, D. C.

Dukes, J. M. C. (1958), "The Application of Printed Circuit Techniques to the Design of Microwave Components, " Proc. IEE (London), 105B, No. 20, pp. 155-172.

Harper, A. E. (1941), Rhombic Antenna Design, D. Van Nostrand Co., Princeton, NJ.

Jasik, H. (1961), Antenna Engineering Handbook, McGraw-Hill Book Co., New York., pp. 4-12 — 4-13 .

Knott, E. F., V. V. Liepa and T. B. A. Senior (1965), "A Surface Field Measurement Facility, " Proc. IEEE, 53, No. 8, pp. 1105-1107.

Knott, E. F. (December 1965), "Design and Operation of a Surface Field Measurement Facility, " The University of Michigan Radiation Laboratory Report No. 7030-7-T, AD 482481, UNCLASSIFIED.

Kraus, J D (1950), Antennas, McGraw-Hill Book Co., New York, pp. 23-32.

Ramsay, J. F., B. V. Popovich and J. F. Gobler (July 1967), "Research on Compact and Efficient Antennas-Final Report", Airborne Instrumenta Laboratory Report ECOM-02111-F, Contract DA28-043 02111(E), Deer Park, New York.

Schelkunoff, S. A. (1955), "Conversion of Maxwell's Equations into Generalized Telegraphist's Equations, " Bell System Technical Journal, pp. 995-1043.

Sinclair, G. (1948), "Electromagnetic Systems Model Theory, " Proc. IRE, 35, No. 11, pp. 1364-1370.

Technology for Communications International (TCI) (1968), Product Catalog, Mountain View, California.

Walton, K. L. and V. C. Sundberg (1964), "Broadband Ridged Horn Design, " Microwave J., pp. 96-101, March issue.

Wolff, E. A. (1966), Antenna Design, John Wiley and Sons, New York, pp. 109-113.

APPENDIX A: RADIATION FIELD OF A VEE ANTENNA

A V-antenna carrying a traveling wave of current may be thought of as a special case of the rudimentary antenna. It is of some interest to compare the performance of a traveling wave V-antenna with that of a rudimentary horn. In the present section we give the complete expressions for the free space radiation fields produced by such an antenna carrying a single traveling wave of current. The results given below are not new; they are included here for the sake of convenience. If necessary the patterns may be computed numerically from the expressions given below and compared with those of rudimentary horn antennas with comparable dimensions.

Let the V-antenna be oriented as shown in Fig. A-1 below and let the current in each area be

$$I=I_0 e^{-ik\ell'} \qquad (A.1)$$

where ℓ' is measured along the arm of the antenna. Let AB=BC=ℓ . The method of analysis is similar to that used in Section 3.2.

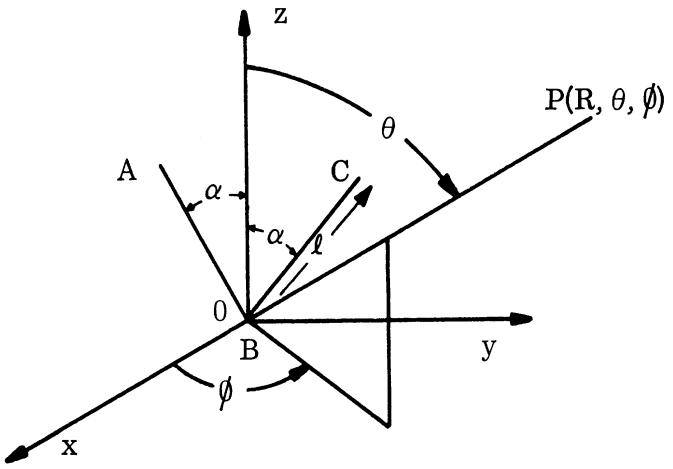

FIG. A-1: GEOMETRICAL REPRESENTATION OF A VEE ANTENNA.

It can be shown that the far field components produced by the antenna are given by the following expressions:

$$E_{\phi}=k\eta_o \ell I_o \sin\alpha \cos\phi \left[e^{-i(1-\cos\psi)k\ell/2} f(\psi)+e^{-i(1-\cos\psi')} f\psi')\right] \quad (A.2)$$

where

$$f(\psi)= \frac{\sin\left[(1-\cos\psi)k\ell/2\right]}{(1-\cos\psi)k\ell/2} \quad (A.3)$$

$$K = \frac{-ike^{-ikR}}{4\pi R} \quad (A.4)$$

$$\cos\psi = \cos\theta\cos\alpha + \sin\theta\sin\alpha\sin\phi \quad (A.5)$$

$$\cos\psi' = \cos\theta\cos\alpha - \sin\theta\sin\alpha\sin\phi, \quad (A.6)$$

$$E_{\theta}=K\eta_o \ell I_o \left[\sin\alpha\cos\theta\sin\phi \left\{e^{-i(1-\cos\psi)k\ell/2} f(\psi) + e^{-i(1-\cos\psi')k\ell/2} f(\psi')\right\} - \cos\alpha\sin\theta\left\{e^{-i(1-\cos\psi)k\ell/2} f(\psi) - e^{-i(1-\cos\psi')k\ell/2} f(\psi')\right\}\right] . \quad (A.7)$$

Thus in the $\phi=0$ plane we have:

$$E_{\theta} \equiv 0 \quad (A.8)$$

$$E_{\phi}= 2K\eta_o \ell I_o e^{-i(1-\cos\theta\cos\alpha)\ell/2} \times \sin\alpha \frac{\sin\left[(1-\cos\theta\cos\phi k\ell/2\right]}{(1-\cos\theta\cos\phi)\, k\ell/2}. \quad (A.9)$$

In the $\phi = \pi/2$ plane:

$$E_{\phi} \equiv 0 \quad (A.10)$$

$$E_{\theta} = K\eta_o \ell I_o \left[e^{-i\left[1-\cos(\alpha-\theta)\right]k\ell/2} \frac{\sin\left[\left\{1-\cos(\alpha-\theta)\right\}k\ell/2\right]}{\left\{1-\cos(\alpha-\theta)\right\}k\ell/2} + e^{-i\left[1-\cos(\alpha+\theta)\right]k\ell/2} \frac{\sin\left[\left\{1-\cos(\alpha+\theta)\right\}k\ell/2\right]}{\left\{1-\cos(\alpha+\theta)\right\}k\ell/2}\right] . \quad (A.11)$$

If necessary, the radiation patterns of V-antennas with standing wave distribution of current can be obtained from standard texts on antennas.

APPENDIX B: CONTOUR MAP OF THE RADIATION FIELD OF ASYMMETRICAL RUDIMENTARY HORNS

In this appendix the three-dimensional behavior of the radiation field of two specific asymmetrical rudimentary horn antennas is discussed. The two antennas chosen for this investigation are the models 9-5C and 7-5C whose design parameters are as given in Tables II-1 and II-2. The important design parameters of these two antenna models are as follows:

9-5C	7-5C
L = 24"	L = 18"
D = 5"	D = 5"

Both the models employ a 15' diameter conducting ground plane. These two models have been selected for measurement in the GHz range because their corresponding physical dimensions at the full scale frequency in the HF range compare favorably with commonly used HF antennas.

The radiation patterns of the above two antenna models have been measured in different ϕ-planes at some selected frequencies lying within the range 1 - 10 GHz. These frequencies are then properly scaled to the full scale frequency which in the present case lies in the HF range. Contour maps of the radiation field have been prepared from the measured radiation patterns and the results are shown in Figs. B-1(a-e) and B-2(a-e). The general behavior of the three-dimensional patterns as a function of frequency can be studied by examining these contour maps.

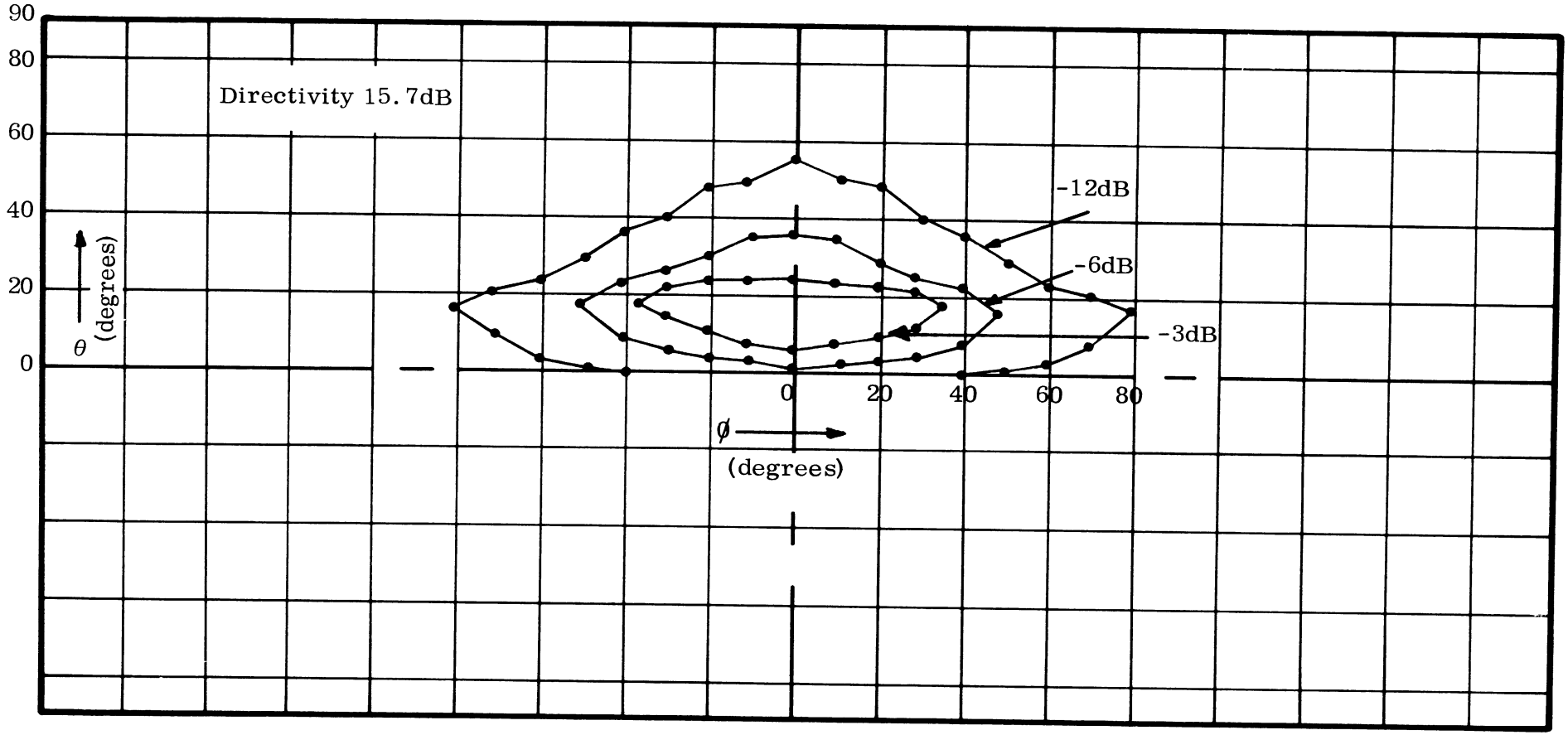

FIG. B-1a: CONTOUR PLOT OF THE RADIATION FIELD OF RUDIMENTARY HORN MODEL 7-5C AT 4.0 MHz.

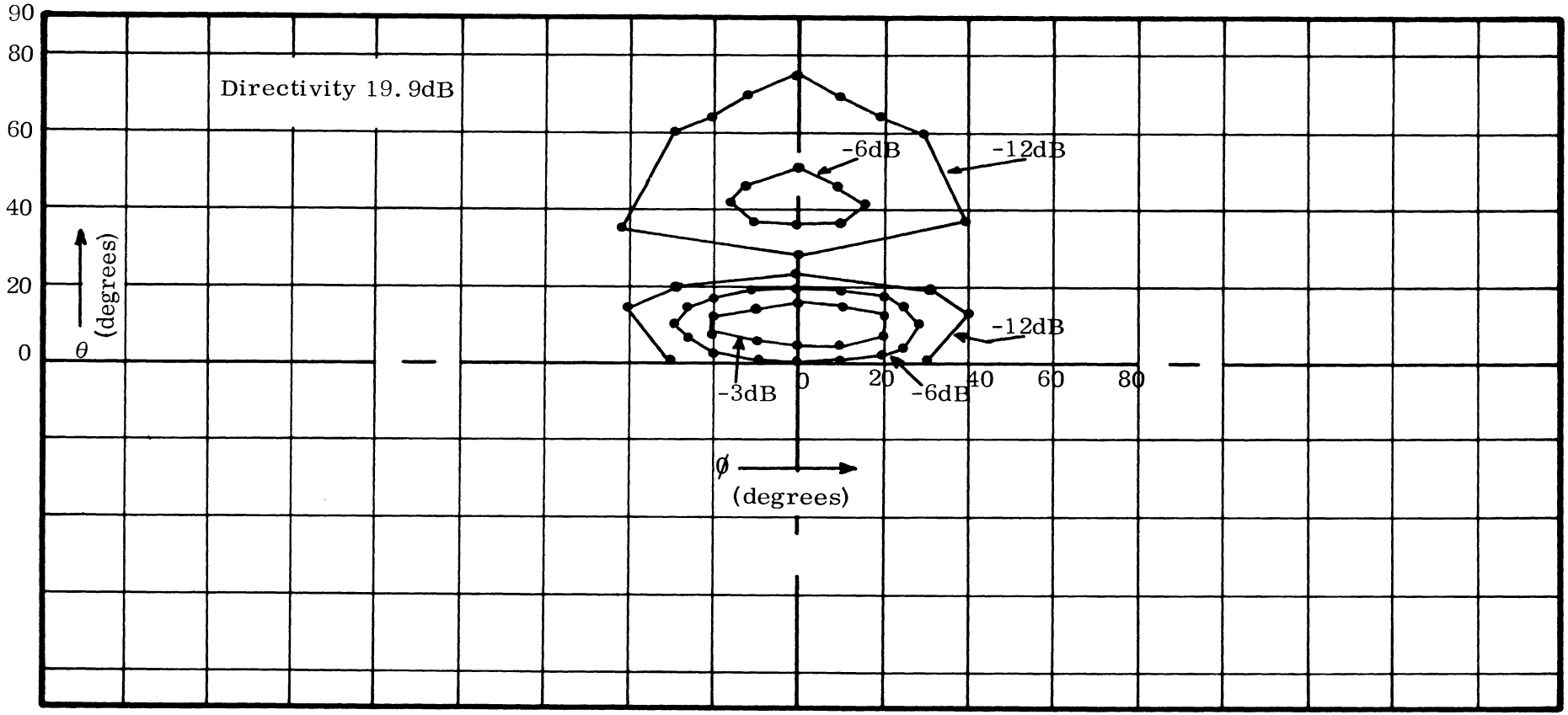

FIG. B-1b: CONTOUR PLOT OF THE RADIATION FIELD OF RUDIMENTARY HORN MODEL 7-5C AT 7.5 MHz.

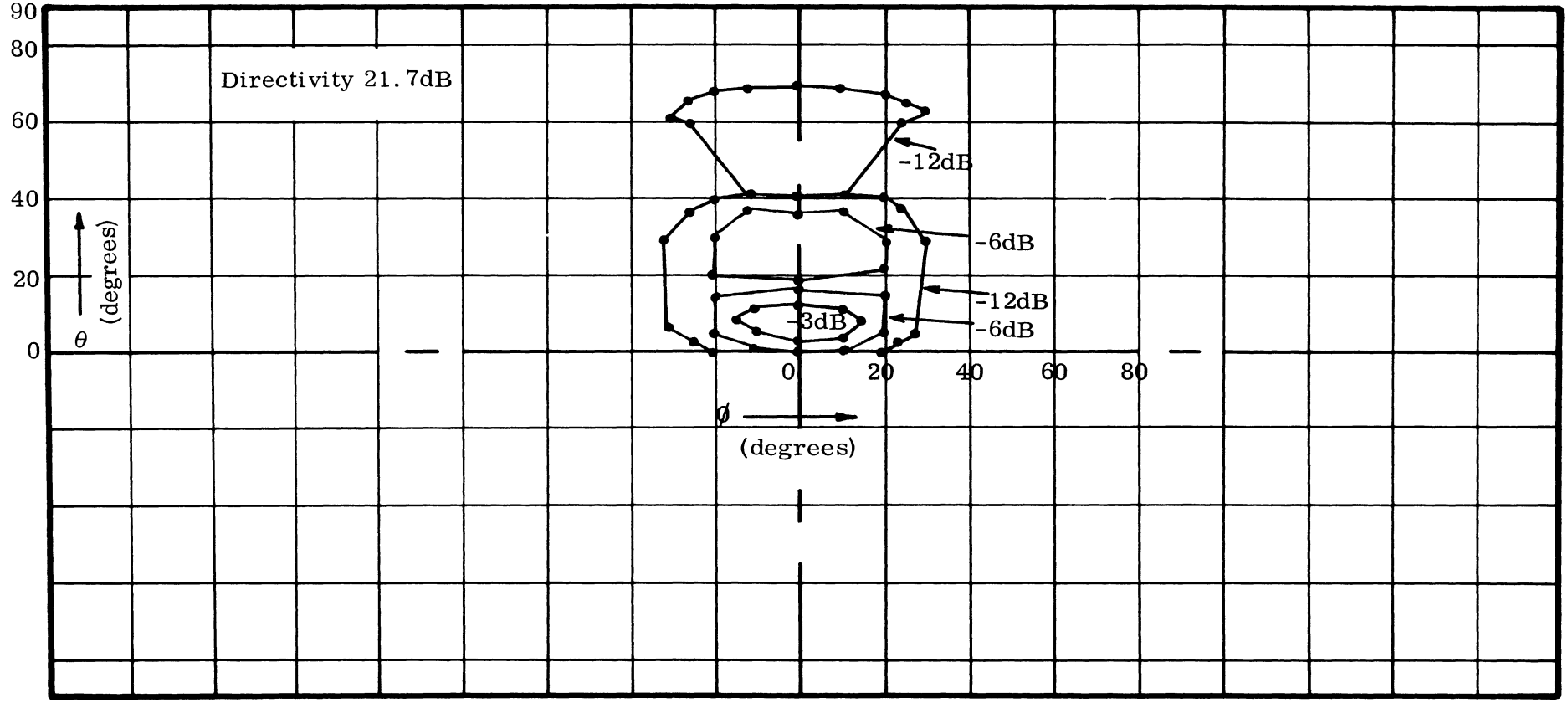

FIG. B-1c: CONTOUR PLOT OF THE RADIATION FIELD OF RUDIMENTARY HORN MODEL 7-5C AT 11.1 MHz.

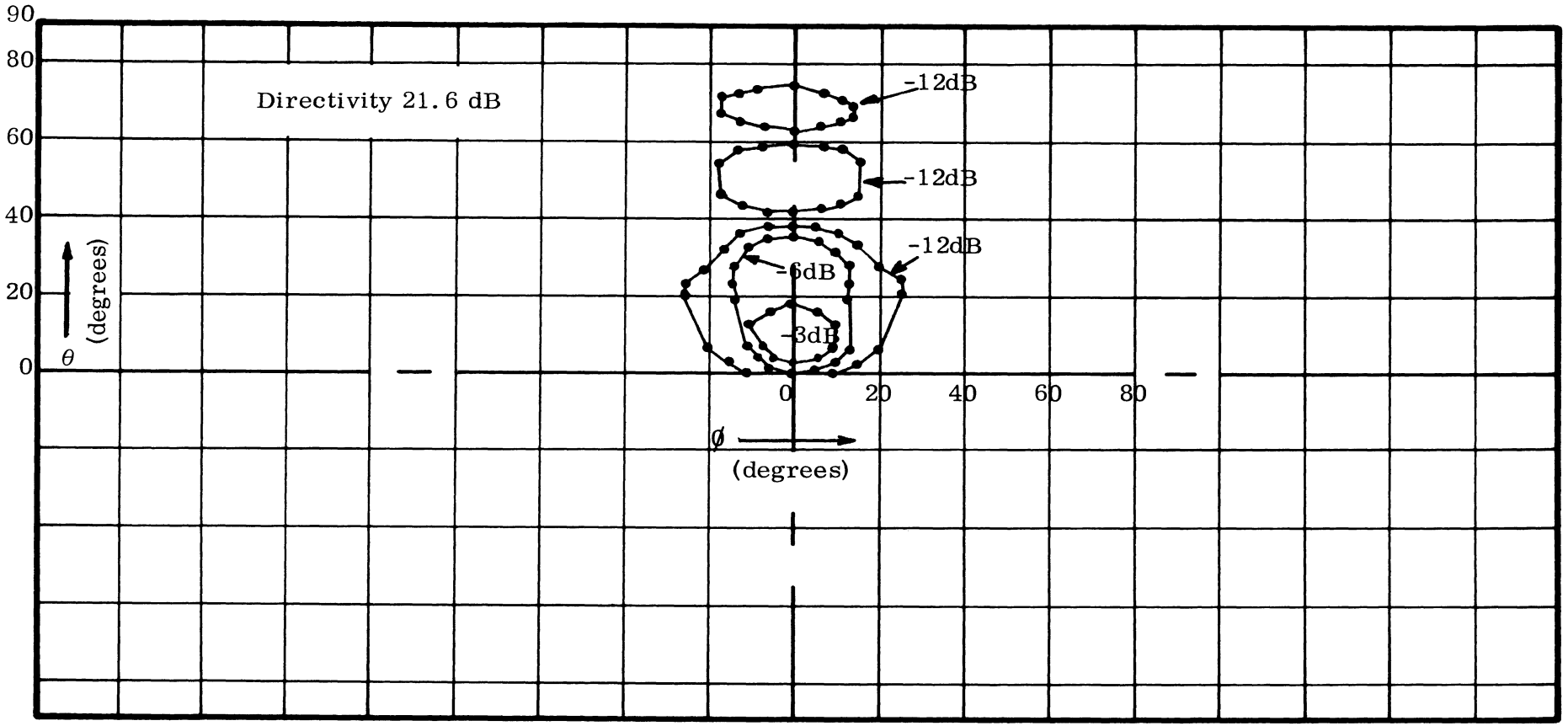

FIG. B-1d: CONTOUR PLOT OF THE RADIATION FIELD OF RUDIMENTARY HORN MODEL 7-5C AT 17.1 MHz.

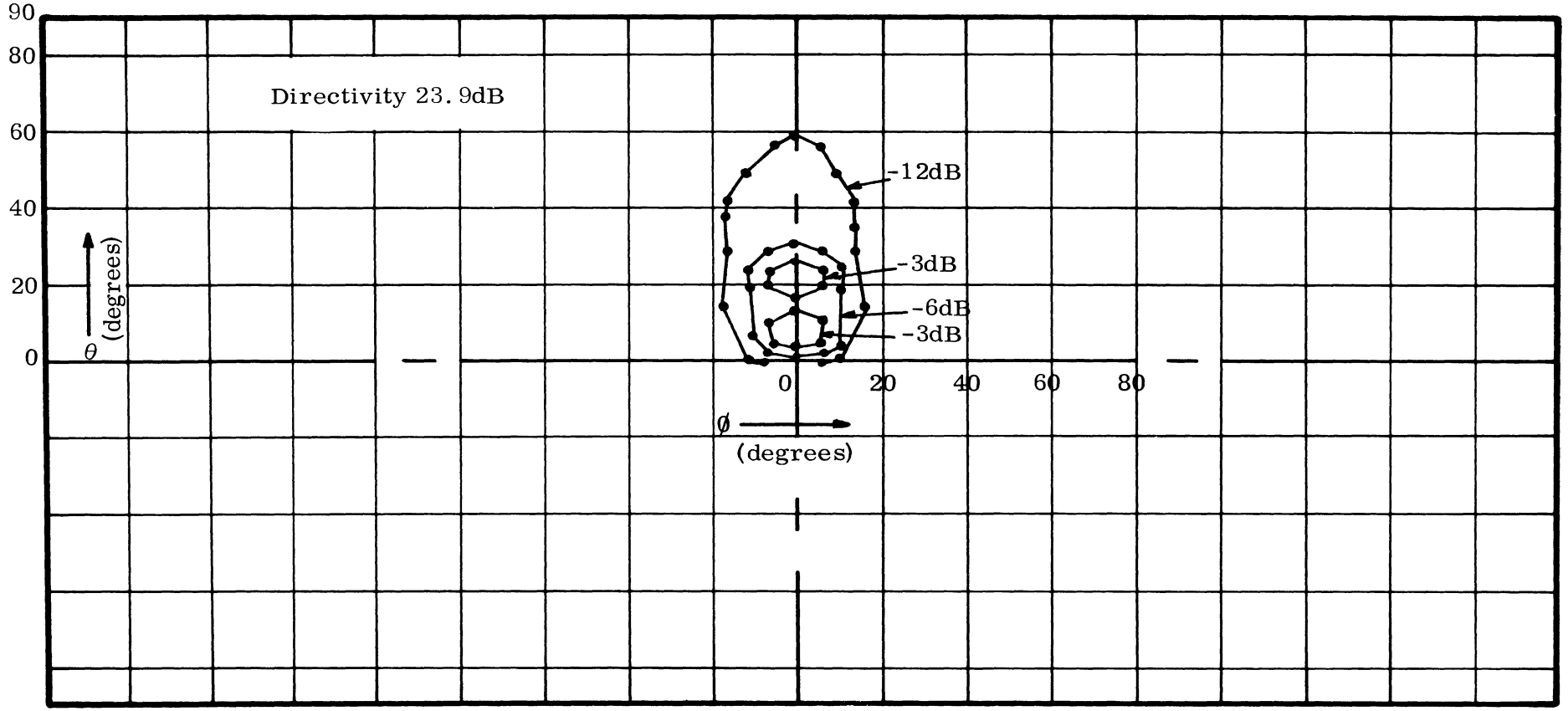

FIG. B-1e: CONTOUR PLOT OF THE RADIATION FIELD OF RUDIMENTARY HORN MODEL 7-5C AT 22.8 MHz.

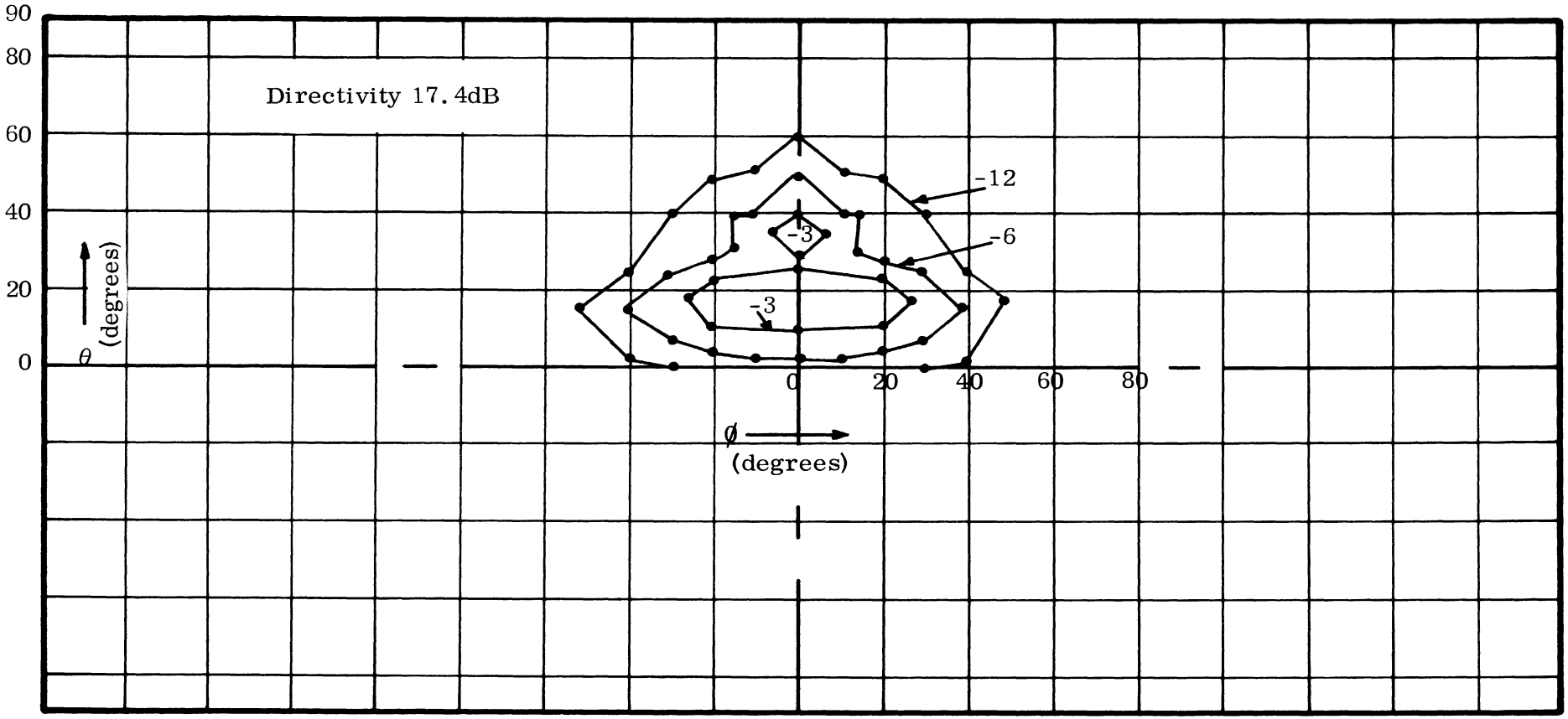

FIG. B-2a: CONTOUR PLOT OF THE RADIATION FIELD OF RUDIMENTARY HORN MODEL 9-5C AT 4.0 MHz.

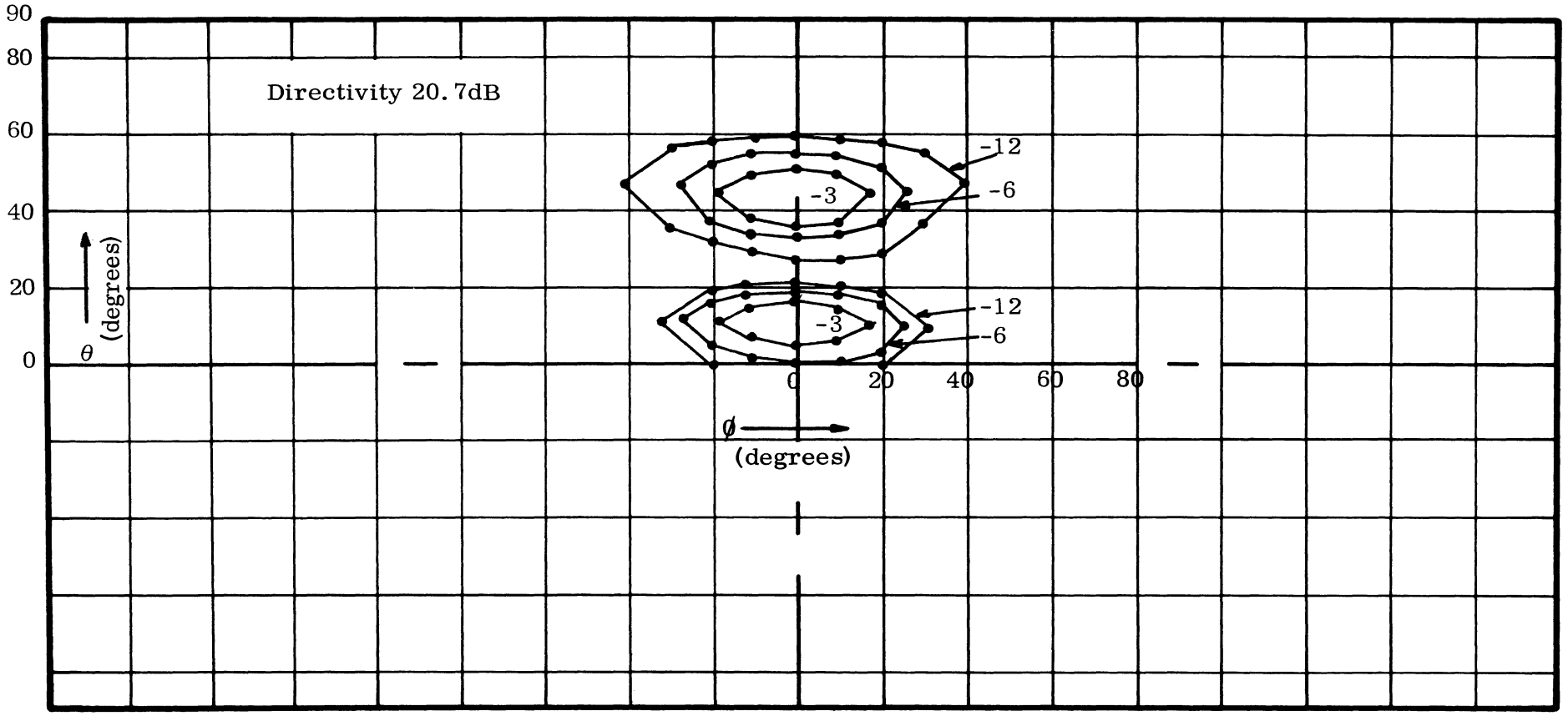

FIG. B-2b: CONTOUR PLOT OF THE RADIATION FIELD OF RUDIMENTARY HORN MODEL 9-5C AT 7.5 MHz.

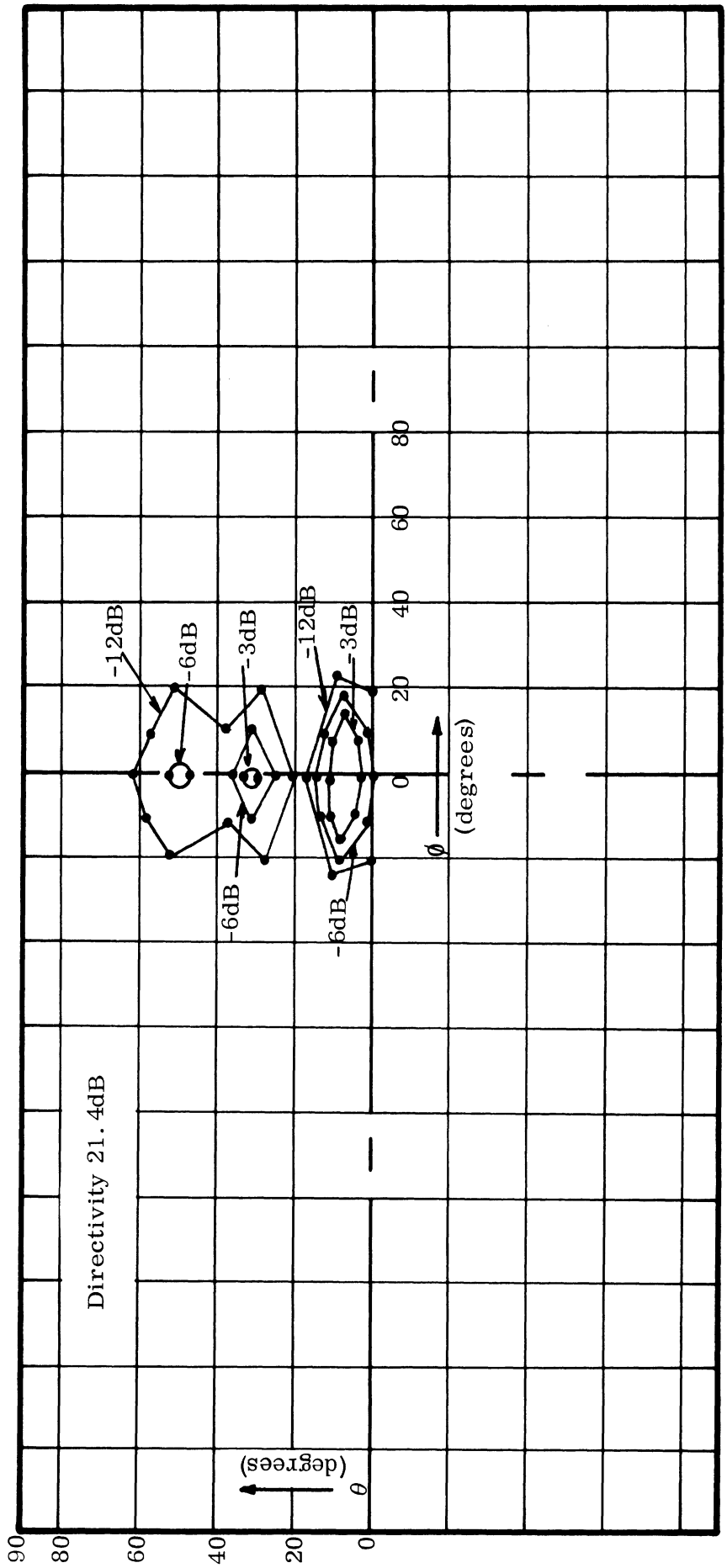

FIG. B-2c: CONTOUR PLOT OF THE RADIATION FIELD OF RUDIMENTARY HORN MODEL 9-5C AT 11.1 MHz.

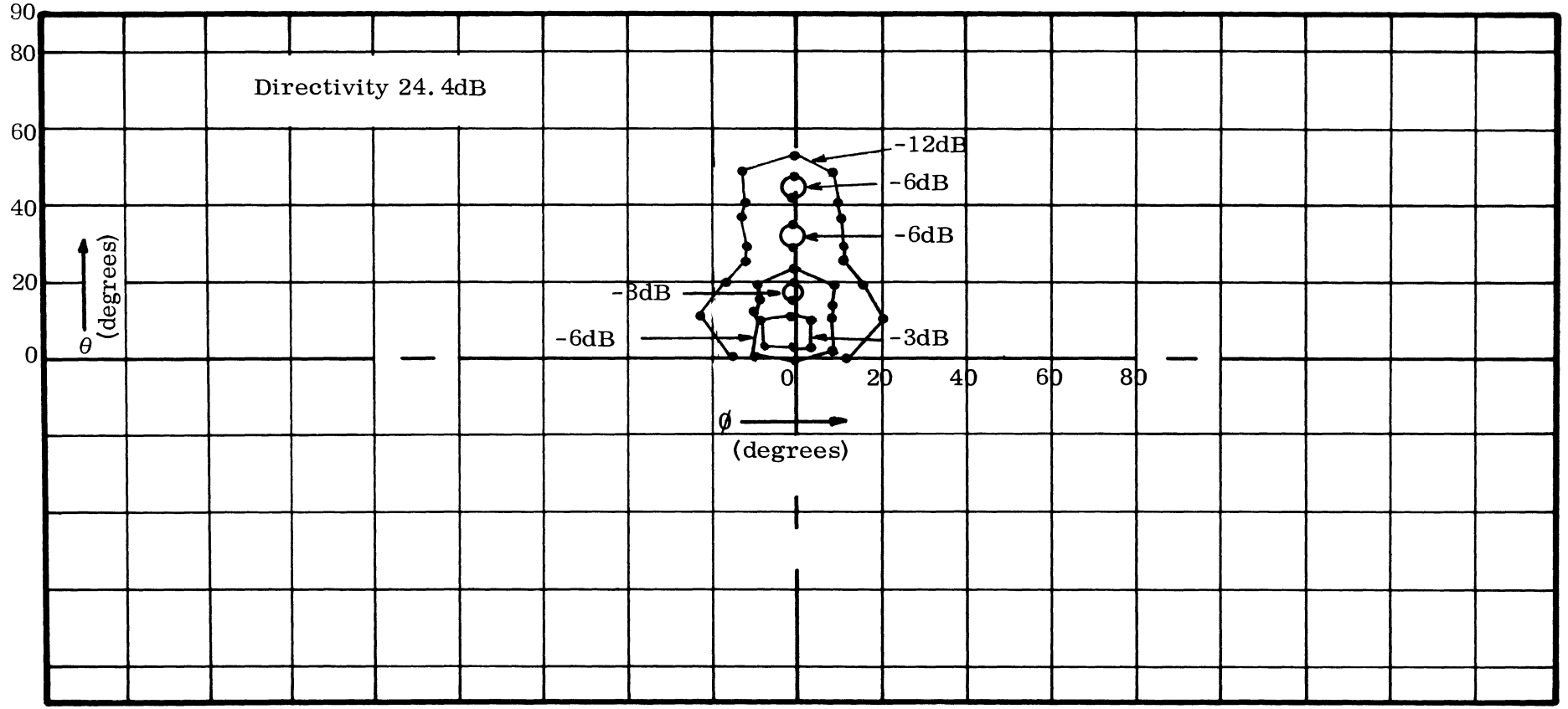

FIG. B-2d: CONTOUR PLOT OF THE RADIATION FIELD OF RUDIMENTARY HORN MODEL 9-5C AT 17.1 MHz.

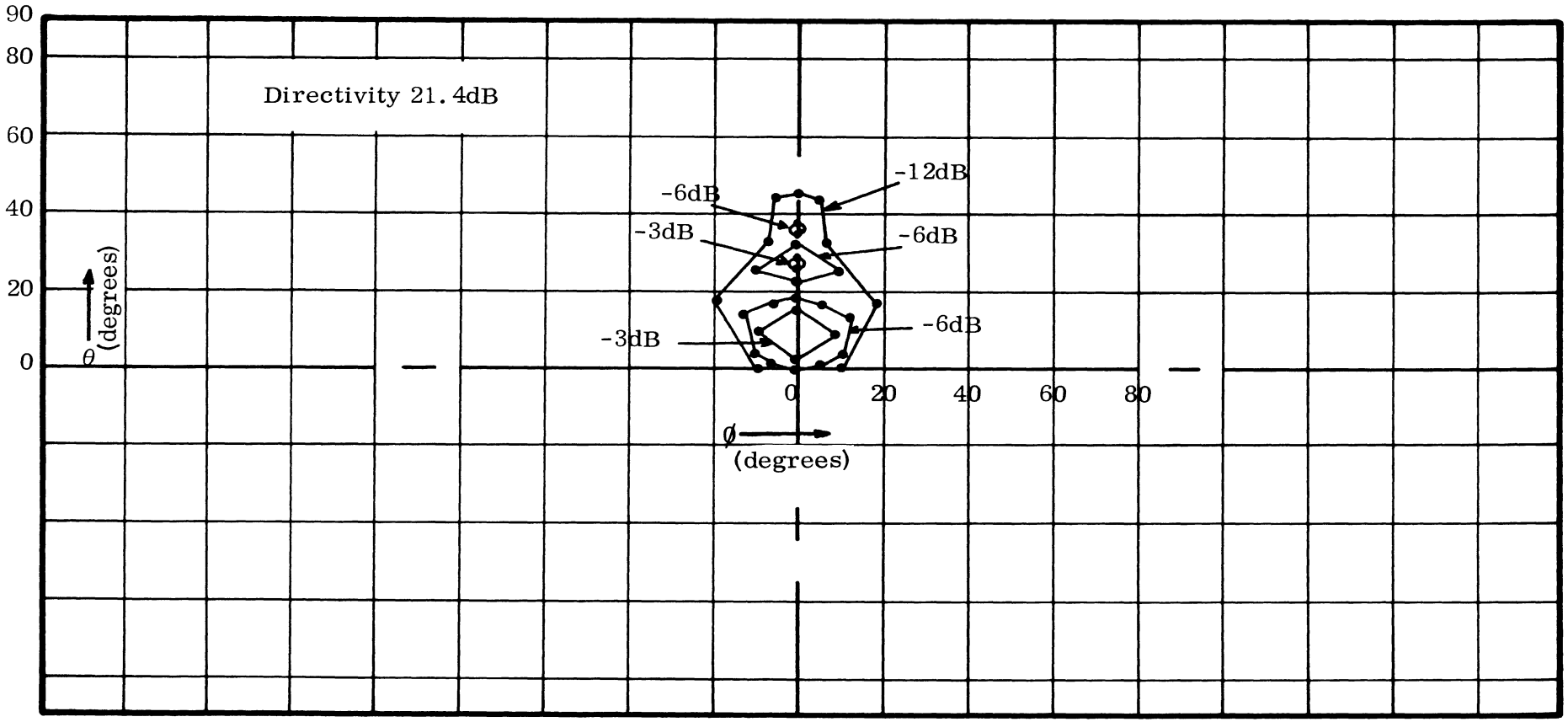

FIG. B-2e: CONTOUR PLOT OF THE RADIATION FIELD OF RUDIMENTARY HORN MODEL 9-5C AT 22.8 MHz.

Distribution List - Final Report ECOM - 0274-F (1778-1-F)
Contract Nr. DAAB07-68-C-0274

Defense Documentation Center
Attn: DDC-IRS
Cameron Station (Bldg 5)
Alexandria, Virginia 22314 — 10

Technical Library
Dir of Defense Research and Engineering
Room 3E-1039, The Pentagon
Washington, DC 20301 — 1

Director, Defense Atomic Support Agency
Attn: Document Library Branch
Washington, DC 20305 — 1

Chief of Naval Research
Attn: Code 427
Department of the Navy
Washington, D.C. 20325 — 1

Naval Ships Systems Command
Attn: Code 20526 (Technical Library)
Main Navy Building, Room 1528
Washington, DC 20325 — 1

Naval Ships Systems Command
Attn: Code 61798
Department of the Navy
Washington, D.C. 20360 — 1

Director
U.S. Naval Research Laboratory
Attn: Code 2027
Washington, D.C. 20390 — 2

Commanding Officer and Director
U.S. Navy Electronics Laboratory
Attn: Library
San Diego, California 92152 — 1

Commander
U.S. Naval Ordnance Laboratory
Attn: Technical Library
White Oak, Silver Spring, Maryland 20910 — 1

Distribution List - continued

AFSC STLO (RTSND) Naval Air Development Center Johnsville, Warminster, Pa. 18974	1
Commandant, Marine Corps (Code A04C) Headquarters, U.S. Marine Corps Washington, D.C. 20380	1
Dir. Marine Corps Landing Force Dev Ctr Attn: C-E Division Marine Corps Schools Quantico, Virginia 22134	1
Rome Air Development Center (EMTLD) Attn: Documents Library Griffiss Air Force Base New York 13440	1
Electronic Systems Division (ESTI) L. G. Hanscom Field Bedford, Massachusetts 01730	2
U.S. Air Force Security Service Attn: ESD San Antonio, Texas 78241	1
Headquarters, AFSC Attn: SCTSE Bolling AFB, Ohio 20332	1
Director Air Force Materials Laboratory Attn: MAAM Wright-Patterson AFB, Ohio 45433	1
Chief of Research and Development Department of the Army Washington, D.C. 20315	2
Ofc of the Chief of Comm-Electronics Department of the Army Attn: CCETC-5 Washington, D.C. 20315	2

Distribution List - continued

Commanding Officer 52D USASASOC Fort Huachuca, Arizona 85613	1
Commanding Officer Aberdeen Proving Ground Attn: Technical Library, Bldg 313 Aberdeen Proving Ground, Md. 21005	2
Headquarters U.S. Army Materiel Command Attn: AMCMA-RM/3 Washington, D.C. 20315	2
Commanding Officer U.S. Army Combat Developments Command Communications-Electronics Agency Fort Monmouth, New Jersey 07703	1
Commander U.S. Army Research Office (Durham) Box CM-Duke Station Durham, North Carolina 27706	1
Commanding Officer U.S. Army Sec Agcy Combat Dev ACTC Arlington Hall Station Arlington, Virginia 22212	1
U.S. Army Security Agency Attn: OAC of S, DEV Arlington Hall Station Arlington, Virginia 22212	1
U.S. Army Security Agcy Processing Ctr Attn: IAVAPC-R and D Vint Hill Farms Station Warrenton, Virginia 22186	1
Commanding Officer U.S. Army Nuclear Defense Laboratory Attn: Library Edgewood Arsenal, Md. 21010	1
Harry Diamond Laboratories Attn: Library Connecticut Avenue and Van Ness Street Washington, DC 20438	1

Distribution List - continued

Commanding General
U.S. Army Electronic Proving Ground
Attn: Technical Information Center
Fort Huachuca, Arizona 85613 — 1

Asst Secretary of the Army (R and d)
Department of the Army
Attn: Deputy Asst for Army (R and D)
Washington, D.C. 20315 — 1

USAECOM Liaison Officer
Aeronautical Systems Division
Attn: ASDL-9
Wright-Patterson AF Base, Ohio 45433 — 1

Commanding General
U. S. Army Electronics Command
Attn: AMSEL-XL-C
Fort Monmouth, New Jersey 07703 — 25

NASA Scientific and Technical Info Facility
Attn: Acquisitions Branch (S-AK/DL)
P. O. Box 33
College Park, Md. 20740 — 1

DASA Info and Analysis Center
General Electric-Tempo
816 State St
Santa Barbara, California 93102 — 1

Commanding General
U.S. Army Communication Systems Agency
Office of the Project Manager STARCOM
Attn: USACSA-EN-4
Fort Monmouth, New Jerseo 07703 — 3

Commanding General
U.S. Army Strategic Communications Command
Attn: USASCCSA-E
Fort Huachuca, Arizona 85613 — 3

Commanding General
U.S. Army Strategic Communications Command CONUS
Attn: USASCCC/DOF-1
4200 Silver Hill Road (Stop. No. 331)
Washington, D. C. 20315 — 2

Distribution List - continued

Commanding Officer USASRATCOM-CONUS Fort Detrick, Md. Facility Attn: SCCC-DM/C Frederick, Maryland 21701	2
Commanding Officer DA Radio Receiver Station Attn: Mr. G. Blythe La Plata, Maryland 20646	2
Commanding Officer U. S. Army Strategic Communications Command Signal Group-Hawaii Attn: SCCP-HPO APO San Francisco, California 96557	1
Commanding Officer U.S. Army STRATCOM-CONUS Davis Calif. Facility Davis, California	1
Mr. M.L. Musselman, Code 5410-846 U.S. Naval Research Laboratory Washington 25 D.C. 20390	1
Commander Naval Communications Command Attn: NC/N421/1kb, Serial 9012 5827 Columbia Pike Bailey's Crossroads, Virginia 22041	1
Commanding Officer Naval Communication Station-Washington Attn: Lt. R.N. Schappacher Washington, D.C. 20390	1
Commanding General, Headwuarters Defense Communications Agency Attn: Mr. S.E. Probst Chief, Frequency Branch South Courthouse Road and 8 Street Arlington, Virginia	1
Mr. David L. Bates Code K3112 National Security Agency Fort G.G. Meade, Md. 20755	1

Distribution List - continued

Mr. William B. Schulthels Central Intelligence Agency Washington, D.C. 20505	1
Mr. Herman V. Cottony ITS Environmental Science Service Admin. Boulder, Colorado 80302	2
Mr. Paul A. Lantz, Code 525 NASA Goddard Space Flight Center Greenvelt, Md.20771	1
Mr. Julius Ross IBS/ET U.S. Information Agency Washington, D.C. 20547	2
Total	99

Security Classification

DOCUMENT CONTROL DATA - R & D

(Security classification of title, body of abstract and indexing annotation must be entered when the overall report is classified)

1. ORIGINATING ACTIVITY (Corporate author) The University of Michigan Radiation Laboratory, Dept. of Electrical Engineering, 201 Catherine Street, Ann Arbor, Michigan 48108	2a. REPORT SECURITY CLASSIFICATION UNCLASSIFIED 2b. GROUP na

3. REPORT TITLE

Investigation of the Rudimentary Horn

4. DESCRIPTIVE NOTES (Type of report and inclusive dates)

Final Report. 26 April 1968 through 25 April 1969

5. AUTHOR(S) (First name, middle initial, last name)

Dipak L. Sengupta and Joseph E. Ferris

6. REPORT DATE	7a. TOTAL NO. OF PAGES	7b. NO. OF REFS
May 1969	105	15

8a. CONTRACT OR GRANT NO.	9a. ORIGINATOR'S REPORT NUMBER(S)
DAAB07-68-C-0274	1778-1-F
b. PROJECT NO. PR and C-68-EL-7303	
c.	9b. OTHER REPORT NO(S) (Any other numbers that may be assigned this report)
d.	ECOM-0274-F

10. DISTRIBUTION STATEMENT

Each transmittal of this document outside the Department of Defense must have prior approval of CG, US Army Communication Systems Agency, Ft. Monmouth, N. J.

11. SUPPLEMENTARY NOTES	12. SPONSORING MILITARY ACTIVITY
	United States Army Electronics Command Fort Monmouth, N J 07703

13. ABSTRACT

The performance of a novel type of antenna named the Rudimentary Horn has been investigated both theoretically and experimentally. Detailed experimental investigation of the VSWR properties as well as the radiation characteristics of the antenna has been carried out over the frequency range 1 - 10 GHz. Over this band of frequencies the antenna has been found to maintain its desirable impedance and radiation characteristics.

A first order theory has been developed for the radiation field produced by a symmetrical rudimentary horn having exponentially curved radiating elements. Fair agreement has been obtained between theory and experiment for the H-plane radiation patterns. Further improvement of the theory is desirable.

The rudimentary horn is found to be a broadband linearly polarized antenna. Its cross-polarization response in the direction of the main beam maximum is at least 30 dB down. The effects of the variation of the different physical parameters on the performance of the antenna are given. General design considerations are also given.

Possible applications of the rudimentary horn are also discussed. In particular, it has been found that in all aspects of electrical performance the rudimentary horn is competitive with commonly used antennas for HF long range communication.

DD FORM 1 NOV 65 1473

Security Classification

14. KEY WORDS	LINK A		LINK B		LINK C	
	ROLE	WT	ROLE	WT	ROLE	WT
Rudimentary Horn Antennas						
Broadband Antennas						
HF Antenna						
Radiation Patterns						
VSWR Characteristics						